

Gas Reactions of Carbon

P. L. WALKER, JR., FRANK RUSINKO, JR.,
AND L. G. AUSTIN

*Fuel Technology Department, The Pennsylvania State University,
University Park, Pennsylvania*

	<i>Page</i>
I. Introduction.....	134
II. Thermodynamics of Gas-Carbon Reactions.....	135
A. Heats of Reaction.....	135
B. Equilibrium Constants and Product-Reactant Ratios.....	136
III. Review of General Mechanisms for the Gas-Carbon Reactions.....	138
A. General Remarks.....	138
B. Mechanisms.....	141
IV. Review of Kinetics for the Gas-Carbon Reactions.....	153
A. Orders of Reactions.....	153
B. Activation Energies of Reactions.....	156
C. Relative Rates of Gas-Carbon Reactions.....	162
V. Role of Mass Transport in Gas-Carbon Reactions.....	164
A. General Remarks.....	164
B. Three Temperature Zones in Gas-Carbon Reactions.....	165
C. General Discussion of Zone II for the Gas-Carbon Reactions.....	167
D. Comprehensive Rate Equations Covering the Three Temperature Zones in Gas-Carbon Reactions.....	171
E. Rates of Gas-Carbon Reactions in Zone III.....	173
VI. Use of Density and Area Profiles on Reacted Carbon Rods for Better Under- standing of Gas-Carbon Reactions.....	178
A. Introduction.....	178
B. Use of Density Profile Data to Determine Rate of Reaction at Any Radius in the Carbon Rod.....	179
C. Mass Transport and Reactant Concentration Profiles through the Rod.....	182
D. Discussion of Experimental Results.....	184
E. Summary.....	200
VII. Some Factors, Other than Mass Transport, Which Affect the Rate of Gas- Carbon Reactions.....	201
A. Crystallite Orientation.....	201
B. Impurities in the Carbon.....	203
C. Crystallite Size.....	205
D. Effect of Heat Treatment of Carbons on Their Subsequent Reactivity to Gases.....	206
E. Addition of Halogens to the Reacting Gas.....	209
F. Irradiation.....	210
Appendix.....	212
References.....	217

I. Introduction

A substantial portion of the world's energy requirements is met directly or indirectly through the utilization of the gas reactions of carbon and carbonaceous materials. To be particularly considered are the reactions of oxygen, steam, carbon dioxide, and hydrogen with carbon. The exothermic reaction of carbon with oxygen has been, and still is, the major source of energy in the world. The endothermic reaction of carbon with steam produces carbon monoxide and hydrogen, which are used either directly as gaseous fuels or as synthesis gas can be converted catalytically to a series of hydrocarbon fuels or organic chemicals. Since carbon dioxide is a direct product of the carbon-oxygen reaction and an indirect product of the carbon-steam reaction through the water-gas shift reaction, the secondary reaction of carbon dioxide with carbon in fuel beds is closely tied to the former gas-carbon reactions. The reaction of hydrogen with carbon to produce methane is not of great industrial significance at the moment but appears to have an important future.

The gas-carbon reactions have other major contributions besides those related directly to fulfilling our energy requirements. Active carbons are produced almost entirely through the activation of carbonaceous materials with steam and/or air. The regeneration of coked or spent catalysts by burning the coke with air is an essential part of the process involving the catalytic cracking of petroleum. The production of carbon monoxide and hydrogen, which serve as reducing agents for the direct processing of ores, shows considerable promise.

Paradoxically, there is a necessity in many operations for retarding the gas-carbon reactions. When carbon is used as an electrode material, it is desired that the carbon not react with either the carbon dioxide produced by reduction of the ore or with the ambient atmosphere. Carbon has excellent high-temperature strength properties which suggest its use for nozzles in rockets and nose cones in missiles, but again good oxidation resistance is a necessity. Graphite is being used to a considerable extent as a moderating material in atomic reactors; and when carbon dioxide is used as the coolant, its reaction with the graphite can be a problem.

Even though the gas-carbon reactions have been an integral part of our industrial economy for many years, a fundamental understanding of their reaction mechanisms and kinetics has lagged far behind their practical use. This primarily has been caused by the lack of experimental techniques to define the properties of one of the reactants—the carbon. With the relatively recent ability to determine quantitatively such properties of solids as surface areas, pore distributions, crystallographic parameters, average crystallite sizes, chemisorption of gases, trace impurities, rates of internal gas transport, and electronic properties, the possibility of clearly understanding the gas-carbon reactions is closer at hand. Certainly, workers in

the field of catalysis, who have employed many of the above experimental techniques to describe their catalysts, have, in recent years, made rapid strides at understanding reactions occurring on solid surfaces. Consequently, many of the concepts developed by workers in the catalysis field have been used extensively by the authors and other workers studying the gas-carbon reactions. Even more extensive use of these connecting and related concepts is to be encouraged. With this main purpose in mind, this article has been written.

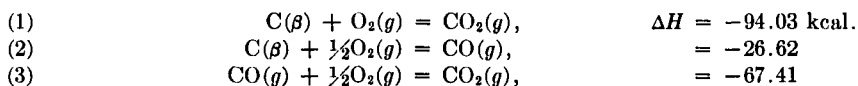
In this article, the authors have attempted to supply a reference to the majority of pertinent papers on gas-carbon reactions. Reasons for the large amount of apparently conflicting data on orders and activation energies for the reactions are advanced. A detailed quantitative discussion of the role which inherent chemical reactivity of the carbon and mass transport of the reactants and products can play in affecting the kinetics of gas-carbon reactions is presented. The possibilities of using bulk-density and surface-area profile data on reacted carbons for better understanding of reaction mechanisms is discussed. Finally, some factors, other than mass transport, affecting gas-carbon reactions are reviewed.

II. Thermodynamics of Gas-Carbon Reactions

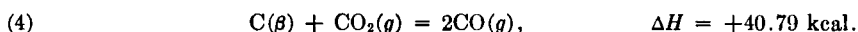
A. HEATS OF REACTION

Heats of reaction at 18° and 1 atm. for the important gas-carbon reactions are presented. When secondary and/or concurrent reactions are possible, data on these reactions are included. In the equations, the carbon is taken to be in the form of β -graphite. On the basis of β -graphite having a zero heat of formation, various types of amorphous carbons are reported (1) to have positive heats of formation ($+\Delta H$) ranging from 1.7 to 2.6 kcal./mole:

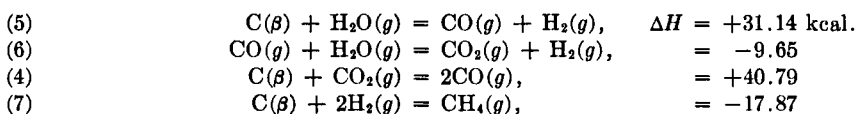
C-O₂



C-CO₂



C-H₂O



C-H₂

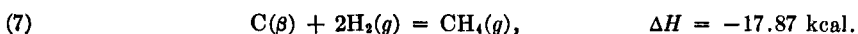


TABLE I
Equilibrium Constants for Gas-Carbon and Associated Reactions

Temperature, °K.	$\log_{10}K_p$						
	1	2	3	4	5	6	7
300	+68.67	+23.93	+44.74	-20.81	-15.86	+4.95	+8.82
400	+51.54	+19.13	+32.41	-13.28	-10.11	+3.17	+5.49
500	+41.26	+16.26	+25.00	-8.74	-6.63	+2.11	+3.43
600	+34.40	+14.34	+20.06	-5.72	-4.29	+1.43	+2.00
700	+29.50	+12.96	+16.54	-3.58	-2.62	+0.96	+0.95
800	+25.83	+11.93	+13.89	-1.97	-1.36	+0.61	+0.15
900	+22.97	+11.13	+11.84	-0.71	-0.37	+0.34	-0.49
1000	+20.68	+10.48	+10.20	+0.28	+0.42	+0.14	-1.01
1100	+18.80	+9.94	+8.86	+1.08	+1.06	-0.02	-1.43
1200	+17.24	+9.50	+7.74	+1.76	+1.60	-0.16	-1.79
1300	+15.92	+9.12	+6.80	+2.32	+2.06	-0.26	-2.10
1400	+14.78	+8.79	+5.99	+2.80	+2.44	-0.36	-2.36
4000	+5.14	+5.84	-0.70	—	—	—	—

B. EQUILIBRIUM CONSTANTS AND PRODUCT-REACTANT RATIOS

Equilibrium constants for the gas-carbon and associated reactions (1) to (7), listed in the previous section, are presented in Table I. The individual concentrations of the species in the equilibrium constants are expressed as partial pressures in atmospheres. From the data (see ref. 2), it is evident that the oxidation of carbon to carbon monoxide and carbon dioxide is not restricted significantly by equilibrium considerations at temperatures even up to 4000° K.

Figures 1 to 3 present calculated equilibrium molar ratios of products to reactants as a function of temperature and total pressure of 1 and 100 atm. for the gas-carbon reactions (4), (7), and (5), (6), (4), (7), respectively. Up to 100 atm. over the temperature range involved, the fugacity coefficients of the gases are close to 1; therefore, pressures can be calculated directly from the equilibrium constant. From Fig. 1, it is seen that at temperatures above 1200°K. and at atmospheric pressure, the conversion of carbon dioxide to carbon monoxide by the reaction $C + CO_2 \rightleftharpoons 2CO$ essentially is unrestricted by equilibrium considerations. At elevated pressures, the possible conversion markedly decreases; hence, high pressure has little utility for this reaction, since increased reaction rate can easily be obtained by increasing reaction temperature. On the other hand, for the reaction $C + 2H_2 \rightleftharpoons CH_4$, the production of methane is seriously limited at one atmosphere pressure and practical operating temperatures, as seen in Fig. 2. Obviously, this reaction must be conducted at elevated pressures to realize a satisfactory yield of methane. For the carbon-steam reaction,

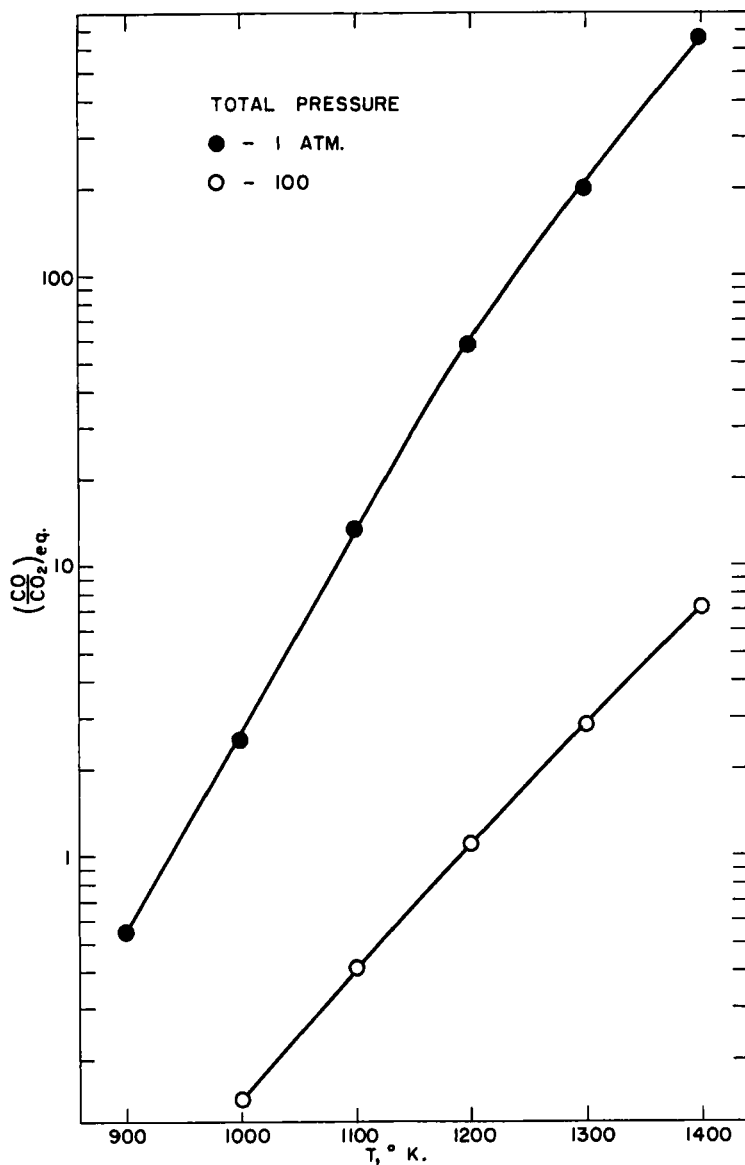


FIG. 1. Equilibrium carbon monoxide-carbon dioxide ratio as a function of temperature and pressure for the reaction $C + CO_2 \rightleftharpoons 2CO$. Perfect gas law assumed.

it is seen in Fig. 3 that the amounts of carbon monoxide and hydrogen which can be produced above 1100° K. up to 100 atm. pressure are essentially equal, even when the possible side reactions are considered. However, as in the carbon-carbon dioxide reaction, the possible extent of con-

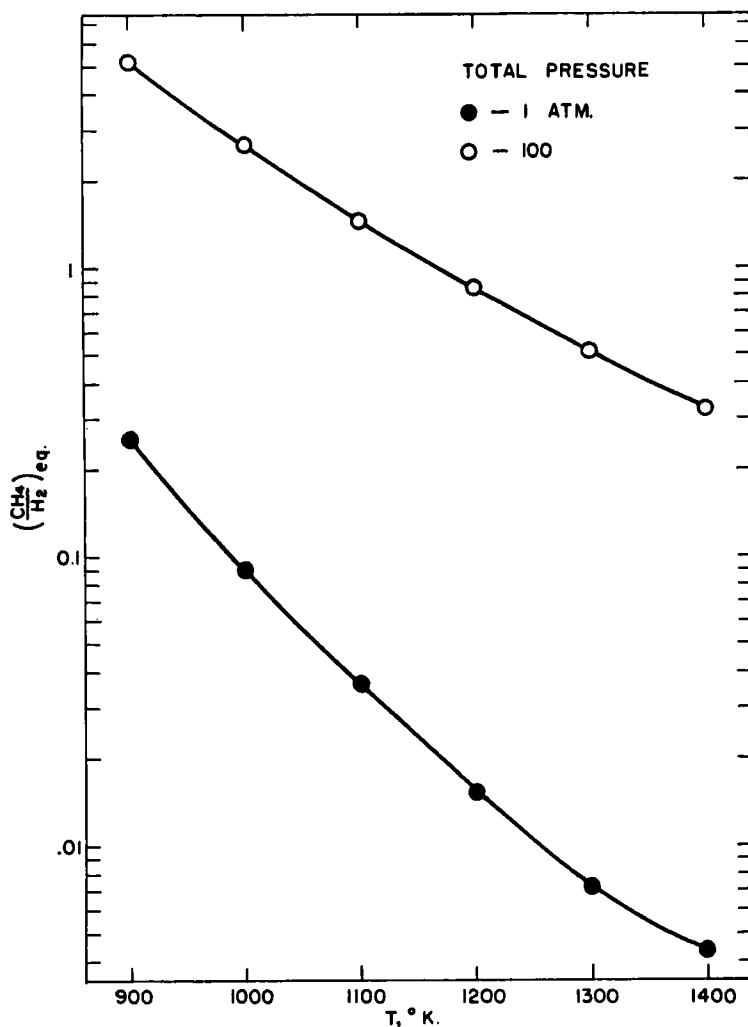


FIG. 2. Equilibrium methane-hydrogen ratio as a function of temperature and pressure for the reaction $C + 2H_2 \rightleftharpoons CH_4$. Perfect gas law assumed.

version of the steam to carbon monoxide and hydrogen decreases with increasing total pressure.

III. Review of General Mechanisms for the Gas-Carbon Reactions

A. GENERAL REMARKS

A large amount of evidence has been accumulated which shows that one of the steps involved in a gas-carbon reaction is the chemisorption of the

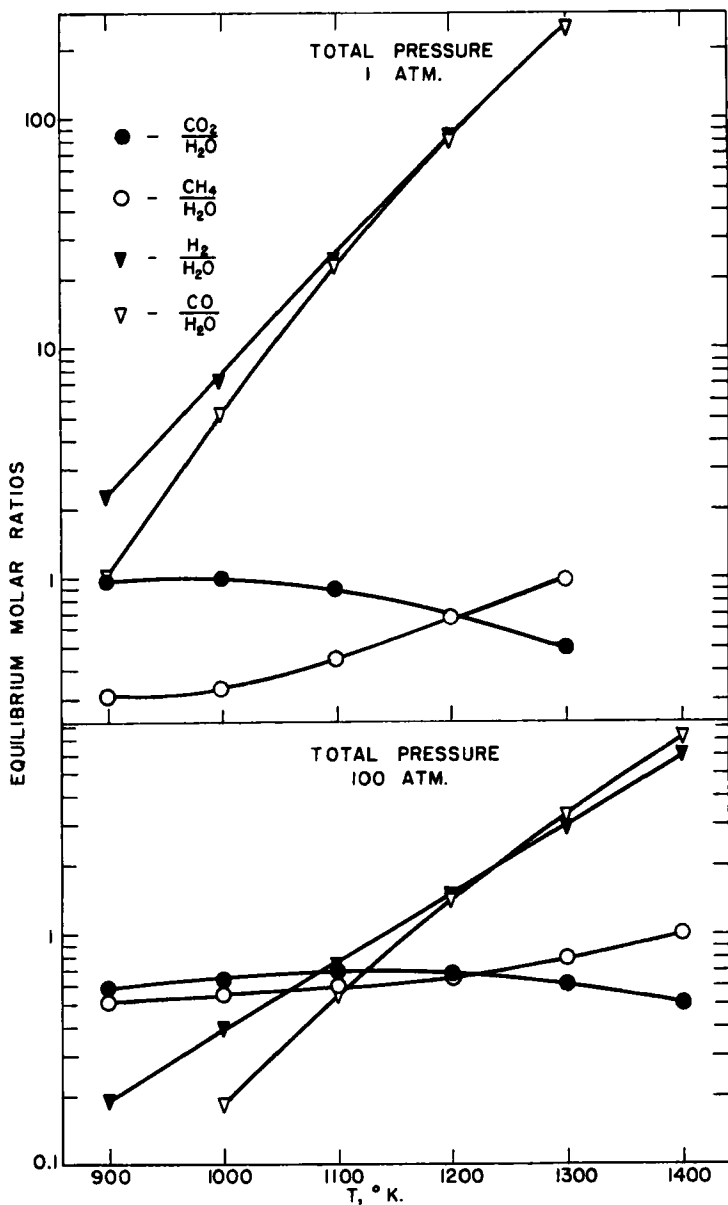


FIG. 3. Equilibrium product-steam ratios as a function of temperature and pressure for the reactions $C + H_2O \rightleftharpoons CO + H_2$, $CO + H_2O \rightleftharpoons CO_2 + H_2$, $C + CO_2 \rightleftharpoons 2CO$, and $C + 2H_2 \rightleftharpoons CH_4$. Perfect gas law assumed.

gas (in whole or in part) on the carbon surface. Further, it is known that some of the products of the gas-carbon reactions chemisorb on the carbon surface under certain conditions. Therefore, an understanding of the chemisorption of gases on carbon is essential to the understanding of the gas-carbon reactions. The modern concepts of chemisorption of gases on solids, including carbon, are reviewed by Trapnell (3).

Briefly, workers are in agreement that the chemisorption of gases on carbon occurs on a relatively small fraction of the total surface. On four amorphous carbons, Loebenstein and Deitz (4) find oxygen to chemisorb on less than 6% of the total surface at 200°. Savage (5) reports that up to 4% of a freshly formed graphite "wear-dust" surface chemisorbs hydrogen and water vapor. Methane is chemisorbed on *ca.* 2% of the surface. Even nitrogen is chemisorbed on *ca.* 0.4% of the surface. No chemisorption of helium or argon is found. Gadsby and co-workers (6) find that only *ca.* 0.5% of a charcoal surface chemisorbs carbon monoxide at 850°. Keifer and Man'ko (7) find that the rate of chemisorption of oxygen (at 182°) and hydrogen (at 485°) by carbons is markedly affected by the type and amount of mineral impurity present.

Zelinski (8) finds that oxygen chemisorbed on artificial graphite imparts either oxidizing or reducing power to the surface, depending upon the adsorption temperature and oxygen pressure. Many workers find that the exposure of carbons to oxygen or carbon dioxide at different temperatures and pressures drastically changes the acid and base-adsorbing power of the surface. Studebaker and co-workers (9), Garten and Weiss (10), and Graham (11) have looked at the nature of carbon-oxygen complexes on carbon surfaces in considerable detail. Probably the major conclusion to be drawn from the numerous findings is that there is more than one type of carbon-oxygen complex which can form on a carbon surface.

Workers find that the chemisorbed oxygen species never can be removed from the carbon surface as such. When the surface is degassed, the oxygen is removed as oxides of carbon. Upon outgassing carbons at elevated temperatures, Anderson and Emmett (12), Carter and Greening (13), and Norton and Marshall (14) find that considerably more carbon monoxide than carbon dioxide is released. The majority of the carbon dioxide is released at temperatures below 600°, and the majority of the carbon monoxide is released at higher temperatures. The workers do find that hydrogen can be desorbed from carbon as such, with the majority of it being released at temperatures above 900°.

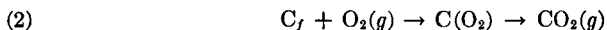
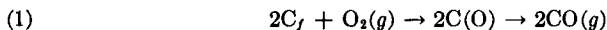
In chemisorption, it is known that the surface atoms must have free valence electrons in order to form strong chemical bonds with gas molecules or atoms. Much recent work (15-18) using electron paramagnetic resonance absorption techniques has confirmed the presence of unpaired

electrons in various types of carbons. Observing the marked effect of exposure of carbon to oxygen on the nature of the resonance absorption, Ingram and Austen (15) conclude that these unpaired electrons are located primarily at, or close to, the carbon surface. Ingram and Austen (15) and Winslow and co-workers (16) find that the number of unpaired electrons is a complex function of carbon heat-treatment temperature, apparently being affected primarily by the number and nature of imperfections in the carbon structure.

It is not surprising that chemisorption experiments have shown the carbon surface to be heterogeneous. In addition to the normal sources of heterogeneity (holes and dislocations in the lattice), carbon is a multi-crystalline material, which means that its surface, in most instances, will be composed of different crystallographic planes. The crystallites in carbon are also of widely varying size, ranging from 10 Å. in some amorphous materials up to thousands of angstroms in natural graphite. The degree of heterogeneity in carbon surfaces will vary depending upon the percentage of different crystallographic planes composing the surface and their size. More will be said about the possible relation between the surface heterogeneity of carbon and its gas reactions later, but it is well to keep this heterogeneity in mind while discussing mechanisms and kinetics.

B. MECHANISMS

1. *Carbon-Oxygen Reaction.* The major question concerning the mechanism of the carbon-oxygen reaction has been whether carbon dioxide is a primary product of the reaction of carbon with oxygen or a secondary product resulting from the gas-phase oxidation of carbon monoxide. The obvious experimental approach to answering this question has been to retard the gas-phase oxidation of carbon monoxide. Mainly, this has been done by three methods: (1) use of low pressures (19-23), (2) use of high gas velocities (24-27), and (3) addition of substances known to inhibit the oxidation of carbon monoxide (24, 28-31). Other workers (32, 33) have conducted the carbon-oxygen reaction at sufficiently low temperatures to be able to assume that the rate of carbon monoxide oxidation is negligible. Almost total agreement has been reached that both carbon monoxide and carbon dioxide are primary products of the oxidation of carbon, or that



where C_f represents a carbon-free site capable of reaction and $C(O)$ and $C(O_2)$ represent a chemisorbed oxygen atom and molecule. Likewise, it is agreed by most workers that the primary CO - CO_2 ratio increases with

increasing reaction temperature. Using a flow method and POCl_3 to inhibit the gas-phase oxidation of carbon monoxide, Arthur (30) determined the CO-CO₂ ratio for two carbons of widely different reactivities at atmospheric pressure in the temperature range 460 to 900°. For these two carbons, he finds that the CO-CO₂ ratio can be expressed as

$$\text{CO}/\text{CO}_2 = 10^{3.4} e^{-12,400/R_g T} \quad (1)$$

over the entire temperature range. Rossberg (32), using two different carbons and thoroughly drying his oxygen to prevent secondary oxidation of carbon monoxide, finds that the temperature dependence of the CO-CO₂ ratio over the temperature range 520 to 1420° is quite similar to that found by Arthur. Arthur and Rossberg feel that the reaction $\text{C} + \text{CO}_2 \rightarrow 2\text{CO}$ is not a factor in affecting the CO-CO₂ ratio even at the highest temperatures which they use. Arthur also states that CO-CO₂ ratios predicted from Equation (1) over the temperature range 900 to 2000° are consistent with the relative rates of formation of these two species observed by other workers (20, 22, 23) in low-pressure experiments at these temperatures.

Lewis and co-workers (33) investigated the oxidation of carbon at a total pressure of 1.1 atm. in a fluidized bed. They confirm that carbon dioxide is a primary product of carbon oxidation, but find that the CO-CO₂ ratio is essentially constant below 520° and is equal to *ca.* 0.3. According to Equation (1), the CO-CO₂ ratio at 520° should be *ca.* 0.9. In agreement with Arthur's findings, Lewis and co-workers report that the CO-CO₂ ratio is relatively independent of the carbon types which they used—hardwood charcoal, metallurgical coke, and natural graphite.

Day (24), studying the carbon-oxygen reaction at atmospheric pressure and high gas velocities, finds the CO-CO₂ ratio to be independent of oxygen concentration in the range of 37 to 99.6 mole % at a total gas velocity of 20,000 ft./min. over the temperature range 1300 to 1900°. He also finds the CO-CO₂ ratio to be independent of gas velocities between 10,000 and 60,000 ft./min. over the same temperature range. At somewhat lower gas velocities (5,000 ft./min., for example), the products leaving the carbon surface are not removed rapidly enough, and gas-phase oxidation of the carbon monoxide is in evidence. Day finds that the type of carbon reacted does affect the CO-CO₂ ratio under otherwise identical conditions. For example, graphitized lampblack-base electrodes have *ca.* a sevenfold smaller CO-CO₂ ratio at comparable temperatures than do the corresponding ungraphitized electrodes. Day finds that the CO-CO₂ ratio increases exponentially with temperature between 1500 and 1900°, but its magnitude is substantially less than that predicted by Equation (1). At 2100°, the maximum CO-CO₂ ratio found is *ca.* 28 compared with a predicted ratio of 123. Day concludes that carbon dioxide is a primary product of carbon oxidation.

Arthur and co-workers (34) have made a study of a number of inhibitors

of the oxidation of carbon monoxide. They find that the best vapor inhibitors are the phosphorus halides and suggest that their main purpose is to remove water molecules from the gas phase. Many workers, including Walker and Wright (35), have shown that water increases the oxidation rate of carbon monoxide. Arthur and Bowring (36) also find that inorganic halides (particularly copper chloride) deposited on carbon markedly increase the CO-CO₂ ratio.

In summary, it is found that

1. Carbon dioxide, as well as carbon monoxide, is a primary product of carbon oxidation.

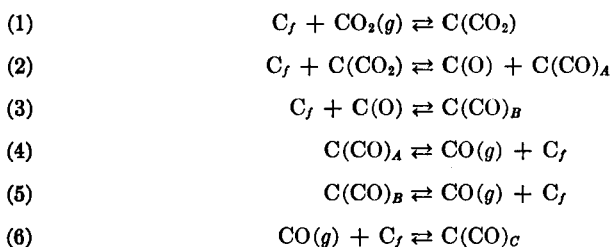
2. The ratio of the primary products, CO/CO₂, generally is found to increase sharply with increasing temperature.

3. It is not well established that the magnitude of the ratio of the primary products is solely a function of temperature and independent of the carbon reacted. Lack of agreement between workers could be caused either by the inability to prevent completely secondary reactions which will change the CO-CO₂ ratio or by actual variations in the primary CO-CO₂ ratio coming from different carbon surfaces.

2. *Carbon-Carbon Dioxide Reaction.* There is general agreement (6, 37-42) that experimental data on the rate of gasification of carbon by carbon dioxide fit an equation of the form

$$\text{Rate} = \frac{k_1 p_{\text{CO}_2}}{1 + k_2 p_{\text{CO}} + k_3 p_{\text{CO}_2}} \quad (2)$$

where p_{CO_2} and p_{CO} are the partial pressures of carbon dioxide and carbon monoxide and the constants k_1 , k_2 , and k_3 are functions of one or more rate constants. There are several hypothetical mechanisms which give the required form of rate Equation (2). A completely general expression is difficult to formulate, but the following steps may be postulated:

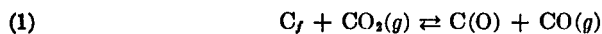


This is analogous to the general scheme used to represent a catalytic reaction:

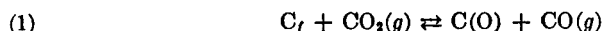


where S represents the catalytic surface, R represents the reactant(s), and P represents the product(s).

To reduce to the simple rate Equation (2), it is necessary that some of the steps in the general scheme occur at a negligible or an extremely fast rate. It has been observed (37) that carbon monoxide gas is an immediate product of the chemisorption of carbon dioxide on carbon and that the adsorption of carbon dioxide is not reversible to give immediate desorption of carbon dioxide. Therefore, it may be assumed that the lives of $C(\text{CO}_2)$ and $C(\text{CO})_A$ are short. Consequently, the general expressions can be simplified to

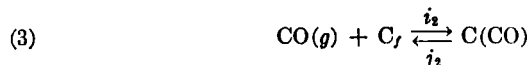
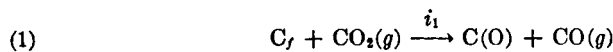


There is the further possibility that the transition $C_f + C(\text{O}) \rightarrow C(\text{CO})_B$ is either slow (Case 1) or fast (Case 2) in comparison with $C(\text{CO})_B \rightarrow \text{CO}(g) + C_f$. The rate expression to be derived is the same in either case, but the interpretation of the individual rate constant, j_3 , in Equation (5) will be different. When Case 1 holds, j_3 represents the rate constant for the surface rearrangement; when Case 2 holds, j_3 represents the rate constant for the desorption of $(\text{CO})_B$. It is not possible, on the basis of present experimental evidence, to decide which case is operative. It is conceivable that each case will be operative but in different temperature ranges. Assuming for the moment that Case 1 holds, the general expressions given above can be simplified to



Equation (2) can now be shown to be consistent with at least two mechanisms where carbon monoxide retards the gasification reaction. Mechanism A applies where the rates of the back reactions of reaction (1) and (2) are negligible.

Mechanism A:



in which i_1 , j_3 , i_2 , and j_2 are the rate constants for these reactions. At steady state, the rates of formation and removal of the surface complexes are equal. If θ_1 and θ_2 are the fractions of the active surface covered by oxygen atoms and by carbon monoxide molecules, respectively, then the relative number of active carbon free sites (C_f) can be expressed as $(1 - \theta_1 - \theta_2)$. Therefore,

$$i_1 p_{\text{CO}_2} (1 - \theta_1 - \theta_2) = j_3 \theta_1 \quad (3)$$

$$i_2 p_{\text{CO}} (1 - \theta_1 - \theta_2) = j_2 \theta_2 \quad (4)$$

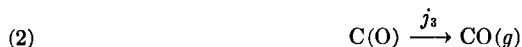
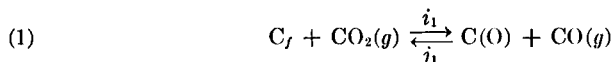
which gives

$$\text{Rate} = j_3 \theta_1 = \frac{i_1 p_{\text{CO}_2}}{1 + \frac{i_2}{j_2} p_{\text{CO}} + \frac{i_1}{j_3} p_{\text{CO}_2}} \quad (5)$$

which is identical to Equation (2), where $k_1 = i_1$, $k_2 = i_2/j_2$, and $k_3 = i_1/j_3$.

Mechanism *B* applies where the rate of the back reaction of reaction (2) is negligible and where reaction (3) is not important.

Mechanism *B*:



Equating the rates of formation and removal of C(O) and again letting θ_1 be the fraction of active surface covered by oxygen atoms,

$$\text{Rate} = j_3 \theta_1 = \frac{i_1 p_{\text{CO}_2}}{1 + \frac{j_1}{j_3} p_{\text{CO}} + \frac{i_1}{j_3} p_{\text{CO}_2}} \quad (6)$$

which is again identical to Equation (2), where $k_1 = i_1$, $k_2 = j_1/j_3$, and $k_3 = i_1/j_3$.

Mechanisms *A* and *B* both state that carbon monoxide retards the gasification of carbon by carbon dioxide by decreasing the fraction of the surface which is covered by oxygen atoms under steady state conditions. In mechanism *A*, θ_1 is decreased by the chemisorption of carbon monoxide by a fraction of the active sites. In mechanism *B*, θ_1 is decreased by the reaction of a portion of the chemisorbed oxygen with gaseous carbon monoxide to produce gaseous carbon dioxide. Reif (37) shows that only one of these reactions can control retardation at one time.

Gadsby and co-workers (6) support mechanism *A* for at least three reasons. First, experiments were performed in which mixtures of carbon

dioxide and carbon monoxide in varying proportions were introduced to charcoal at 750° for a period of 20 min., after which the quantity of oxygen adsorbed on the surface was determined. They report that a wide variation in the final pressure of carbon dioxide was not accompanied by a corresponding change in the amount of oxygen complex adsorbed but followed more closely the smaller variation in the final pressure of carbon monoxide. This led to the conclusion that a large part of the oxygen on the surface at the end of this time interval was probably due to the adsorption of carbon monoxide.

Second, assuming mechanism *B* to be correct, Gadsby and co-workers find an activation energy of -16.8 kcal. for reaction (1) reverse. This they conclude cannot be correct. Third, two of the above authors (43) discuss at length their findings that both carbon monoxide and hydrogen retard the carbon-carbon dioxide reaction but only hydrogen retards the carbon-steam reaction. They argue that the carbon-steam reaction can take place on edge carbon atoms possessing only one unshared electron and that carbon monoxide, which would be expected to chemisorb only on carbon atoms containing two unshared electrons, would not be expected to poison the carbon-steam reaction. On the other hand, it is suggested that the carbon-carbon dioxide reaction takes place on edge carbon atoms containing two unshared electrons; hence, these reacting sites can be blocked by the chemisorption of either carbon monoxide or hydrogen. If retardation in the carbon-steam reaction were occurring by reduction of the surface-oxygen complex, carbon monoxide, as well as hydrogen, should inhibit the reaction. The conclusion is that retardation in both the carbon-steam and carbon-carbon dioxide reaction is by chemisorption.

Reif (37), on the other hand, supports mechanism *B*. He argues that Gadsby *et al.* incorrectly interpret their chemisorption experiments (reason one above) and further states that his own chemisorption experiments for carbon monoxide on a coke surface (37, 44) make mechanism *A* unlikely. Insofar as reason two offered above is concerned, Reif (37) counters with the fact that Wu (40) finds an activation energy of +21.4 kcal. for reaction (1) reverse under mechanism *B*. Reif does not comment on reason three given by Gadsby and co-workers but acknowledges that there is a possibility that the two retarding reactions may be operative for different types of carbon under different conditions of temperature and pressure.

Ergun (45) presents results which very strongly support mechanism *B*. Experiments were conducted in a fluidized bed using three different types of carbon (Ceylon graphite, activated carbon, and activated graphite). These samples had a considerable range of mineral content (from a trace to 0.5%); and although not reported, it is certain that they also had a wide

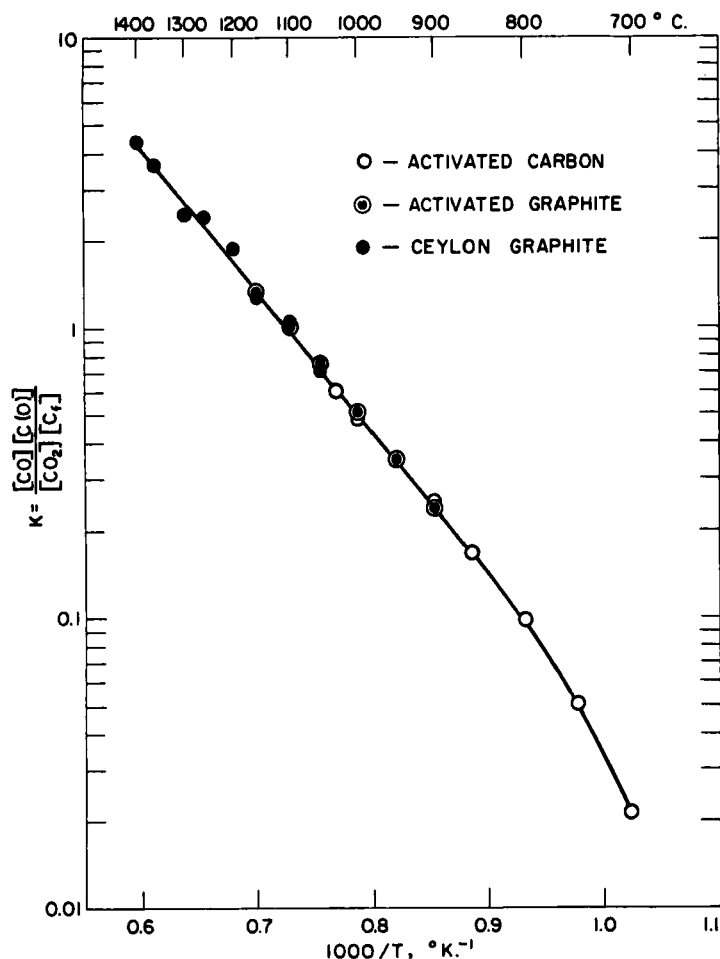


FIG. 4. Equilibrium constant of reaction (1) for mechanism *B* in the carbon-carbon dioxide reaction as a function of temperature. [After S. Ergun, *J. Phys. Chem.* **60**, 480 (1956).]

range of specific surface area. In spite of this, as is shown in Fig. 4, Ergun finds the equilibrium constant for reaction (1) of mechanism *B* to be independent of the carbon used and the reaction to have an average ΔH of +23 kcal./mole over the temperature range 800 to 1400°. Because of its high temperature coefficient, Ergun feels that the equilibrium has a pronounced effect on the rate of gasification. If, for example, in the gas phase, the CO-CO₂ ratio equals 1, the fraction of the total active sites which are

occupied, $C(O)$ in this case, increases from 0.0215 to 0.81 in going from 700 to 1400°. Since the gasification rate is proportional to the number of occupied sites, the effect of the equilibrium constant on the rate is through its influence on the concentration of occupied sites.

Key (46) and Strickland-Constable (47) also support mechanism *B* for the carbon-carbon dioxide reaction. Strickland-Constable concludes from earlier measurements (48) that the rate of adsorption of carbon monoxide on carbon is too low to account for the retardation.

At 450° and a total pressure of 1.1 atm., Paxton (49) finds that for oxygen pressures between 0.21 and 0.5 atm. the reaction rate with carbon monoxide dilution is more than twice that with nitrogen dilution. This finding also appears to support indirectly mechanism *B* for the carbon-carbon dioxide reaction. If chemisorption of carbon monoxide were occurring at a significant rate in Paxton's work, blockage of additional carbon-free sites would occur, which should retard the carbon-oxygen reaction. Instead, the carbon monoxide is presumably removing relatively stable carbon-oxygen complex, which is produced by the product carbon dioxide through the back reaction, as discussed shortly.

Workers have used radioactive carbon, C^{14} , as a tracer to study oxygen and carbon exchange reactions occurring during the over-all gasification of carbon with carbon dioxide. Bonner and Turkevich (50) find that reaction (1) of mechanism *A* and reaction (1) forward of mechanism *B* is rapid on charcoal at temperatures of 735 and 840° and initial carbon dioxide pressures of 180 and 330 mm. Hg. On the other hand, under these conditions they find reaction (2) of both mechanisms to be slow. They confirm that some carbon from the original carbon dioxide has also transferred to the charcoal surface. Brown (51) investigated carbon transfer to the surface of graphite and sugar carbon during their reaction with carbon dioxide. He finds carbon transfer for both materials but states that it is much greater for the sugar carbon. He suggests that when carbon dioxide reacts with a small fraction of the active surface (perhaps 2% of the active surface for the sugar carbon), the carbon dioxide deposits its carbon atom on the surface and its oxygen atoms depart with two new carbon atoms. Orning and Sterling (52) find that the rate of oxygen transfer to a carbon surface depends upon the nature of the solid, presence of catalytic agents, and gas composition. Potassium carbonate, which is known to catalyze carbon gasification, also enhances oxygen transfer to a high temperature coke. Orning and Sterling find the specific radioactivity of the product gas equal to that of the entering gas as long as the temperature is low enough for gasification to be negligible. This indicates that chemisorption of carbon monoxide is also negligible under these conditions.

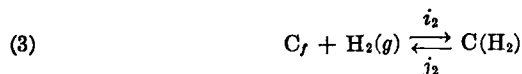
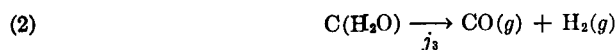
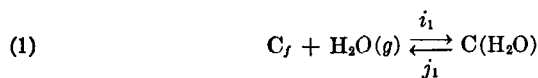
3. *Carbon-Steam Reaction.* There is general agreement (41, 43, 53-55)

that experimental data on the rate of gasification of carbon by steam fit an equation of the form

$$\text{Rate} = \frac{k_1 p_{\text{H}_2\text{O}}}{1 + k_2 p_{\text{H}_2} + k_3 p_{\text{H}_2\text{O}}} \quad (7)$$

where $p_{\text{H}_2\text{O}}$ and p_{H_2} are the partial pressures of steam and hydrogen and the constants k_1 , k_2 , and k_3 are functions of one or more rate constants. The form of this equation is identical to that for the carbon-carbon dioxide reaction.* The mechanism suggested by Gadsby *et al.* (53) and Johnstone *et al.* (54) is as follows:

Mechanism A:



At steady state, the rates of formation and removal of the surface complexes are equal. If θ_3 and θ_4 are the fractions of the active surface covered by water and hydrogen molecules, respectively, then

$$i_1 p_{\text{H}_2\text{O}}(1 - \theta_3 - \theta_4) = j_1 \theta_3 + j_3 \theta_3 \quad (8)$$

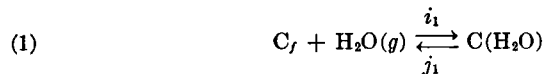
$$i_2 p_{\text{H}_2}(1 - \theta_3 - \theta_4) = j_2 \theta_4 \quad (9)$$

which gives

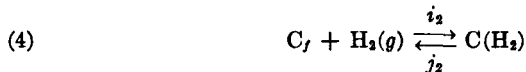
$$\text{Rate} = j_3 \theta_3 = \frac{\frac{i_1 j_3}{j_1 + j_3} p_{\text{H}_2\text{O}}}{1 + \frac{i_2}{j_2} p_{\text{H}_2} + \frac{i_1}{j_1 + j_3} p_{\text{H}_2\text{O}}} \quad (10)$$

If the rate of evaporation of water molecules from the surface is negligible (j_1 is small), $k_1 = i_1$, $k_2 = i_2/j_2$, and $k_3 = i_1/j_3$.

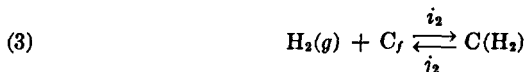
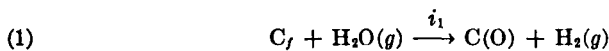
Mechanism A can be written in slightly more detailed form as



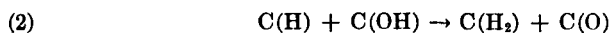
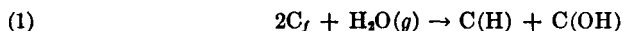
* As in the carbon-carbon dioxide reaction, mechanisms A and B can be treated for the cases where either the surface rearrangement or desorption of the carbon-oxygen complex is the slow step. This has no effect on the discussion except that the significance of the rate constant j_3 in Equation (10) is altered, as previously discussed.



If $j_4 \ll j_3$ and j_1 is small, the correct rate equation may be derived. Alternatively, it is found that if $j_1 \ll j_4$ and $j_3 \ll j_4$, which implies that the surface reaction is fast compared with the desorption of $\text{C}(\text{O})$ as CO , a rate expression identical to Equation (10) is obtained. Under these conditions the mechanism can be expressed more simply by equations similar to those for mechanism *A* of the carbon-carbon dioxide reaction as

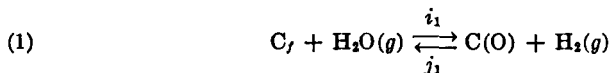


The mechanism of the carbon-steam reaction is discussed in more detail by Long and Sykes (43). They propose that the steam molecule decomposes at the carbon surface into a hydrogen atom and hydroxyl radical both of which chemisorb rapidly on adjacent carbon sites. This is followed by the hydrogen atom on the chemisorbed hydroxyl radical joining the hydrogen atom on the adjacent carbon site and leaving as a hydrogen molecule. Therefore, a further breakdown of the steps in mechanism *A* may be written as



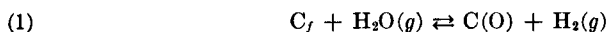
A second mechanism for the carbon-steam reaction, similar to mechanism *B* of the carbon-carbon dioxide reaction, may be operative.

Mechanism *B*:

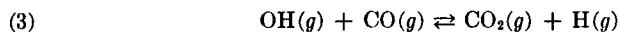
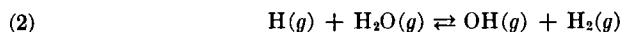


This mechanism also gives Equation (7) directly.

Whereas there has been considerable discussion as to the possibility that the retardation of the carbon-carbon dioxide reaction by carbon monoxide is caused by reduction of the amount of chemisorbed oxygen on the carbon surface, the like possibility for hydrogen retardation in the carbon-steam reaction generally has not been discussed. Reif (57), using Key's suggestion that the carbon-steam reaction follows an analogous reaction mechanism to the carbon-carbon dioxide reaction and noting that the attainment of equilibrium in the water-gas shift reaction is catalyzed by carbon (56, 57), suggests the following equations as part of the carbon-steam reaction



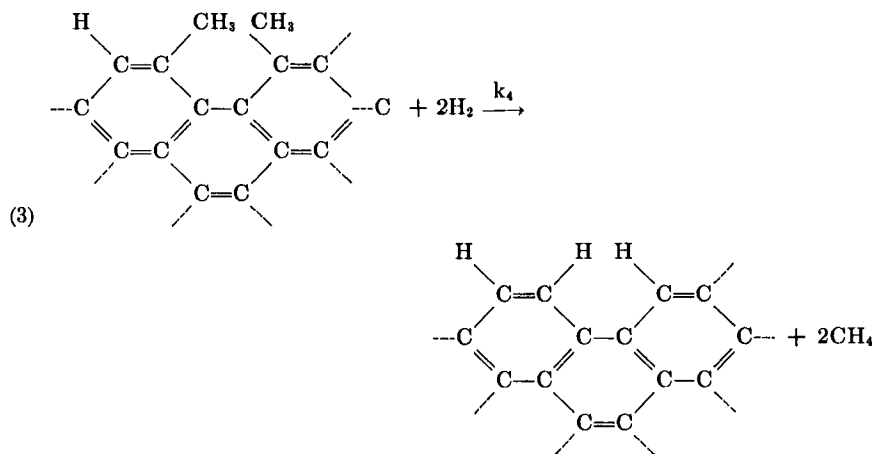
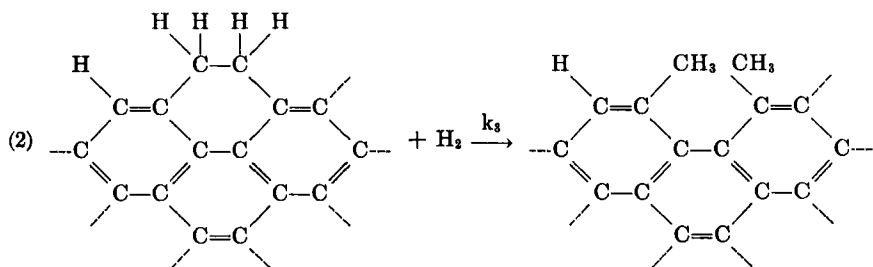
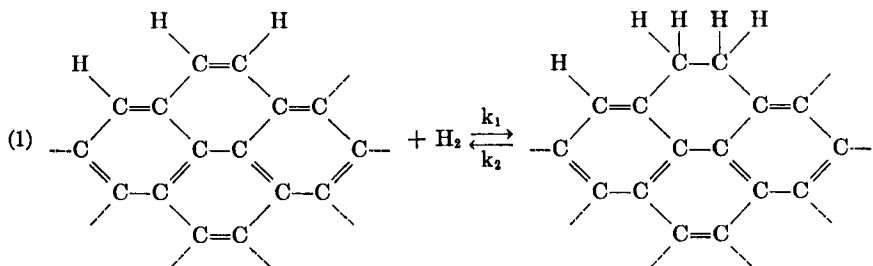
In addition to these reactions causing the rapid attainment of equilibrium in the water-gas shift reaction, they should retard the rate of carbon gasification by reduction of the concentration of chemisorbed oxygen on the carbon surface. However, Gadsby and co-workers (53) find that the addition of carbon monoxide does not inhibit the gasification of carbon with steam other than its resulting in the production of more hydrogen which does inhibit the reaction. Recently, Ingles (58) concludes that a carbon surface accelerates the water-gas shift reaction by acting as a chain initiator to the following reactions



which means that the acceleration of the water-gas shift reaction by carbon and the lack of retardation of the gasification reaction by carbon monoxide (and possibly hydrogen) need not contradict each other.

Strickland-Constable (47), observing that hydrogen is not only strongly but very rapidly adsorbed on carbon, supports the view the hydrogen retardation in the carbon-steam reaction is caused by its chemisorption on active sites.

3. *Carbon-Hydrogen Reaction.* Surprisingly little work has been published on the carbon-hydrogen reaction. Zielke and Gorin (59) investigated the gasification of a low-temperature char in a fluidized bed at temperatures between 810 and 928° and hydrogen pressures of 1 to 30 atm. They propose the following mechanism for the conversion of carbon and hydrogen to methane:



Zielke and Gorin suggest that edge groups $-\text{CH}=\text{CH}-$ are always regenerated by resonance considerations. On the basis of the assumptions that (1) on the average, an equal number of new active sites represented by $-\text{CH}=\text{CH}-$ are regenerated for each one consumed, (2) reaction 3 is rapid compared to reactions 1 and 2, and (3) a steady-state concentration of the product of the forward reaction 1 is established, they state that the rate of methane production is given as

$$\frac{d_{\text{CH}_4}}{dt} = \frac{(k_1 k_3 A)(p_{\text{H}_2})^2}{k_2 + k_3 p_{\text{H}_2}} \quad (11)$$

where A represents the number of active groupings per unit of carbon. However, they do not find that this equation correlates the rate data at 870°. They suggest that this is a result of a conglomeration of different types of carbon reacting at different rates. At 928°, they say that they would expect the carbon to become more uniform and they indeed find that an equation similar to Equation (11) of the form

$$\frac{d_{\text{CH}_4}}{dt} = \frac{a(p_{\text{H}_2})^2}{1 + bp_{\text{H}_2}} \quad (12)$$

does correlate the rate data at 10 and 20 atm. hydrogen pressure at different percentages of carbon gasified. The authors further confirm that methane does not retard the carbon-hydrogen reaction other than through equilibrium considerations.

It is obvious to the writers that much more research must be done on the carbon-hydrogen reaction before it is well understood.

IV. Review of Kinetics for the Gas-Carbon Reactions

A. ORDERS OF REACTIONS

When the rate of a gas-carbon reaction is being controlled solely by the inherent chemical reactivity of the solid (and not in part by mass transport of the reacting gas to the surface of the solid), a relatively simple qualitative discussion of reaction order is possible. For simplicity, the rate of reaction (weight loss of carbon) for the carbon-carbon dioxide, carbon-oxygen, and carbon-steam reactions can be assumed to be determined by the rate of surface rearrangement of the carbon-oxygen complex to a rapidly desorbable product. (The discussion would follow in a similar manner if the rate of reaction was determined by the rate of release of the desorbable product.) If the fraction of the surface covered by a carbon-oxygen complex is θ , the rate of reaction is proportional to the product of θ and a rate constant. At a particular temperature, the order of reaction depends upon the relationship between the change in θ with the change in pressure of the reacting gas. At one extreme, if θ approaches one throughout the range of pressure change investigated, the reaction will be zero order. At the other extreme, if θ is small, the change in θ will be directly proportional to the change in pressure, and the reaction will be first order. At intermediate values of θ , the order of the reaction will vary from zero to one.

The value of θ is a function of the magnitude of the individual rate constants for the formation of the surface complex and its conversion to a desorbable product and the pressure of the reacting gas. If the product of the rate constant for the formation of the surface-oxygen complex and the pressure of the reacting gas is large compared with the rate constant for

the conversion of the surface-oxygen complex to a rapidly desorbable product, $\theta \rightarrow 1$. On the other hand, if the product of the rate constant for the formation of the surface-oxygen complex and the pressure of the reacting gas is small compared with the rate constant for the conversion of the surface-oxygen complex to a rapidly desorbable product, $\theta \rightarrow 0$.

It is apparent that at a particular temperature, where the values of the rate constants for the formation and conversion of the surface-oxygen complex are fixed, the pressure of the reacting gas can affect θ and, hence, the order of the reaction. If the pressure is sufficiently low, the product of the rate constant for the formation of the surface-oxygen complex and the pressure will be small compared with the rate constant for the conversion of the surface-oxygen complex and $\theta \rightarrow 0$. At sufficiently high pressures, $\theta \rightarrow 1$. Therefore, the order of the reaction at a particular temperature can range from zero to one, as the pressure of the reacting gas is decreased over a wide range.

Reaction temperature can also affect the order of a reaction. It is generally agreed that the rate constant for the conversion (or desorption) of the surface-oxygen complex has a higher activation energy than the rate constant for the formation of the complex. Therefore, a reaction which is zero order at low temperatures and a given pressure can become first order at the same pressure and a sufficiently high temperature.

Unfortunately, insofar as a clear understanding of the true orders of gas-carbon reactions is concerned, the problem is made more difficult when the gasification rate is affected by product retardation and by the rate of mass transport of reactants to the surface of the solid. Product retardation can result in the obtaining of orders of reaction which are too low, while mass transport retardation can either raise or lower the apparent order depending upon the true order of reaction and the nature of the mass transport control. In Secs. V and VI, these complicating factors will be discussed in more detail. In the remainder of this Section, pertinent references on the orders of gas-carbon reactions will be given.

1. *Carbon-Carbon Dioxide Reaction.* It is seen from Equation (2) that the carbon-carbon dioxide reaction will be zero order when $k_2 p_{\text{CO}} \ll 1$ and $k_3 p_{\text{CO}_2} \gg 1$. At low temperatures, the production of carbon monoxide is small and the first inequality is satisfied. At high carbon dioxide pressures, the second inequality is satisfied. On the other hand, it is seen from Equation (2) that the carbon-carbon dioxide reaction will be first order when $k_2 p_{\text{CO}} \ll 1$ and $k_3 p_{\text{CO}_2} \ll 1$. These inequalities will be satisfied at low temperatures and low carbon dioxide pressures. Workers have shown (6, 39, 40) that k_2 and k_3 decrease sharply with increasing temperature; therefore, at high temperatures and increasing pressures the inequalities $k_2 p_{\text{CO}} \ll 1$ and $k_3 p_{\text{CO}_2} \ll 1$ still can be found to hold, resulting in a first-order reaction.

Workers reporting orders of reaction for the carbon-carbon dioxide reaction include Graham (41), Strickland-Constable (48), Vulis and Vitman (60), Thring and Price (61), Armington (62), Vastola (63), Duval (64), and Karzhavina (65). As expected, they find reaction orders which vary from zero to one depending upon temperature, pressure, type of carbon reacted, purity of carbon, and geometric dimensions of the sample.

2. *Carbon-Steam Reaction.* The analysis of the order of the carbon-steam reaction as deduced from Equation (7) is identical to that for the carbon-carbon dioxide reaction. Orders ranging from 0 to 1 are expected. As for the carbon-carbon dioxide reaction, it has been shown that k_2 and k_3 in Equation (7) decrease exponentially with temperature (41, 53, 54), resulting in a first-order reaction at sufficiently high temperatures. Batchelder, Busche, and Armstrong (66) have taken the data of Johnstone *et al.* (54) for the variation of k_2 and k_3 with temperature and have shown that at a total pressure of 1 atm., the carbon-steam reaction is expected to be first order above 1370°. Workers reporting on orders of reaction for the carbon-steam reaction include Graham (41), Strickland-Constable (48), Mayers (67), Pilcher, Walker, and Wright (68), Key and Cobb (69), James (70), Goring and co-workers (71), Tuddenham and Hill (72), and Binford and Eyring (73). They find reaction orders varying from 0 to 1.

3. *Carbon-Oxygen Reaction.* Discussion on the reaction orders of the carbon-oxygen reaction was deliberately postponed until after presenting results for the carbon-carbon dioxide and carbon-steam reactions to emphasize the considerable difference in experimental findings between these reactions. The majority of results under varied experimental conditions show the carbon-oxygen reaction to be first order, or close to first order, only. The findings of Strickland-Constable (22), Day (24), Rossberg (32), Lewis *et al.* (33), Armington (62), Mayers (74), Scott and Jones (75), Sihvonen (76), and Chen *et al.* (77) substantiate this statement. From the previous discussion, the implication of the first-order reaction is that under all experimental conditions used by the above authors, the fraction of the total active carbon surface occupied by an oxygen complex at any given instant during the reaction approaches zero.

Two notable exceptions to the carbon-oxygen reaction being first order are found. Gulbransen and Andrew (78), working with spectroscopic graphite, find that at reaction temperatures of 450 and 500° the order is nearly zero at pressures below 0.15 cm. Hg. They do state further that at pressures above 10 cm. Hg the reaction is first order. Blyholder and Eyring (79) reacted extremely thin coatings of graphite, which were supported on a ceramic base, with oxygen at 800° and pressures less than 100 μ Hg. From limited data (at least as presented in the paper), they conclude that the reaction is of zero order. These results are of extreme interest, since they

appear to contradict the reasoning behind the orders of heterogeneous reactions. As was discussed previously, a reaction should become zero order when $\theta \rightarrow 1$. This state should be favored at high reacting pressures, not at the low pressures reported by the above authors. Further, Gulbransen and Andrew's statement that the reaction order increases with increasing pressure is difficult to explain on theoretical grounds. Indeed, their data at 450° over the entire pressure range could be better expressed as a half-order reaction, as pointed out by Blyholder and Eyring (79). The results of the above two groups of workers indicate the necessity of more experimental work being done before the reasons behind orders of reaction for the carbon-oxygen reaction are well understood.

4. *Carbon-Hydrogen Reaction.* Limited data are available on the reaction orders of the carbon-hydrogen reaction. Equation (11) suggests that at low pressures a maximum order of two should be obtained; and at high pressures, the order should go to one. Zielke and Gorin (59) find that at 928°, at hydrogen pressures between 10 and 20 atm., and at 20% carbon gasified, the reaction order is 1.60. Between 20 and 30 atm., the reaction order decreases to 1.27. On some very limited data, Gilliland and Harriott (80) conclude that at low hydrogen pressures and 540° the reaction may be 0.5 order.

B. ACTIVATION ENERGIES OF REACTIONS

It has been popular for workers to determine activation energies for the gas-carbon reactions. However, the correct interpretation of the meaning of the activation energies frequently has not been made. Primarily they have failed to recognize the part which mass-transport resistance can play in affecting the activation energy values. In Secs. V and VI the effect of varying degrees of mass transport control on activation energies will be discussed. At the moment, we are concerned about the values for activation energies of gas-carbon reactions when the rate of reaction is controlled solely by resistance to chemical reactivity.

Wicke and his school (31, 32, 81, 82) have been particularly concerned about the true activation energies for the gas-carbon reactions. Rossberg (32) suggests that the slow step in these reactions is the separation of an oxygen atom from the reactant species. Therefore, he suggests that the activation energies for the different reactions should be related to the energy necessary to dissociate the reacting species. Table II presents a comparison between the dissociation energies of the reactant gas and the true chemical activation energies of the corresponding gas-carbon reactions, which, according to Rossberg (32), confirms the above hypothesis. It would appear inconsistent, however, in light of the previous discussion on orders of reaction, to say that the separation of an oxygen atom from the reac-

TABLE II
Comparison of True Activation Energies in Reactions of Carbon with Oxygen-Containing Gases and the Dissociation Energy of an O Atom from the Reactant (after Rossberg^a)

Reaction	True activation energies, kcal./mole	Dissociation reaction and energy, kcal./mole
$C + CO_2 \rightarrow 2CO$	86	$CO_2 \rightarrow CO + O, \Delta H = +126$
$C + H_2O \rightarrow CO + H_2$	ca. 80	$H_2O \rightarrow H_2 + O, = +116$
$C + \frac{1}{2}O_2 \rightarrow CO$	50-58	$\frac{1}{2}O_2 \rightarrow O, = +59$
$C + N_2O \rightarrow CO + N_2$	40-50	$N_2O \rightarrow N_2 + O, = +39$

^a Rossberg, M., *Z. Elektrochem.* 60: 952 (1956).

tant species need necessarily be the slow step in the over-all gasification reaction. Indeed, at least for the carbon-carbon dioxide and carbon-steam reactions at low temperatures and at pressures not too far removed from atmospheric, the reaction is found to be of zero order. As discussed, the implication of the zero order reaction is that the over-all gasification rate is being controlled by the rate of removal or rearrangement to a desorbable product of the surface-oxygen complex and not by the rate of its formation. Therefore, the activation energy is that for the breakdown of the surface-oxygen complex to release carbon oxides.

Even for the carbon-oxygen reaction proceeding under first order conditions, it is doubtful whether Rossberg's concept has any significance, since it would appear unsound to compare half the dissociation energy of oxygen with the activation energy of the reaction. Clearly, the activation energy will be the same whether the reaction rate is expressed in terms of moles of oxygen or atoms of oxygen reacting per unit time; therefore, the correct dissociation energy for comparison is 118 kcal./mole and not the value of 59 used by Rossberg (unless it is postulated that oxygen chemisorbs in the form of a peroxide structure).

Perhaps a more reasonable explanation for the relative activation energies for the reactions between carbon and the oxygen-containing gases (oxygen, carbon dioxide, and steam) is more in line with the following picture, which has been indirectly suggested in a paper by Long and Sykes (43). For these reactions, the process of going from a reacting gas molecule and a carbon free site to a surface-oxygen complex, $C(O)$, is exothermic. The exothermicity of this process for the carbon-oxygen reaction is estimated to be nearly twice that for the carbon-steam or carbon-carbon dioxide reactions. The magnitude of this excess energy could determine the lifetime of the carbon-oxygen complex on the surface. For the carbon-oxygen reaction, this duration could be relatively small, the surface coverage

in turn small, and the over-all activation energy determined by the adsorption step. For the carbon-steam and carbon-carbon dioxide reactions, this duration could be relatively long, the surface coverage in turn large, and the over-all activation energy determined by the desorption step.* Since it is generally agreed that the desorption of the carbon-oxygen complex has a higher activation energy than the initial adsorption of the complex, the carbon-steam and carbon-carbon dioxide reactions would be expected to have an over-all higher activation energy than the carbon-oxygen reaction. The same reasoning can be extended to the carbon-nitrous oxide reaction if desired. In any event, there appears to be reasonable experimental evidence that the activation energy for the carbon-oxygen reaction is almost always less than that for the carbon-carbon dioxide and carbon-steam reactions. Some particular results on the different gas-carbon reactions can now be considered.

1. *Carbon-Carbon Dioxide Reaction.* It is important to realize that the activation energy determined for the carbon-carbon dioxide reaction need not refer to the same rate-controlling step in every case. In Equation (5), it is seen that at low temperatures and pressures the rate of reaction is proportional to i_1 , the rate constant for the formation of the surface-oxygen complex. At low temperatures and higher pressures, the rate constant is proportional to j_3 , the rate constant for the removal of the surface-oxygen complex. Where none of the terms can be dropped from the denominator of Equation (5), an understanding of the exact physical meaning of an over-all activation energy is made difficult.

Rossberg (32) bases his recommended activation energy of 86 kcal./mole for all carbons undergoing gasification with carbon dioxide in the chemical control region on the experimental findings of Wicke (31), who finds the same activation energy for a high-purity electrode carbon and a medium-purity activated charcoal. Since Wicke's experiments were conducted in a flow system close to atmospheric pressure, the rate-determining step presumably was the desorption of the surface-oxygen complex. Indeed, observing that the frequency factors determined from the reaction rates are not consistent with the concept of activation energies produced by molecules impinging on the surface, Wicke also concludes that desorption from

* In support of the hypothesis regarding the relative lifetime of the carbon-oxygen complexes on the surface for the different reactions, Paxton (49) finds the carbon-oxygen reaction to be accelerated by carbon monoxide. The writers suggest that the addition of carbon monoxide to the incoming oxygen drives the reaction $C(O) + CO(g) \rightleftharpoons CO_2(g) + C_f$ in the forward direction and reduces the extent of surface coverage by the relatively stable carbon-oxygen complex, which is produced by the product carbon dioxide through the back reaction. Other workers who have shown that a stable surface-oxygen complex can retard the carbon-oxygen reaction are Arthur, Newitt, and Raftery (83) and Lambert (84).

the surface, energetically supported by thermal vibrations of the graphite lattice, probably is the rate-determining step. This is important for this means that Wicke's activation energy probably represents the value belonging to j_3 in Equation (5).

Ergun (45) reports the activation energy for the product (j_3)(C_t) for three different types and purities of carbon (Ceylon graphite, activated carbon, and activated graphite), using a fluidizing bed operating close to atmospheric pressure. He finds the same activation energy in each case (59 kcal./mole), and assuming that C_t (the total number of active sites) does not change with temperature, concludes that this is the activation energy for the rate constant j_3 . Within each set of results, both Wicke and Ergun have confirmed that different carbons can have the same activation energy for the carbon-carbon dioxide reaction, but obviously the lack of agreement of the two investigators on the same activation energy still leaves the issue unsettled.

Armington (62) estimates the activation energy for the gasification of a series of graphitized carbon blacks and graphite "wear-dust" at 0.1 atm. carbon dioxide pressure. A zero-order reaction is found for all samples investigated, indicating that the over-all gasification rate is proportional to j_3 . For seven different samples, Armington finds the activation energies to vary from about 73 to 97 kcal./mole, with the arithmetic average being 88 kcal./mole. These values are in considerably better agreement with Wicke's value than with Ergun's value. The range of activation energies found, however, does keep open the question, "In the region of chemical reactivity control, do all carbons have the same over-all activation energy for a given gas-carbon reaction?"

Other workers (67, 85-89) have determined over-all activation energies for the carbon-carbon dioxide reaction, but the values have been affected to some extent by mass-transport control. Workers (6, 39, 40, 41) have also determined activation energies for the individual rate constants in Equation (5) but do not agree on their magnitude. The values of activation energy reported for rate constant i_1 vary from 26.5 (41) to 61.5 kcal./mole (40).

2. *Carbon-Steam Reaction.* The discussion of activation energies for the carbon-steam reaction using Equation (10) is analogous to the prior discussion for the carbon-carbon dioxide reaction using Equation (5). It is not clear from which source Rossberg (32) obtained his recommended activation energy of *ca.* 80 kcal./mole for the carbon-steam reaction. According to Hedden (90), however, recent data on the carbon-steam reaction, using the same experimental arrangement and carbons as used by Wicke (31) on the carbon-carbon dioxide reaction, yield an activation energy of 71 kcal./mole for i_1 in Equation (10). Recently, James (70),

using a flow system and reacting graphite rods with steam close to atmospheric pressure, determined an over-all activation energy of 69 kcal./mole in the chemical control region. Since the reaction was also reported to be of zero order, this should be the activation energy for the rate constant j_3 in Equation (10). Binford and Eyring (73), using a flow system and reacting graphite rods at pressures below 100 μ Hg, report an activation energy of 60 kcal./mole concurrent with a zero order reaction. Again, this activation energy should be for rate constant j_3 in Equation (10).

Other workers (68, 91-93) have determined over-all activation energies for the carbon-steam reaction, which in most cases undoubtedly are low because of some mass-transport control. Again, workers (41, 43, 53, 54) have determined activation energies for the individual rate constants in Equation (10) but do not agree on their magnitude. This apparently is not surprising, for, as Johnstone, Chen, and Scott (54) show, the activation energies even vary with per cent burn-off of the carbon. Long and Sykes (94) investigated the effect of removal of impurities from coconut shell charcoal on the individual rate constants. They find that the activation energy for the step in which adsorbed oxygen atoms are converted to gaseous carbon monoxide is increased from 55 ± 7 to 83 ± 5 kcal./mole upon purification of the charcoal.

3. *Carbon-Oxygen Reaction.* Rossberg (32) apparently bases his recommended activation energy of 50 to 58 kcal./mole on two experiments. Wicke (31), working with the same experimental set-up as used for the carbon-carbon dioxide reaction, reports a value of 58 ± 4 kcal./mole for crushed electrode carbon. Rossberg (32), using spectrographic carbon tubes of apparently the same source as those used by Wicke, finds an activation energy of 49.5 kcal./mole. Rossberg is certain that his lower value is not caused by partial mass-transport control. Actually, upon looking at Rossberg's data, it is seen that his activation energy cannot be reported to an accuracy better than ± 5 kcal./mole, which means that there is little, if any, significant difference between the two above results.

Armington (62), reacting three graphitized carbon blacks and two graphite "wear-dust" samples in 0.1 atm. of oxygen between 550 and 600°, reports activation energies ranging from 46 to 58 kcal./mole. He finds the reaction to be close to first order.

As in the case of the order of reaction, the results of Gulbransen and Andrew (78) and Blyholder and Eyring (79) again are difficult to resolve on the basis of the above data. Both groups have determined activation energies under conditions where mass transport should not affect the results. Gulbransen and Andrew, reacting thin spectroscopic graphite plates between 425 and 575° under 0.1 atm. of oxygen, report an activation energy of 36.7 kcal./mole. They base their value on reaction-rate data at

zero time. Armington (62) finds considerable difficulty in duplicating rate data at extremely low burnoffs ($t \rightarrow 0$) but has little difficulty at burnoffs above 2%, using an apparatus quite similar to that of Gulbransen and Andrew. Using Gulbransen and Andrew's rate data at 425 and 575° after 1-hr. reaction time, the writers calculate a somewhat higher activation energy, *ca.* 40 kcal./mole. Unfortunately, rate data are not available at 575° for longer periods of time.

The writers have found in their laboratory that invariably after a certain burnoff (depending upon the reactor, temperature, and sample), a subsequent extended period of constant reaction rate, expressed in grams of carbon reacting per unit time, is attained. In this burnoff region, there obviously is equilibrium between the rate of formation of the surface-oxygen complex and its removal with a carbon atom. It is felt that this is the reaction rate most characteristic of a given temperature and should be used in kinetic calculations. In principle, Wicke (31) concurs with this reasoning and reports reactivity data only after the sample has attained a total surface area which is virtually constant.

Blyholder and Eyring (79), reacting very thin coatings of spectroscopic graphite, report an activation energy of 80 kcal./mole at pressures below 100 μ Hg and temperatures around 800°. As discussed before, the reaction is reported to be zero order. While the writers do not understand why the order of the reaction is zero, the activation energy is in line with such a value. The zero order is indicative of the building up of a more stable surface-oxygen complex in a manner similar to the carbon-carbon dioxide and carbon-steam reactions. Therefore, the activation energy for Blyholder and Eyring's experiment should be, and is, comparable to that for the gasification reactions.

Other workers reporting activation energies for the carbon-oxygen reaction include Meyer (21), Lewis *et al.* (33), Chen *et al.* (77), Lambert (95), Letort and Magrone (96), Golovina (97), Klibanova and Frank-Kamenetskii (98), and Earp and Hill (99). Activation energies are found to vary from 17 (33) to 100 ± 30 kcal./mole (98). Some of the lower activation energies are influenced by mass transport resistance. Both sets of experimenters who found high activation energies (21, 98) worked at low pressures, as did Blyholder and Eyring (79).

4. *Carbon-Hydrogen Reaction.* Zielke and Gorin (59) determined the activation energy for the reaction of a low temperature char between 810 and 928° at a hydrogen pressure of 30 atm. They find that the activation energy increases from 15 to 48 kcal./mole as the per cent burnoff increases from 0 to 60. They attribute this increase to the heterogeneous char structure approaching that of graphite progressively more closely with increasing burnoff. The possibility that the lower activation energies are in part con-

trolled by mass transport resistance is considered but concluded not to be a factor. Unfortunately, insofar as understanding the activation energy data is concerned, the char had seen a maximum temperature of only 600°, prior to the above runs, which means that a material of different properties was reacted at each temperature.

Gilliland and Harriott (80) investigated the reactivity with hydrogen at one atm. pressure of carbons deposited from hydrocarbons on porous carriers. The porous carrier usually consisted of 28 to 200 mesh silica gel impregnated with nickel. The carbon deposition and subsequent reactivity studies with hydrogen were both carried out in a batch fluidized reactor. In the temperature range 538 to 660°, the activation energy for the reaction of all carbons with hydrogen is found to be roughly the same, 36 ± 6 kcal./mole. The authors also conclude that mass transport resistance is not affecting the gasification rates and, hence, the activation energies.

C. RELATIVE RATES OF GAS-CARBON REACTIONS

Under fixed experimental conditions, the rate of a gas-carbon reaction (rate of removal of carbon atoms from the surface) is dependent upon the reacting gas and the nature of the carbon. A discussion of the effect of the nature of the carbon on particular gas-carbon reactions is postponed until Sec. VII. In this section, existing data on the relative rates of gas-carbon reactions, where an investigator has reacted the same carbon, is presented. Results of primary interest are those where the reaction rates are not affected by mass transport resistance.

Obviously, since the gas-carbon reactions have different activation energies and orders of reaction, the relative rates of these reactions will be a function of the temperature and pressure selected for the correlation. Unfortunately, the authors can find no reactivity data for all four of the gas-carbon reactions using the same carbon. Furthermore, data for even two of the gas-carbon reactions on the same carbon are limited. The available data will be taken and extrapolated, where necessary, to give at least a qualitative idea of relative rates of the gas-carbon reactions at 800° and 0.1 atm. gas pressure. Extrapolation of these relative reactivities to other temperatures and pressures by the reader will require the assumption of activation energies and orders of reaction.

Gadsby and co-workers (53) report that for a coal charcoal, the rate of the carbon-steam reaction is greater by a factor of about three than the carbon-carbon dioxide reaction at 800° and a pressure range of 50 to 500 mm. Hg. The results of Pilcher *et al.* (68) and Walker *et al.* (85), using the same graphitized carbon rods and apparatus, essentially agree with this finding. At 1100°, the former workers report a reaction rate of 1.6 g./hr. at a steam partial pressure of 142 mm. Hg, which can be extrapolated to 4.8

g./hr. at 1 atm. using their experimental order of reaction of 0.66. The latter authors report a reaction rate of 1.7 g./hr. for the carbon-carbon dioxide reaction at 1100° and 1 atm. pressure, giving a ratio of reaction rates of 2.8. The important point to be made from these results is that the rates of the carbon-steam and carbon-carbon dioxide reactions are quite similar.

On the other hand, available data show the rates of the carbon-oxygen and carbon-carbon dioxide reactions to be markedly different. Gulbransen and Andrew (78), reacting spectrographic graphite plates, find reaction rates of 2.5×10^{-8} g./cm.²/sec. at 575° and 0.1 atm. of oxygen and 1.1×10^{-9} g./cm.²/sec. at 900° and 0.1 atm. of carbon dioxide. Using activation energies of 36.7 kcal./mole for the carbon-oxygen reaction (78) and 84 kcal./mole for the carbon-carbon dioxide reaction (62), the ratio of the rates of 800° and 0.1 atm. is calculated to be 6×10^4 .

Wicke (31), reacting spectroscopic electrode carbon at 0.1 atm. reactant pressure, gives the following equations for the rates of the carbon-oxygen and carbon-carbon dioxide reactions

$$\text{Rate}_{\text{C-O}_2} = 2.9 \times 10^9 e^{-58 \pm 4 / R_0 T} \quad (13)$$

$$\text{Rate}_{\text{C-CO}_2} = 2.6 \times 10^9 e^{-85 \pm 3 / R_0 T} \quad (14)$$

where the units are cc. of gas consumed per sq. cm. of surface per sec. If these rates are to be on the basis of weight of carbon consumed and if carbon monoxide is assumed to be the primary product of the carbon-oxygen reaction, the ratio, $\text{rate}_{\text{C-O}_2} / \text{rate}_{\text{C-CO}_2}$, should be multiplied by 2. At 800° and 0.1 atm. pressure, the ratio of the rates is calculated to be 6×10^5 .

Armington (62) reports the reactivity of graphite "wear-dust" to be 4.9×10^{-11} g./cm.²/sec. at 600° and 0.1 atm. of oxygen and 6.2×10^{-12} g./cm.²/sec. at 900° and 0.1 atm. of carbon dioxide. Using his activation energies of 46 and 84 kcal./mole for the carbon-oxygen and carbon-carbon dioxide reactions, the ratio of the rates at 800° and 0.1 atm. is calculated to be 4×10^4 . For a graphitized carbon black (P-33), Armington also reports reaction rates of 1.1×10^{-11} g./cm.²/sec. at 600° and 0.1 atm. of oxygen and 7.3×10^{-13} g./cm.²/sec. at 900° and 0.1 atm. of carbon dioxide. Using his activation energies of 54 and 89 kcal./mole for the carbon-oxygen and carbon-carbon dioxide reactions, the ratio of the rates at 800° and 0.1 atm. is calculated to be 2×10^5 .

No data have come to the authors' attention on a direct comparison of the reaction rates for the carbon-oxygen and carbon-steam reactions.

To the authors' knowledge, the only data available which can relate the relative rate of the carbon-hydrogen reaction to the rates of the above gas-

TABLE III
*Approximate Relative Rates of the Gas-Carbon Reactions at 800° and
 0.1 Atm. Pressure*

Reaction	Relative rates
C-O ₂	1 × 10 ⁵
C-H ₂ O	3
C-CO ₂	1
C-H ₂	3 × 10 ⁻³

carbon reactions are that of Goring and co-workers (71). They present data for the reactivity of a low-temperature char with hydrogen and hydrogen-steam mixtures at 870° and total pressures from 1 to 6 atm. after 10% carbon burnoff. Extrapolation of the data to 0.1 atm. and 870° gives rates of 5.5×10^{-5} and 1.3×10^{-8} g. carbon gasified per g. carbon in reactor per second for steam and hydrogen, respectively. Using activation energies of 69 and 27 kcal./mole for the carbon-steam (70) and carbon-hydrogen reactions (59), the ratio of the rates at 800° and 0.1 atm. is estimated to be 1×10^3 .

Table III presents relative rates for the gas-carbon reactions at 800° and 0.1 atm. based on the experimental data discussed. It is to be emphasized that these are approximate, relative rates. However, it is seen that there is a wide variation possible in the rates of gas-carbon reactions depending upon the reacting gas.

V. Role of Mass Transport in Gas-Carbon Reactions

A. GENERAL REMARKS

Heterogeneous reaction rates involving a porous solid and a gas may be controlled by one or more of three major steps:

1. Mass transport of reacting gas and product or products across a relatively stagnant gas film between the exterior surface of the solid and the main gas stream.

2. Mass transport of the reacting gas from the exterior surface to an active site beneath the surface and mass transport of the products in the opposite direction.

3. Chemisorption of reactant, wholly or in part; a rearrangement of chemisorbed species on the surface to a desorbable product(s); and desorption of product or products from the surface.

It is imperative that anyone attempting to understand the kinetics of the gas-carbon reactions also understand the role which the above steps (separately or in combination) can play in affecting values determined for orders of reaction, activation energies, and reaction rates. In the field of

catalysis, Thiele (100), Wheeler (101, 102), Weisz and Prater (103), and Frank-Kamenetskii (104) have made major contributions to the understanding of the role which steps 2 and 3 jointly play in affecting the kinetics of reactions. In this section, their quantitative concepts will be used and extended in an attempt to clarify the kinetics of gas-carbon reactions.

B. THREE TEMPERATURE ZONES IN GAS-CARBON REACTIONS

Ideally, the variation of reaction rate with temperature for gas-carbon reactions can be divided into three main zones, as shown in Fig. 5 and as previously discussed by Wicke (31) and Rossberg and Wicke (32). In the low-temperature zone, Zone I, the reaction rate is controlled solely by the chemical reactivity of the solid (step 3). The measured or apparent activa-

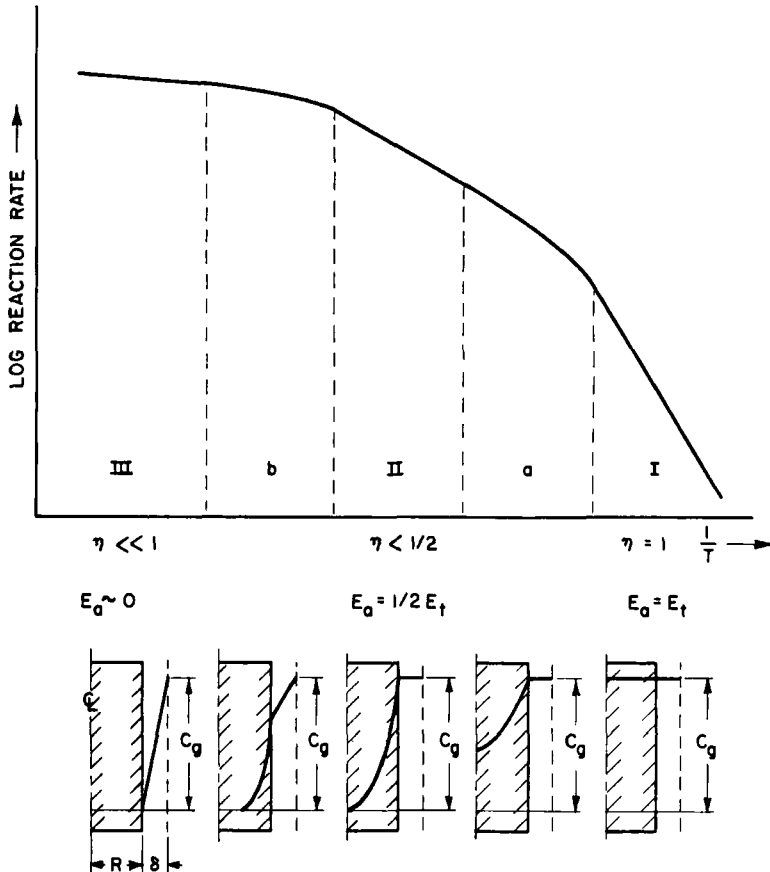


FIG. 5. Ideally, the three zones representing the change of reaction rate of a porous carbon with temperature.

tion energy, E_a , is equal to the true activation energy, E_t . Furthermore η , which is defined as the ratio of the experimental reaction rate to the reaction rate which would be found if the gas concentration were equal to C_g throughout the interior of the sample, virtually equals 1. (Obviously, there must be some concentration gradient of reactant through the sample, even in Zone I; but it is so small that a concentration of C_g can be assumed.) In the intermediate-temperature zone, Zone II, the concentration of the reactant species goes to zero at a distance from the exterior surface less than the radius R . The reaction rate is controlled jointly by steps 2 and 3. Wheeler (101) and Weisz and Prater (103) have shown that the apparent activation energy is one-half of the true activation energy in this zone. Further, η is less than one-half. In the high-temperature zone, Zone III, the concentration of the reactant species goes to a small value at the exterior surface of the solid. (This does not necessarily mean that reaction penetration into the porous carbon is zero.) The reaction rate is controlled by step 1. Increasing temperature affects the reaction rate by determining how much additional reactant can reach the exterior surface per unit time. Since bulk mass transport processes have low activation energies, the apparent activation energies for the gas-carbon reactions in Zone III are also low. Obviously, η is $\ll 1$.

Before discussing in more detail the intermediate and high temperature zones under ideal conditions, it is well to emphasize that in practice there are good reasons why the simplified picture presented in Fig. 5 is not necessarily obeyed:

1. The reactant concentration gradient across the stagnant film thickness, δ , can deviate significantly from zero before the reactant concentration goes to zero in the solid. This results in the disappearance of Zone II and a longer transition region from Zones I to III. This situation is most likely to occur with low gas flow rates past the sample (δ becomes larger) and with small particle sized samples, where the external-surface-area-to-volume ratio becomes large and the possibility of the reactant concentration going to zero in the particle becomes less.

2. The rate controlling part of step 3 (the chemical step) can change with increasing temperature. If, for example, this rate-controlling part of step 3 changes from desorption in Zone I to adsorption in Zone II, the true activation energy for the over-all reaction will have changed. The apparent activation energy in Zone II will correspond to one-half the true activation energy in this zone, which will be different from one-half the true activation energy for Zone I.

3. In Zone I, the concentration of products within the porous solid is negligible and reaction retardation is likewise negligible. In Zone II, the concentration of products within the solid becomes comparable with that

of the reactant, and reaction retardation can become significant. The true activation energy for the over-all reaction rate then becomes a complex mixture of activation energies for different rate constants, as discussed in Sec. III and IV.

C. GENERAL DISCUSSION OF ZONE II FOR THE GAS-CARBON REACTIONS

1. *Relation between True Activation Energy and Apparent Activation Energy Found in Zone II.* It has been shown (101, 103) that the rate of reaction in the diffusion controlled zone is given by

$$\frac{dw}{dt} = C_R^{(m+1)/2} \sqrt{k_v D_{\text{eff}}} \quad (15)$$

where dw/dt is the rate of reaction per unit area of exterior surface, C_R is the reactant gas concentration at the exterior surface of the reacting specimen, k_v is the specific rate constant per unit volume, m is the order of reaction, and D_{eff} is the effective diffusion coefficient through the material. It is of considerable importance to be aware of the assumptions made in this derivation, especially when applied to porous carbons, which have a complicated internal pore structure. It is assumed that all of the pore surface area at a given penetration corresponding to a gas concentration C_r is available for reaction at the concentration C_r . Also, the derivation implicitly assumes that the penetration of gas into porous carbons takes place along a series of pores of varying dimensions and shapes (105), each pore joining into other pores, thus providing a tortuous path to the interior. Statistically, it is assumed that the gas concentration at any depth of penetration into the specimen is constant over the specimen; that is, the gas concentration profile is the same in each series of pores reaching the center of the sample. This will be true if the pores are interconnected at relatively short distances. As discussed in Sec. VI, there is some experimental evidence that this assumption is not justified. The general Equation (15) still holds when applied to any part of the reaction occurring in pores of constant effective diffusion coefficient; but if a unit of exterior surface area is composed of elements of area dA , in which is found a range of effective diffusion coefficients, determined by the pore size in element dA , then Equation (15) becomes

$$\frac{dw}{dt} = C_R^{(m+1)/2} \sqrt{k_v} \int_{A=0}^{A=1} \sqrt{D_{\text{eff}}} dA. \quad (16)$$

Experimental evidence, presented in Sec. VI and elsewhere (31, 106), suggests that after a relatively small burnoff (ca. 5%) the surface area available for reaction and the over-all reaction rate remains virtually constant over a

considerable burnoff range. Further, as discussed in Sec. VI, the specific surface area at any point in the carbon which has undergone the initial burnoff does not vary greatly with reaction temperature. These are additional assumptions made in the derivation of Equation (15), in the case of gas-carbon reactions.

Assuming the change in effective diffusion coefficient with temperature to be small compared with the change of specific rate constant with temperature, Equation (15) may be re-expressed as

$$\frac{\left(\frac{dw}{dt}\right)_2}{\left(\frac{dw}{dt}\right)_1} = \sqrt{\frac{k_2}{k_1}}. \quad (17)$$

Thus, the increase in the over-all reaction rate is proportional to the square root of the specific or true rate constant. Since the apparent activation energy for the reaction is defined by

$$\frac{dw}{dt} = (\text{constant}) e^{-E_a/R_0T} \quad (18)$$

and the true activation energy by

$$k = (\text{constant}) e^{-E_t/R_0T} \quad (19)$$

and since dw/dt is proportional to \sqrt{k} ,

$$\frac{dw}{dt} \propto e^{-E_t/2R_0T} \propto e^{-E_a/R_0T} \quad (20)$$

where $E_a = E_t/2$.

The physical meaning of Equation (17) is simply this: if the specific rate constant goes up, say nine times, because of an increase of temperature, the concentration profile must be steeper in order to diffuse in the extra amount of reactant gas. Consequently, the penetration into the carbon decreases. Obviously, equilibrium is reached when the concentration gradient increases threefold, the penetration distance decreases threefold, and the over-all reaction rate (proportional to k times penetration distance) increases threefold, where 3, in this example, is the square root of the factor of specific-rate-constant increase. For these conditions, the over-all reaction rate has increased threefold, but so has the diffusion gradient; that is, equilibrium has been reached.

2. *Criteria for the Prediction of Gas-Carbon Reactions Entering Zone II.* Thiele (100) has derived equations to predict under what conditions plane or spherical specimens undergoing reaction will enter Zone II. Aris (107) has discussed the effect of specimen shape on the Thiele equations. The au-

thors, using an approach similar to Thiele, derive an equation to be used to determine when cylindrical (rod) specimens undergoing reaction will enter Zone II. Equations pertaining to all three geometric shapes are reviewed and implications of the equations discussed.

Let the reaction be first order, and assume that the specific rate constant and effective diffusion coefficient are constant throughout the rod. It can easily be shown that, for a cylindrical specimen, the differential equation to be solved is

$$\frac{d^2C}{dr^2} + \frac{1}{r} \frac{dC}{dr} + \left(\frac{-k_v}{D_{\text{eff}}} \right) rC = 0 \quad (21)$$

where C is the reactant gas concentration at a penetration r from the center axis of the specimen. This equation can be solved using Bessel functions (as shown in the Appendix). The over-all rate of reaction per unit area of external surface of the rod, dw/dt , is given by

$$\frac{dw}{dt} = D_{\text{eff}} \frac{r}{R} \left(\frac{dC}{dr} \right)_R \quad (22)$$

Therefore, in Zone II, when $\phi > 4$, ($\phi = R\sqrt{k_v/D_{\text{eff}}}$)

$$\frac{dw}{dt} = C_R \sqrt{k_v D_{\text{eff}}} \quad (23)$$

and

$$\eta = 2/\phi \quad (24)$$

where η is the Thiele utilization factor defined as the ratio of the actual rate of reaction to that which would occur if the reacting gas concentration were uniform throughout the material.

The criteria used for the prediction of gas-carbon reactions entering Zone II, for first order reactions, are presented in Table IV, with the results of Thiele (100) for plane and spherical specimens included. Zone II is entered when $\phi > \phi_{\text{II}}$, where ϕ_{II} is the value of ϕ for the start of Zone II and is 2, 4, or 6 for a plane, cylinder, or sphere, respectively. In all cases, the specimens approach uniform internal reaction, that is chemical control, when ϕ is $< ca. 0.2$ or 0.3 ; and in this range, the true activation energy is obtained.

Implications of the equations presented in Table IV can be summarized as follows:

1. A reacting sample will be completely in Zone II when $\phi > \phi_{\text{II}}$. The rate of reaction per unit external surface area in Zone II is given by

$$C_R \sqrt{k_v D_{\text{eff}}} \quad \text{or} \quad C_R \sqrt{k_a S_v D_{\text{eff}}},$$

irrespective of the geometric shape of the sample.

TABLE IV
 Criteria for the Prediction of Gas-Carbon Reactions Entering Zone II for
 Various Geometrically Shaped Samples

Geometric shape	ϕ	η for $\phi > \Delta \phi_{II}$		Rate of reaction per unit area of exterior surface for uniform gas concentration throughout sample	Rate of reaction per unit area of exterior surface when $\phi > \phi_{II}$
		η	ϕ_{II}		
Plane: thickness R	$R\sqrt{k_v/D_{eff}}$	$\frac{1}{\phi}$	2	$k_v C_R R$	$\frac{dw}{dt} = C_R \sqrt{k_v D_{eff}}$
Cylinder: radius R	$R\sqrt{k_v/D_{eff}}$	$\frac{2}{\phi}$	4	$k_v C_R \frac{R}{2}$	$\frac{dw}{dt} = C_R \sqrt{k_v D_{eff}}$
Sphere: radius R	$R\sqrt{k_v/D_{eff}}$	$\frac{3}{\phi}$	6	$k_v C_R \frac{R}{3}$	$\frac{dw}{dt} = C_R \sqrt{k_v D_{eff}}$

2. The transition region between Zones I and II will occur over a temperature range sufficient to increase ϕ by *ca.* 20. Since $\phi = R\sqrt{k_v/D_{eff}}$ and $dw/dt = k_v C_R \frac{R}{n} \eta$,

$$\phi^2 \eta = \frac{Rn}{C_R D_{eff}} \frac{dw}{dt} \quad (25)$$

where $n = 1$ for a plane
 = 2 for a cylinder
 = 3 for a sphere

Thus, $\phi^2 \eta \propto dw/dt$, and since over the transition region ϕ increases by *ca.* 20 while η goes from 1 to $\frac{1}{2}$, the over-all reaction rate, dw/dt , must increase by *ca.* 200 over the transition range. This implies, as discussed by Weisz and Prater (103), that the transition region between Zones I and II can cover a considerable temperature range.

3. Equation (25) can be used to determine whether a reaction is proceeding in Zone I or II. Since Zone I is closely approximated when $\phi < 0.3$ and η is close to 1, if $\phi^2 \eta$ is *<ca.* 0.1, the reaction is in Zone I.* On the other hand, it is easily shown that if $\phi^2 \eta$ is *>2n²*, the reaction is in Zone II.

* This is a more stringent requirement than that given by Weisz and Prater (103) who give $\phi^2 \eta < 1.0$ in the chemical control zone. Weisz (108) later gives the safe limit of Zone I as $\phi^2 \eta < 0.6$ for $\eta \geq 0.95$ (taking into account uncertainty in order of reaction).

4. If the order of the reaction is m , then the formulas given in Table IV are modified as follows:

$$\phi = R \sqrt{(k_v C_R^{m-1})/D_{\text{eff}}} \tag{26}$$

and dw/dt is given by Equation (15).

D. COMPREHENSIVE RATE EQUATIONS COVERING THREE TEMPERATURE ZONES IN GAS-CARBON REACTIONS

When a solid is reacting with a gas stream flowing over its surface and the reaction rate is dependent on the partial pressure of the reacting gas, the over-all picture of the process of reaction may be represented as shown in Fig. 6. The general over-all rate and mass transfer relations can be expressed as follows:

$$\frac{dw}{dt} = \frac{(C_o - C_R)}{\delta} D_{\text{free}} \tag{27}$$

and

$$\frac{dw}{dt} = \frac{R}{n} k_s S_v C_R^m \eta + C_R^m k_s f \tag{28}$$

where dw/dt is the rate of reaction per unit of external surface; D_{free} is the diffusion coefficient of the reactant through the "stagnant film" of thickness δ ; k_s is the rate constant per unit of reacting surface; S_v is the specific internal surface area expressed per unit volume; m is the true order of reaction; $n = 1, 2, 3$, for a plane, cylinder, or sphere, respectively; and f is the roughness factor for the external surface.

The first term on the right-hand side of Equation (28) represents reaction occurring within the solid, while the second term represents reaction occurring on the exposed external face. Since carbons have internal surface

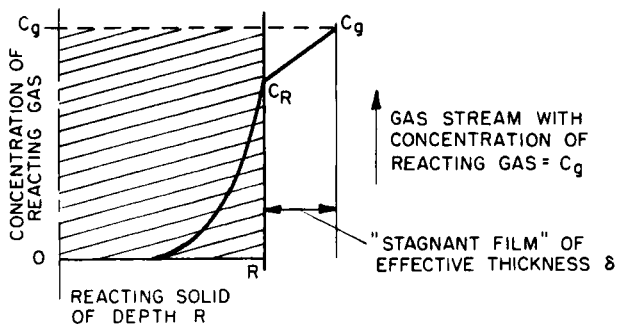


FIG. 6. Illustration of general case of gas-solid reaction.

areas of the order of at least several $\text{m.}^2/\text{cc.}$, while the second term involves an area of only a few $\text{cm.}^2/\text{cc.}$ (unless the solid is in a very finely divided form), the second term can be neglected except at very high rates of reaction and almost zero penetration into the carbon.

If the effect of volume change within the reacting specimen is small, the following formulas represent η to a sufficiently close approximation:

Plane,

$$\eta = \frac{\tanh \phi}{\phi} \quad (29)$$

Rod,

$$\eta = \text{Bessel function of } \phi \text{ (see Appendix)} \quad (30)$$

Sphere,

$$\eta = \frac{3}{\phi} \left(\frac{1}{\tanh \phi} - \frac{1}{\phi} \right) \quad (31)$$

Clearly, the elimination of the unknown concentration C_R between Equations (27), (28), and (29-31) is difficult. However, since the effective diffusion coefficient within the pores of carbon is considerably smaller than the free diffusion coefficient in the stagnant film (109) and since the thickness of the stagnant film is usually much smaller than R , it can be assumed that for large specimens the reaction in the solid will be mainly in Zone II before $(C_o - C_R)$ becomes appreciable. Therefore, at low rates of reaction

$$\frac{dw}{dt} = \frac{R}{n} k_s S_v C_o^m \eta \quad (32)$$

where $\eta \sim 1$ in Zone I and is given by Equations (29-31) in the transition region between Zones I and II.

When the reaction is in Zone II, $\eta = n/\phi$ and Equations (27) and (28) can be expressed as

$$\frac{dw}{dt} = \left(\frac{C_o - C_R}{\delta} \right) D_{\text{free}} = \frac{R}{n} k_s S_v C_R \frac{n}{R \sqrt{(k_s S_v C_R^{m-1})/D_{\text{eff}}}} + C_R^m k_s f \quad (33)$$

or

$$\frac{dw}{dt} = \left(\frac{C_o - C_R}{\delta} \right) D_{\text{free}} = C_R^{(m+1)/2} \sqrt{k_s S_v D_{\text{eff}}} + C_R^m k_s f \quad (34)$$

Eliminating C_R from the three terms in Equation (34) gives

$$\frac{dw}{dt} = \left(C_o - \frac{dw}{dt} \frac{\delta}{D_{\text{free}}} \right)^{(m+1)/2} \sqrt{k_s S_v D_{\text{eff}}} + \left(C_o - \frac{dw}{dt} \frac{\delta}{D_{\text{free}}} \right)^m k_s f \quad (35)$$

At the high temperatures required to enter the stagnant film-controlled zone (Zone III), many reactions will tend to first order. Therefore, substituting $m = 1$ in Equation (35) and rearranging,

$$\frac{dw}{dt} = \frac{C_g}{\frac{1}{\sqrt{k_s S_v D_{\text{eff}}} + k_s f} + \frac{\delta}{D_{\text{free}}}} \quad (36)$$

When reaction occurs at an appreciable penetration into the solid, $k_s f$ is negligible compared with $\sqrt{k_s S_v D_{\text{eff}}}$ and

$$\frac{dw}{dt} = \frac{C_g}{\frac{1}{\sqrt{k_s S_v D_{\text{eff}}}} + \frac{\delta}{D_{\text{free}}}} \quad (37)$$

However, for very high rates of reaction, $\sqrt{k_s S_v D_{\text{eff}}}$ is negligible compared with $k_s f$ and

$$\frac{dw}{dt} = \frac{C_g}{\frac{1}{k_s f} + \frac{\delta}{D_{\text{free}}}} \quad (38)$$

Equation (38) will also apply when the carbon is nonporous, that is, $D_{\text{eff}} = 0$.

As k_s becomes very large, Equations (37) and (38) will give

$$\frac{dw}{dt} = \frac{C_g D_{\text{free}}}{\delta} \quad (39)$$

Equation (39) represents the reaction rate in Zone III. The reaction is clearly first order with respect to the reactant concentration in the main gas stream. This is clearly shown by Day (24) for the carbon-oxygen reaction, as shown in Fig. 7.

Depending on the specific surface area of the carbon and the effective diffusion coefficient of the reactant through the carbon, it is not necessary for the reaction to be represented by Equation (37) going to Equation (36), Equation (36) going to Equation (38), and Equation (38) going to Equation (39) as the rate of reaction increases. In some cases, Equation (37) goes directly to Equation (39) without reaction on the exterior surface area becoming an appreciable rate controlling factor.

E. RATES OF GAS-CARBON REACTIONS IN ZONE III

Using heat transfer data, Rice (110) shows that the film thickness of a fluid flowing over an object can be expressed as

$$\delta = \psi \left(\frac{\mu R}{\rho V} \right)^{0.5} \quad (40)$$

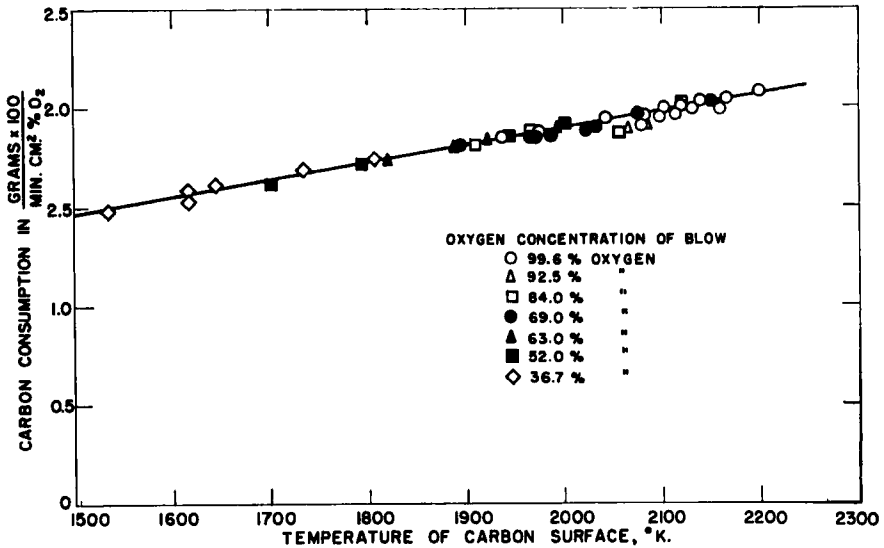


FIG. 7. Illustration of first-order kinetics for the carbon-oxygen reaction in Zone III. [After R. J. Day, Ph.D. Thesis, The Pennsylvania State University, 1949.]

where μ and ρ are the viscosity and density of the fluid, V is the linear flow velocity of fluid over the surface, and R is the radius of the solid. Using this relation and the additional relations, $\mu \propto T^{0.5}$, $\rho \propto T^{-1.0}$, $C_g \propto T^{-1.0}$, and $D_{free} \propto T^{1.75}$, Equation (39) can be expressed as

$$\frac{dw}{dt} \propto \left(\frac{V}{R}\right)^{0.5} \quad (41)$$

which states that the reaction rate is predicted to be independent of temperature. Actually, there is some doubt as to the variation of viscosity and diffusivity with temperature; but in any case, the reaction rate in Zone III varies only slightly with temperature.

Many workers have attempted to confirm the variation of reaction rate for the carbon-oxygen reaction with linear gas flow rate, as expressed by Equation (41). Parker and Hottel (111), reacting brush carbon with air at 1227°, find the rate varies with the 0.37 power of velocity. Mayers (112), using 40- by 60-mesh coke in 1-in. high beds, obtains a value of 0.5 for the exponent; Chukhanov and Karzhavina (113), in their high-velocity experiments using beds of particles 3 by 5.5 mm. in diameter, find a value of 0.4; Kuchta and co-workers (114), using carbon rods, report an exponent of 0.45; Day (24), using carbon and graphite rods, reports a value of 0.5; and Tu *et al.* (115) report a value of 0.49. Graham *et al.* (116), studying the variation in reaction rate of the carbon-steam reaction under high ve-

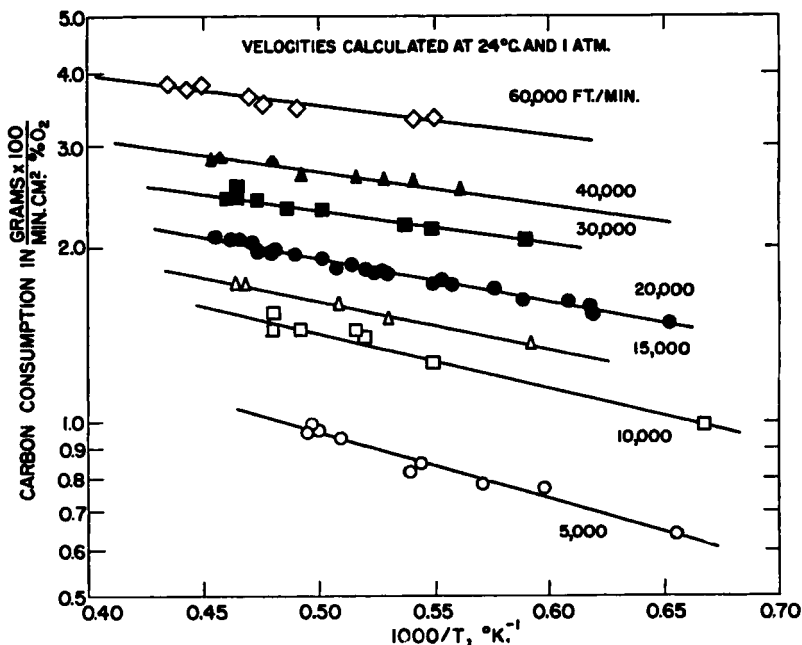


FIG. 8. Arrhenius plots for the carbon-oxygen reaction at different linear gas velocities in Zone III. [After R. J. Day, Ph.D. Thesis, The Pennsylvania State University, 1949.]

locity conditions, find that the rate varies with the power of velocity ranging from 0.23 to 0.33. They conclude that when the power is less than 0.5, the reaction is not in Zone III but is in the transition region.

Day (24), who apparently is completely in Zone III for his studies on the carbon-oxygen reaction, confirms the small dependence of reaction rate on temperature, as shown in Fig. 8. Between 1227 and 2027°, the activation energy is less than 8 kcal./mole at all flow velocities used.

For a particular gas-carbon reaction, Equation (39), with one reservation, leads to the conclusion that under identical reaction conditions (i.e., C_o , D_{free} , and δ are constant), the rate of reaction in Zone III is independent of the type of carbon reacted. The reservation is that in the carbon-oxygen reaction, the nature of the carbon may affect the CO-CO₂ ratio leaving the surface and hence the reaction rate per unit of oxygen diffusing to the surface. Unfortunately, little data are available on reactivities of different carbons where the reaction has been conducted completely in Zone III. Day (24) reports that the reaction rates of petroleum coke, graphitized lamp-black, and graphitized anthracite rods agree within 12% at a temperature of 1827° and at a constant gas velocity.

For reaction at the same temperature, it is of interest to predict the relative rates of the different gas-carbon reactions in Zone III, when using a sample of fixed dimensions, a constant linear gas velocity, and a fixed concentration of reacting gas in the main stream.* Under these conditions, Equation (39) can be expressed as

$$\frac{dw}{dt} \propto \frac{nD_{\text{free}}}{(\mu/\rho)^{0.5}} \quad (42)$$

where $n = 1$ for the carbon-carbon dioxide and carbon-steam reactions and $n = 2$ for the carbon-oxygen reaction. The relative value of n is based on the assumption that at the high temperatures encountered in Zone III, the CO-CO₂ primary product ratio for the carbon-oxygen reaction becomes large (30). Consequently, each molecule of oxygen reaching the surface will result in the gasification of *ca.* two carbon atoms, whereas each molecule of carbon dioxide or steam reaching the surface will result in the gasification of one carbon atom.

To simplify the calculation of relative values of D_{free} , μ , and ρ for the gas in the stagnant film, the following average gas compositions in the film are assumed:

C-O₂ : 34% O₂, 66% CO

C-CO₂ : 34% CO₂, 66% CO

C-H₂O : 34% H₂O, 33% H₂, 33% CO

Relative diffusivities for the mixtures are calculated assuming

$$D_{\text{free}} \propto M^{-0.5}$$

Relative viscosities are calculated from viscosities for the individual components at 0° (117), weighting them on a mole fraction basis. The change in diffusivities and viscosities with temperature and pressure is assumed to be independent of gas mixture. If desired, more accurate calculations of diffusivities and viscosities of gas mixtures can be made using the approaches of Wilke (118) and Bromley and Wilke (119), respectively. Table V presents relative values for D_{free} , μ , and ρ across the stagnant film for the gas-carbon reactions. Substituting these values in Equation (42), the relative reaction rates in Zone III for the gas-carbon reactions are calculated and also presented in Table V. Qualitatively, the rates of the carbon-oxygen and carbon-steam reactions are predicted to be about twice the rate

* The reaction $C + 2H_2 \rightarrow CH_4$ is not included in this consideration because, as discussed in Sec. II, at high temperatures and atmospheric pressure, equilibrium greatly restricts this gasification reaction. That is, C_R never approaches zero and, to the contrary, approaches C_G closely. This means that the concentration gradient across the stagnant film is small and dw/dt is correspondingly small.

TABLE V
Predicted Relative Rates of Carbon Gasification in Reaction Zone III for Similar Shapes of Carbon Specimens and Constant Linear Gas Flow Rate

Reaction	Relative physical data across stagnant film			Relative reaction rate in Zone III
	D_{free}	μ	ρ	
C-O ₂	1	1	1	2.0
C-CO ₂	0.9	0.9	1.2	1.0
C-H ₂ O	1.9	0.6	0.6	1.9

of the carbon-carbon dioxide reaction. The rate of the carbon-oxygen reaction is high because of the removal of *ca.* two carbon atoms from the surface for each molecule of reacting gas. The rate of the carbon-steam reaction is high because of the relatively high diffusivity value for the steam molecule across the stagnant film.

Figure 9 graphically shows the marked effect which temperature level is

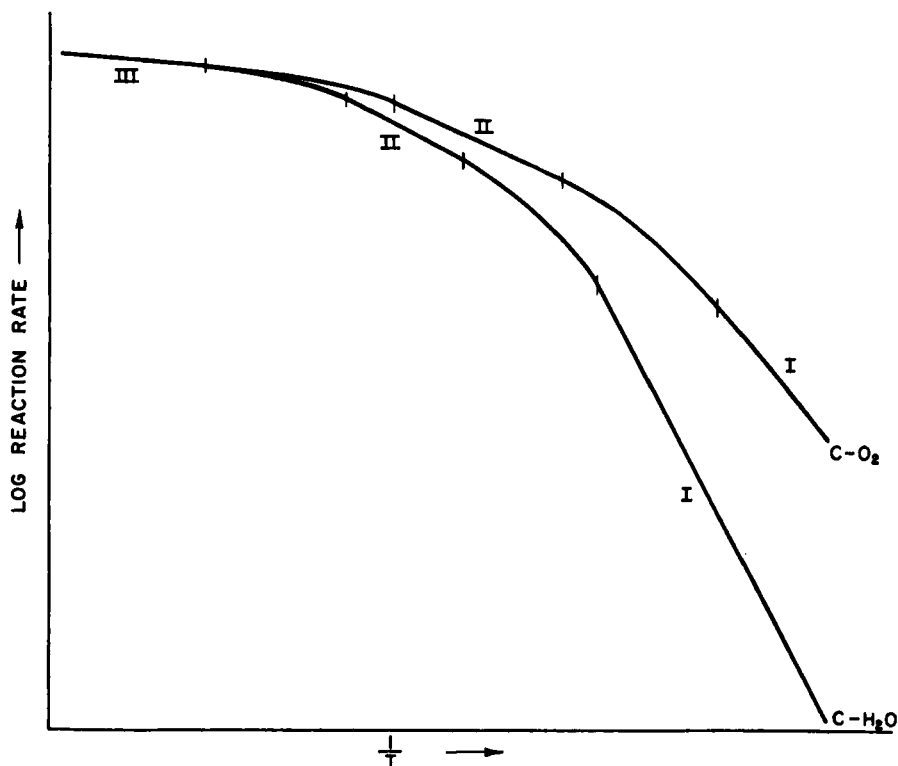


FIG. 9. Ideally, the predicted variation in the relative rates of the carbon-oxygen and carbon-steam reactions with temperature for a porous carbon.

expected to have on the relative rates of the carbon-oxygen and carbon-steam reactions. At low temperatures, in Zone I, as discussed in Sec. IV, the carbon-oxygen reaction is many times more rapid than the carbon-steam reaction. Because of the higher true activation energy of the carbon-steam reaction and the higher temperature at which this reaction enters the comparable temperature zones, this difference in reaction rates rapidly decreases. Finally in line with the prediction presented in Table V, the reaction rates for these two reactions should be quite comparable in Zone III.

VI. Use of Density and Area Profiles on Reacted Carbon Rods for Better Understanding of Gas-Carbon Reactions

A. INTRODUCTION

The availability of data on the change in physical structure of carbons after different degrees of burnoff at different temperatures can aid in the understanding of gas-carbon reactions. In the broadest sense, use of profile data after fractional burnoff enables a clear determination to be made of the temperature zone in which the reaction has occurred, as follows:

1. If the density profile is uniform through the sample, the reaction occurred in Zone I.
2. If the density at some depth into the sample equals the starting density, the reaction occurred in Zone II or III.

Petersen (87, 120) discusses the use of profile data to understand better the mechanism of the carbon-carbon dioxide reaction. He reacted $\frac{1}{2}$ -in. diameter rod samples in an apparatus previously described (85). Profile data were determined on the reacted rods as follows: A $\frac{1}{8}$ -in. hole was drilled through the center of the rod prior to placing it on an ordinary screw-cutting engine lathe. Following incremental cuts of approximately 0.25 mm. from the exterior surface, the rod was removed from the lathe and weighed, and its diameter was determined by a micrometer caliper. For each cut, the apparent density of the material removed was calculated from the weight loss and volume of carbon removed.

Profile data reported in this section were determined in a similar way, following reaction of spectroscopic carbon rods (National Carbon's L113SP) with carbon dioxide in the apparatus previously described (85). Briefly, the apparatus consisted of a vertical mullite reactor tube $1\frac{1}{2}$ -in. i.d. Carbon samples 2 in. long by $\frac{1}{2}$ in. in diameter with a $\frac{1}{8}$ -in. hole through their center (the rods weighing *ca.* 8.8 g.) were suspended in the reactor by connecting them through a $\frac{1}{8}$ -in. mullite rod to a balance. Reaction at the top and bottom of the carbon rods was minimized by $\frac{1}{2}$ -in. diameter mullite plates. Following reaction to *ca.* 11% burnoff (1 g.) at temperatures of 925, 1000, 1200, and 1305°, density and surface area profile data were determined. The area data were determined in a conventional

B.E.T. apparatus (121), using nitrogen as the adsorbate at liquid nitrogen temperatures. Reactivity data were also determined at a number of other temperatures between 900 and 1350°, but subsequent profile data are lacking.

The experimental results obtained from the measurement of surface area remaining after each lathe cut can be plotted as cumulative surface area against radius. If S_r' is the surface area per cm. of radial distance at radius r , the cumulative surface area is given by

$$S_c = \int_{r_1}^{r_2} S_r' dr \quad (43)$$

If S_r is the specific surface area at r in $\text{cm.}^2/\text{cc.}$, $S_r' = S_r(r/R)A$, where A is the external surface area of the rod (excluding the ends) in cm.^2 and R is the external radius. Therefore,

$$\frac{dS_c}{dr} = S_r \frac{r}{R} A \quad (44)$$

or

$$S_r = \left(\frac{dS_c}{dr} \right)_r \frac{R}{rA} \quad (45)$$

Thus, the specific surface area at any radius in the rod can be estimated from the dimensions of the rod and the slopes of the cumulative surface area curve.

In a similar manner, the porosity at any radius in the rod can be estimated from the corresponding slopes of the curve of cumulative weight *vs.* radius by the equation

$$\rho_r = \left(\frac{dw_c}{dr} \right)_r \frac{R}{rA} \quad (46)$$

where ρ_r is the apparent density of the carbon at r and w_c is the cumulative weight. Then

$$\Theta_r = 1 - \frac{\rho_r}{\rho_t} \quad (47)$$

where Θ_r is the porosity of the carbon at r and ρ_t is the true density of carbon, which, in this case, equals 2.268 g./cc.

B. USE OF DENSITY PROFILE DATA TO DETERMINE RATE OF REACTION AT ANY RADIUS IN THE CARBON ROD

The most accurate way to obtain the rate of reaction at any radius in the rod would be to react a series of identical rods under identical conditions to different burnoffs, followed by the cutting of each rod as described. The

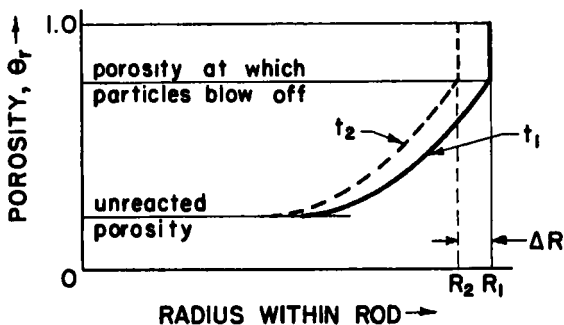


FIG. 10. Illustration of the porosity profile through a rod at two times, t_1 and t_2 , when reaction is occurring at a constant rate in temperature Zone II.

rate of reaction, $(dn/dt)_r$, at any radius could then be estimated from the changes in porosity with time. This would be a tedious process. In this study, $(dn/dt)_r$ is determined more simply and probably about as accurately by an alternative method.

At sufficiently high temperatures, the reaction in the rod will proceed so fast that the carbon dioxide concentration will be zero at some point in the rod (Zone II). After an initial burnoff, the porosity at the surface will reach a value at which the carbon no longer has sufficient structural strength to remain attached to the rod. Carbon then will be lost by particles blowing off in the reacting gas stream. When this point is reached, it is obvious by intuition that the rate of reaction will be constant for a small decrease in external radius; and the profile functions through the rod will be duplicated after a time interval Δt but moved in a radius ΔR (equilibrium burning). The condition of the rod at two different times is illustrated in Fig. 10. Clearly, the over-all rate of reaction per cm^2 of external surface b is given by

$$b = \frac{\Delta R}{\Delta t} \rho_u \tag{48}$$

where ρ_u is the apparent density of the unreacted carbon and b is constant for a small change in external surface area. Considering 1 cm^2 of external rod surface,

$$\left(\frac{dn}{dt}\right)_r = \left(\frac{d\theta}{dt}\right)_r \frac{r}{R} \rho_t \tag{49}$$

but

$$\frac{d\theta}{dt} = \frac{d\theta}{dr} \frac{dr}{dt}$$

Therefore,

$$\left(\frac{dn}{dt}\right)_r = \left(\frac{d\theta}{dr}\right)_r \frac{r}{R} \frac{\rho_t}{\rho_u} b \quad (50)$$

Determination of $(dn/dt)_r$ is possible, since $(d\theta/dr)_r$ can be found from the slope of the θ vs. r plot and b can be found from the experimental reactivity curve. It should be noted that $(dn/dt)_r$ is the rate of reaction per cm. thickness of section, whereas the actual rate of reaction in an infinitesimal section of thickness dr is $(dn/dt)_r dr$.

From profile data to be discussed shortly, it was found that Zone II was approximated only at reaction temperatures of 1305° and higher. The overall rate of reaction curve for this temperature is given in Fig. 11. If it is assumed that the abrupt change in reaction rate after 4-min. reaction time occurs at the onset of equilibrium burning, the measured decrease in external radius of the rod can be assumed to have occurred between 4 and 8 min., and b can be calculated. The value of b is found to agree well with the rate calculated from Fig. 11.

It is of interest to note that several workers (99, 116) have assumed $\Delta R/\Delta t$ to represent the rate of reaction of a carbon specimen only when the reaction is proceeding entirely on the external surface. The above reasoning shows that $\Delta R/\Delta t$ can be a constant and represent the over-all rate of reaction when the reaction is occurring internally and the utilized surface area is far greater than the external surface area. Graham and co-workers (116), studying the carbon-steam reaction under high-velocity conditions,

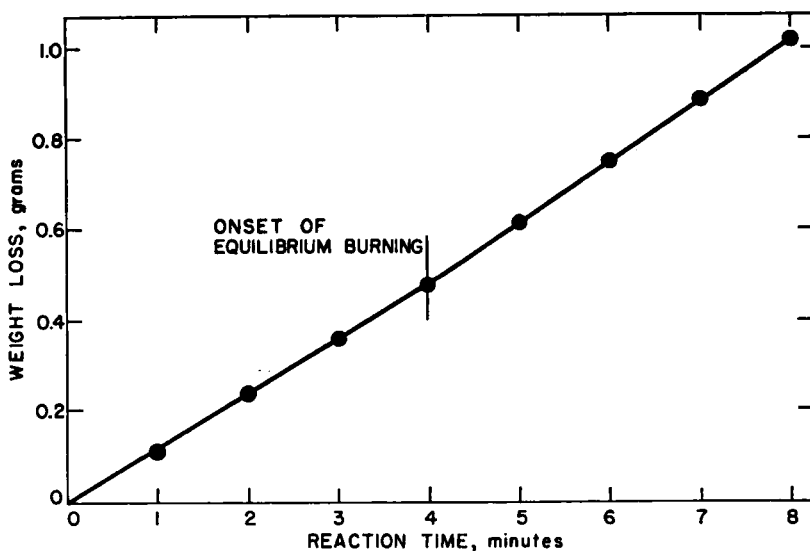


FIG. 11. Plot of weight loss vs. time for reaction of spectroscopic carbon rod with carbon dioxide at 1305° (Zone II) to 11% burnoff.

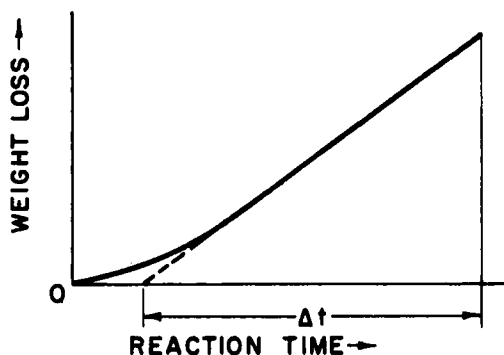


FIG. 12. Typical plot of weight loss vs. time for reaction of spectroscopic carbon rod with carbon dioxide at temperatures below Zone II.

determine reaction rates from the change in external sample radius with time, using Equation (48). On the assumption that Equation (48) holds only when reaction takes place solely on the exterior surface, they calculate reaction probabilities, which they acknowledge to be about a thousandfold too high on the basis of other workers' findings. Since they report that their reactant concentration at the exterior surface of the carbon does not go to zero but only to *ca.* $C_0/2$, there is no doubt that some internal reaction is occurring. Using the formulas developed in Sec. V to estimate the degree of internal reaction and the true surface area undergoing reaction, reaction probabilities some thousandfold lower are calculated, in agreement with accepted values.

At temperatures below Zone II, equilibrium burning (as illustrated in Fig. 10) obviously is not obtained. It is found, however, that after some burnoff (usually less than 5%) the reaction rate is essentially constant over a wide burnoff range. A typical reactivity plot is shown in Fig. 12. If it is assumed that the porosity measured at the close of the run is derived from uniform burning over time Δt , then

$$\left(\frac{dn}{dt}\right)_r = \frac{\Delta\theta_r}{\Delta t} \frac{r}{R} \rho_t \quad (51)$$

where $\Delta\theta_r$ is the increase in porosity above the unreacted porosity at r . This estimation can only be used where the rate of reaction has been constant over most of the reaction time.

C. MASS TRANSPORT AND REACTANT CONCENTRATION PROFILES THROUGH THE ROD

From a knowledge of the rates of reaction through the rod and the effective diffusion coefficient at any radius, it is possible to determine the con-

centration profile through the rod without making any assumptions regarding the order of the reaction or the surface areas taking part in the reaction. Three limiting cases are possible depending on the manner in which mass transport is occurring through the rod. Equations for the three cases for the carbon-carbon dioxide reaction are derived in the Appendix and presented below.

1. Knudsen diffusion only is occurring (Case 1):

$$C_r - C_0 = \int_0^r \frac{f(r)}{(D_{\text{eff}})_r} \frac{R}{r} dr \quad (52)$$

where

$$f(r) = \int_0^r \left(\frac{dn}{dt} \right)_r dr.$$

At high rates of reaction, the reactant concentration in the center of the specimen, C_0 , approaches zero closely.

2. Bulk diffusion occurring but pores too fine to allow Poiseuille flow (Case 2):

$$C_r = (\rho + C_r) - \frac{(\rho + C_r - LC_r)}{\text{antilog} \left[\frac{F(r)}{2.3\rho} \right]} \quad (53)$$

where $C_0/C_R = L$, $\rho = C_R + C_R'$ in g. of carbon per cc. of gas, and

$$F(r) = \int_0^r \frac{f(r)}{(D'_{\text{eff}})_r} \frac{R}{r} dr$$

[see Appendix for definition of $(D'_{\text{eff}})_r$]. C_R' is the concentration of carbon monoxide at the surface. When the reaction is not in the stagnant film-controlled zone, $C_R = \rho$; and at sufficiently high reaction rates, $L \simeq 0$. Therefore, Equation (53) can be simplified to

$$C_r = 2C_R(1 - e^{-F(r)/C_R}) \quad (54)$$

3. Bulk diffusion occurring with a maximum of Poiseuille flow under conditions where $C_0 \simeq 0$ and $\rho = C_R$ (Case 3):

$$C_r = C_R(e^{F(r)/C_R} - 1) \quad (55)$$

where

$$F(r) = \int_0^r \frac{f(r)}{(D_{\text{eff}})_r} \frac{R}{r} dr$$

D. DISCUSSION OF EXPERIMENTAL RESULTS

1. *Density and Area Profiles.* Figure 13 presents porosity profiles for the original carbon rod and for the carbon rods after reaction to *ca.* 11% burn-off at four different temperatures. The samples could only be cut down to a radius of *ca.* 0.35 cm. Attempts at cutting to a smaller radius resulted in breaking through the thin carbon wall. The porosity point at *ca.* 0.25 cm. represents the mean porosity of the carbon remaining after the last cut. At 1305°, reaction occurred at a considerable penetration into the rod, even though equilibrium burning was obtained. Reaction was effectively zero

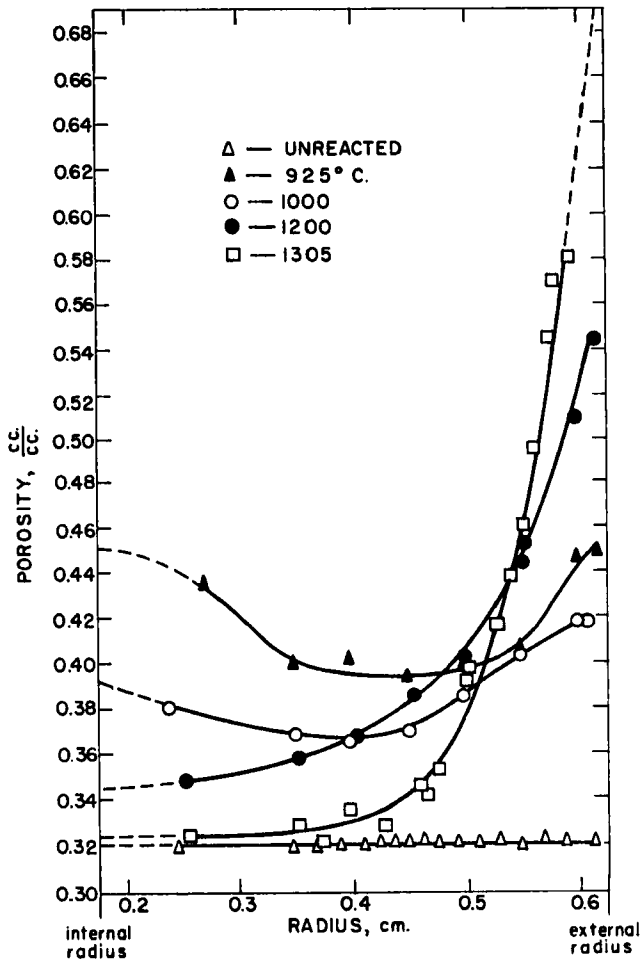


FIG. 13. Porosity profiles through spectroscopic carbon rods before and after *ca.* 11% burnoff at different temperatures.

towards the center of the rod. Extrapolation indicates that the porosity at the external surface is *ca.* 0.7 to 0.8. Since the external radius was decreased significantly during reaction, this suggests that the maximum porosity reached at the surface before carbon particles dropped from the rod ranged from 0.7 to 0.8. In this experiment, carbon deposits were found in the top of the reaction tube. Apparently only about 70 % of the total weight loss at this temperature was a direct result of carbon gasification.

At 1200°, no decrease in external radius occurred, with the surface porosity reaching a value of only 0.56. At this temperature, there was a significant increase in porosity even near the center hole in the rod; consequently, it may be assumed that the carbon dioxide concentration was not zero in this part of the rod. Therefore, reaction was in the transition region between Zones I and II. The reaction should be in Zone II when $\phi^2\eta = (R/C_R D_{\text{eff}})dw/dt > 4$, as previously discussed. Since R is *ca.* 0.48 cm., and at 1200°, C_R is 1×10^{-4} g. of carbon per cc., dw/dt is 0.22×10^{-2} g. of carbon/min./cm.² and the mean D_{eff} (as discussed shortly) is *ca.* 0.1 cm.²/sec., $\phi^2\eta = 1.7$. Thus, the reaction should be near, but not in, Zone II, in agreement with the interpretation of the porosity profile.

It is seen that at 1000° the reaction is much more uniform through the rod but is still not in the chemical control zone. At this low rate of reaction, it appears that carbon dioxide is diffusing sufficiently rapidly between the inner wall of the carbon rod and the ceramic support rod to maintain an appreciable concentration of reactant at the inner exposed surface of the rod. As expected, the minimum porosity (smallest amount of reaction) is found about half-way between the inner and outer radius, that is, at 0.4-cm. radius.

Even at 925°, the reaction is not uniform through the rod. This is difficult to explain because the criterion for chemical control indicates that for the reaction rate at this temperature, the reaction should be well within Zone I. It can hardly be ascribed to a temperature gradient within the rod, since heat-transfer calculations show that the gradient through the rod to supply the necessary heat of reaction at this low reaction rate is negligible (85). Furthermore, since heat is being supplied to the sample from the outside, a minimum in temperature at an intermediate radius (to explain the minimum in reaction rate at a radius of *ca.* 0.4 cm.) is not conceivable. Possibly, the assumption of a complete interconnection of the pores within carbon rods is not correct. If the interior of the carbon rod was being supplied with reactant gas through both large and small pores which are not greatly interconnected, the nonuniformity of the profile at 925° could be caused by the reaction still being in Zone II in the small pore system. The experimental D_{eff} used to estimate the reaction zone would be determined almost entirely by diffusion through the large pores in the system and would

be considerably too high to be used to calculate the temperature zone operative for the small pore system. If it is postulated that the gas-carrying pore system within the rod behaves as a series of pores with effective diffusion radii ranging over a complete distribution from small to large, with effective diffusion coefficients for the smallest radii group of diffusing pores being, perhaps, one-hundredth of that for the largest, then the nonuniform porosity found at low rates of reaction is clearly explained. Much of the work described in the following pages would need to be recalculated using distributions of surface area and porosity with diffusion coefficients and integrating the effects of the systems. It should be emphasized, how-

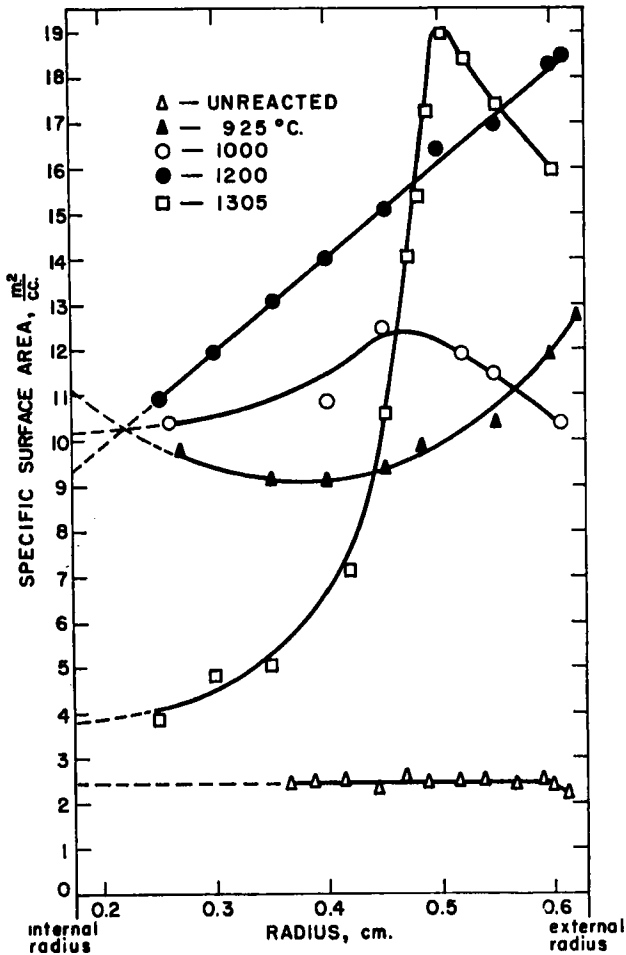


Fig. 14. Specific surface area profiles through spectroscopic carbon rods before and after ca. 11% burnoff at different temperatures.

ever, that it is difficult on the basis of our present understanding of the physical structure of carbon rods (106) to envision anything but an interconnected pore system.

Figure 14 presents specific surface area profiles on the same carbon rods on which porosity profile data were determined. As expected, the specific surface areas of the samples reacted at 1305 and 1200° decrease markedly as the radius decreases. For the rod reacted at 1305°, it is seen that a negligible increase in porosity at the internal radius results in a 60% increase in specific surface area at the same radius. This can be attributed to a significant amount of closed pore volume being opened up at small burnoffs (122, 123). The additional volume is negligible, but the additional surface area provided by the micropores is comparatively large. Again, looking at the profile for the rod reacted at 1305°, it is seen that the specific surface area goes through a maximum at a radius of *ca.* 0.5 cm. This is in line with the findings of Walker and Raats (106) and Wicke (31) that the specific surface area goes through a maximum as a function of burnoff or sample porosity. The area profiles for the rods reacted at 925 and 1000° are, in general, as expected. They show relatively little variation in area with radius.

By cross-plotting the data in Figs. 13 and 14, the relation between the specific surface area and the porosity of the carbon rods after reaction at different temperatures can be presented, as in Fig. 15. It is seen that the surface area developed in the rods is not only a function of the porosity developed but also a function of the reaction temperature. The development

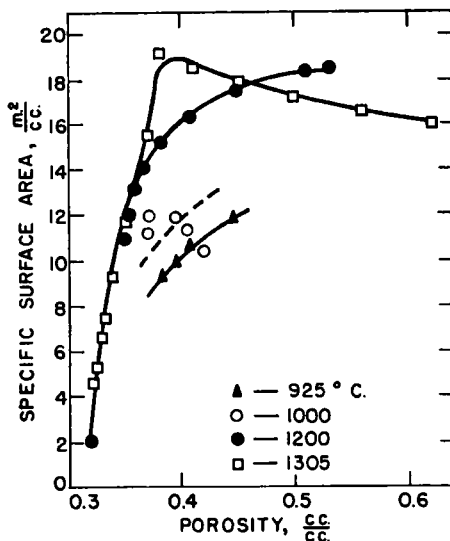


FIG. 15. Relation between specific surface area and porosity for spectroscopic carbon rods after *ca.* 11% burnoff at different temperatures.

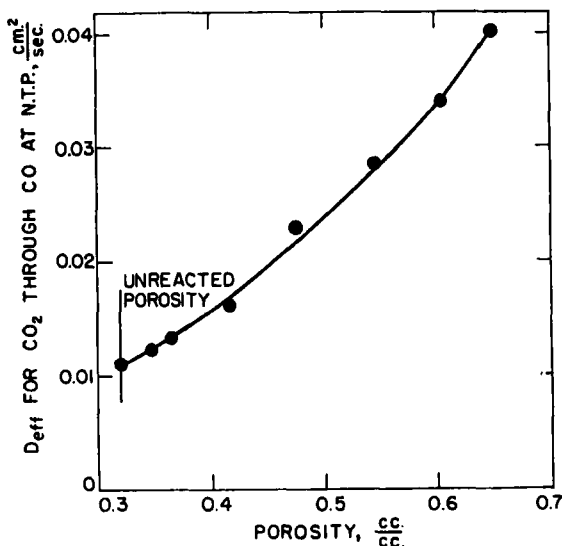


FIG. 16. Variation of effective diffusion coefficient of carbon dioxide through carbon monoxide at N.T.P. with porosity of spectroscopic carbon rods. Porosity developed by reaction with carbon dioxide at 950°.

of an increasing surface area after constant burnoff as the reaction temperature is increased in the range of about 900 to 1200° has been previously discussed (106, 124). It has been shown that variation in the over-all specific surface area developed in rods after reaction at different temperatures cannot be attributed only to variations in porosity, as again shown in Fig. 15.

2. *Variation of D_{eff} with Porosity of Carbon Rods.* Before being able to calculate reactant concentrations through the rods at different reaction temperatures, it was necessary to determine experimentally values for D_{eff} in the rods as a function of porosity. It has not been established that D_{eff} is only a function of porosity for a given carbon material and independent of the temperature at which this porosity is produced, but for simplicity this has been assumed to be the case. Carbon rods $\frac{1}{8}$ in. in diameter and $\frac{1}{8}$ in. long were cut from the original rods (the axis of the small rods being perpendicular to the axis of the original rods, since D_{eff} perpendicular to the axis is the value desired) and reacted at 950° to various degrees of burnoff. The samples were then mounted in the diffusion apparatus described by Weisz and Prater (103) and D_{eff} for hydrogen through nitrogen were determined at room temperature.* D_{eff} values for three samples at each burnoff were determined, and the values agreed within $\pm 3\%$ at burn-

* The writers are indebted to P. B. Weisz of the Socony-Mobil Laboratories for determining the D_{eff} data.

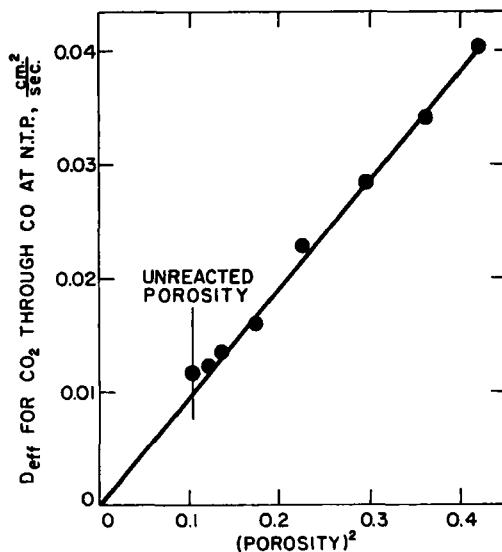


FIG. 17. Relation between effective diffusion coefficient of carbon dioxide through carbon monoxide at N.T.P. and square of porosity for spectroscopic carbon rods.

offs below 33%. At higher burnoffs, the agreement between values was within $\pm 10\%$.

The diffusion coefficients, corrected to carbon dioxide through carbon monoxide by multiplying by $\sqrt{2/44}$, are presented in Fig. 16 as a function of porosity. At porosities greater than 65%, the pellets become too fragile to handle. Contrary to expectations, it is found that initial, small amounts of burnoff do not greatly increase D_{eff} . This indicates that the marked increase in surface area for small amounts of burnoff occurs primarily by unblocking of pores which are not part of the main system of macropores through which the majority of diffusion is occurring. Apart from the data at very low burnoffs, it is found that D_{eff} is directly proportional to the square of the porosity, as shown in Fig. 17, or

$$D_{eff} = A\theta^2 \quad (56)$$

where $A = 0.095 \text{ cm.}^2/\text{sec.}$ at N.T.P. This can be compared with the well-known formula

$$D_{eff} = \frac{D_{free}}{\gamma} \theta \quad (57)$$

where γ is the tortuosity factor.* Possibly after a small initial burnoff,

* It is relevant to note that tortuosity defined by Equation (57) is by no means the same as that defined by (L_e/L) , where L_e is the effective tortuous path length

$\gamma = 1/\theta$ ($\gamma = 1$ when $\theta = 1$) and

$$D_{\text{eff}} = D_{\text{free}}\theta^2 \quad (58)$$

From Equation (58), D_{free} has the value of 0.095 cm.²/sec. at N.T.P., compared to the value of 0.14 cm.²/sec. found from free-diffusion experiments (126). As discussed, the values of D_{eff} were obtained from diffusion of hydrogen through nitrogen converted to carbon dioxide through carbon monoxide by multiplying by $\sqrt{2/44}$. Since hydrogen is much smaller than nitrogen, carbon dioxide, or carbon monoxide, it is probably more accurate to correct D_{eff} using the factor

$$\sqrt{\frac{28 + 44}{44 \times 28} \frac{2 + 28}{2 \times 28}} \quad (127).$$

When this conversion factor is used, D_{free} calculated from Equation (58) is 0.147 cm.²/sec., in good agreement with the experimental value.

Since porosity-radius curves have been obtained, it is possible to plot curves of D_{eff} against radius for the reacted rods. To correct to the temperature of reaction, it is assumed that D_{eff} is proportional to $T^{1.3}$ (128).

3. *Reactant Concentration Profile through Rod during Reaction at 1200°.* Equations (52), (54), and (55) are used to calculate the reactant concentration profile through the rod during reaction at 1200°. C_0 is initially assumed ≈ 0 , but as will be seen later, its value can be approximated. The most significant conclusion that can be drawn from the concentration data in Table VI is that there is no major difference in the decrease of concentration through the rod for the three different cases, even at high rates of reaction. At low rates of reaction, Equations (52), (54), and (55) all give the same result, since there is little pressure build-up or forced flow in the rod. As would be expected, Cases 2 and 3 require that the concentration gradient be somewhat steeper to diffuse in the required amount of carbon dioxide for reaction. In Table VI, the concentration through the rods also is expressed as a percentage of the surface concentration.

It is probable that the actual mass-transport process is a combination of all three cases. However, since the percentage falloff of concentration in the rod is not much different in the three cases, the results may be used on a

and L the measured thickness of the sample. As discussed by Carman (125), it is difficult to justify theoretically values of (L_s/L) which depart much from $\sqrt{2}$. The value of tortuosity defined by Equation (57) must be considered as a correction factor which includes (L_s/L) , but it is also a function of how the various-sized pores in a solid are interconnected. The tortuosity factor equals (L_s/L) only when the pores available for diffusion are not of widely different size and the interconnections between them are not constrictions. This can best be seen by noting that as the pore interconnections become small, D_{eff} tends to zero; therefore, γ tends to infinity even though the diffusion path and the porosity do not necessarily change very much.

comparative basis as long as it is remembered that the absolute magnitude of the concentrations is in doubt. It will be noted that the predicted concentrations of carbon dioxide at the surface of the rod (C_R) are 0.35, 0.56, and 0.39×10^{-4} g. of carbon per cc. for Cases 1, 2, and 3, respectively. Under the conditions of the reaction, C_0 is about 1.0×10^{-4} . From Equation (27) (where δ is calculated using Equation (40) with $\psi = 2.0$), it is estimated that $C_0 - C_R = 0.04 \times 10^{-4}$ g. of carbon per cc. Therefore,

$$C_R \simeq 1.0 \times 10^{-4},$$

indicating that the discrepancy between the values of carbon dioxide concentration calculated from concentration profiles and Equation (27) cannot be attributed to significant control of the reaction by mass transport resistance across the "stagnant film." A minor part of the difference can be attributed to C_0 not being zero, which can be seen by extrapolating the original rate-concentration curves to zero concentration, as discussed shortly. The major part of the discrepancy is almost certainly caused by the assumed variation between D_{eff} and temperature ($D_{\text{eff}} \propto T^{1.3}$). If D_{eff} were to vary with temperature to about the 0.9 power, the correct carbon dioxide concentration at the outside of the rod would be calculated. Unfortunately, no data are available for this relation for these particular carbon samples.

4. *Variation of Reaction Rate with Temperature for Spectroscopic Carbon Reacting with Carbon Dioxide.* Figure 18 presents the Arrhenius plot showing the variation in reaction rate with temperature for the spectroscopic carbon reacting with carbon dioxide. At temperatures below 950° , an activation energy of 93 kcal./mole is obtained, the value probably approaching E_t reasonably closely (32, 62). Between 950 and 1000° , there is an abrupt change in apparent activation energy, which might be interpreted as the entire transition region between Zones I and II. However, this interpretation is not valid. The porosity profile for the carbon reacted at 1200° (Fig. 13) indicates that the reaction is still in the transition region. Further, using Equation (25), the start of Zone II is calculated to occur when dw/dt is ca. 6 g. of carbon reacting per hour. Although this value is approximate, it is over 50 times the value of dw/dt at 1000° .

Also presented in Fig. 18 is the ideal change in reaction rate of the spectroscopic carbon with temperature, assuming a true activation energy of 93 kcal./mole. Zone II should start at a reaction rate of ca. 6 g. of carbon per hour and knowing that $\eta \simeq 0.5$ at the start of Zone II, the temperature can be approximated. It is of interest to note that the ideal activation energy in Zone II, 46.5 kcal./mole, is closely approximated by the change in experimental reaction rate with temperature above ca. 1250° .

It might be expected that the smaller values of experimental reaction

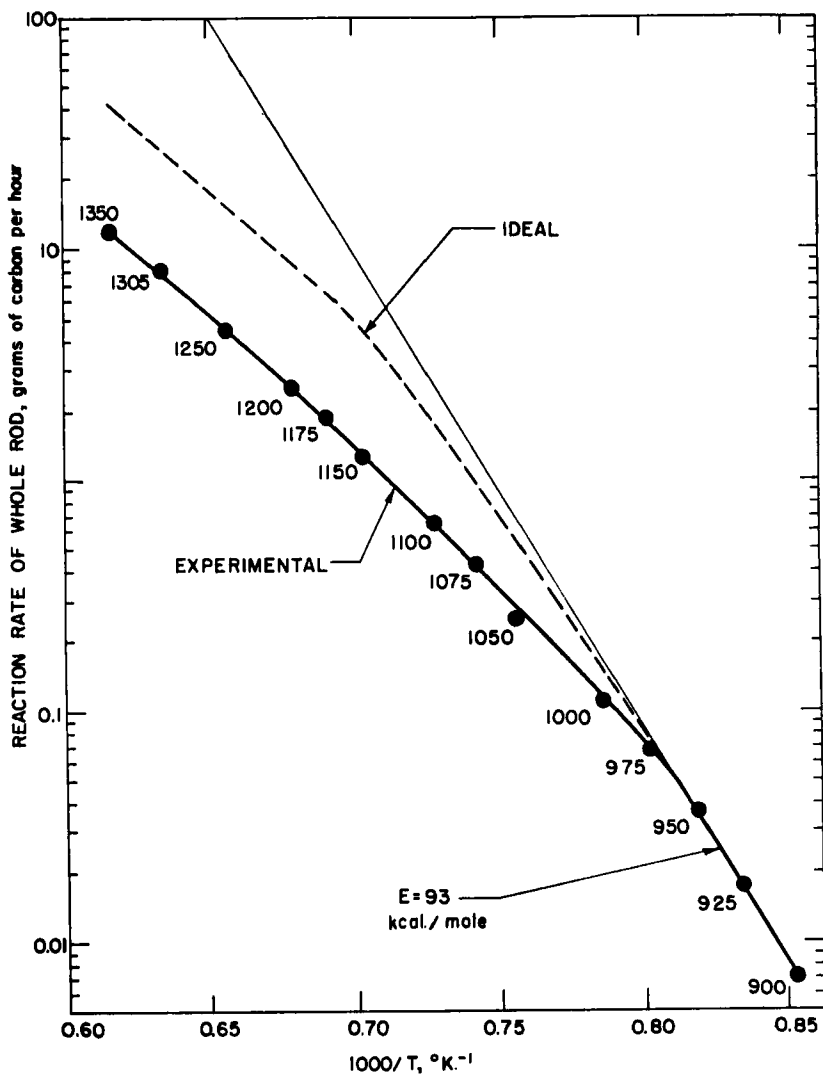


FIG. 18. Arrhenius plot for reaction of spectroscopic carbon rods with carbon dioxide at 1 atm. pressure.

rate which are observed in the transition region between Zones I and II are a result of forced flow or pressure buildup in the rod opposing the entry of carbon dioxide. However, the concentrations listed in Table VI indicate that these factors cannot account for such a marked discrepancy in reaction rate. It is probable that the buildup of carbon monoxide concentration in the rod at temperatures above 1000° results in retardation of the reaction.

5. *True and Apparent Order of Reaction.* From a knowledge of $(dn/dt)_r$, through the rod, the over-all rate of reaction can be determined by graphical integration. When this is done for the rod reacted at 1200° , it is found that the integrated rate of reaction in the rod (0.127 g. of carbon reacting per hour per cm^2 of external area) agrees well with the total rate of reaction determined from the experimental rate curve (0.131). The corresponding values for the rod reacted at 1305° are 0.30 and 0.41, which indicates that 28% of the over-all reaction is a result of carbon blowing from the external surface. This agrees well with the extent of mechanical loss of carbon predicted from the 1305° porosity profile (Fig. 13).

At any radius r , the rate of reaction per unit area can be calculated from the quotient, $(dn/dt)_r/S_r$. Consequently, the specific rate of reaction and calculated carbon dioxide concentration (both taken at the same value of r) can be plotted to determine the true order of reaction, independent of diffusion control. Figure 19 presents such data for the carbon rod reacted at 1200° , assuming the relative concentrations for Case 3 in Table VI to be applicable. From an auxiliary plot similar to Fig. 19, a finite reaction rate at zero carbon dioxide concentration is found. Since the concentrations of carbon dioxide were calculated assuming C_0 to be zero, it is clear that this reaction rate is due to a finite C_0 concentration at the center of the rod. The actual values of concentration at values of r were estimated by extrapolat-

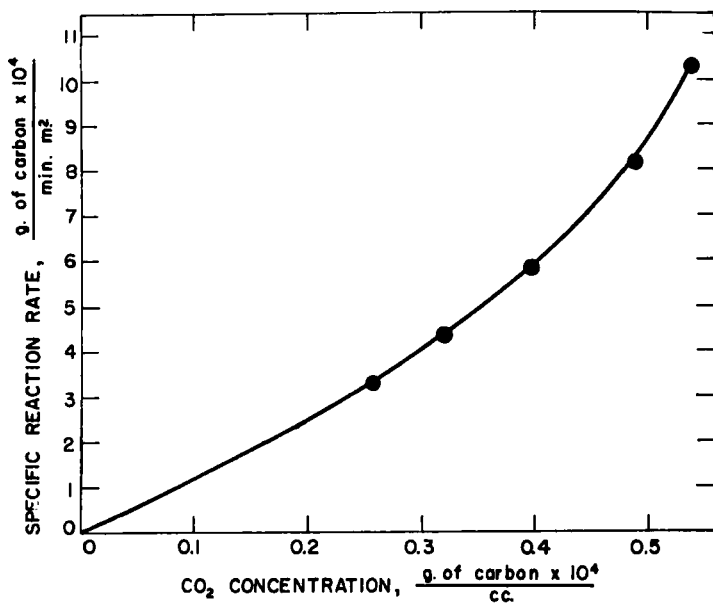


FIG. 19. Relation between specific reaction rate and carbon dioxide concentration in rod undergoing reaction at 1200° .

TABLE VI
*Concentrations of Carbon Dioxide through Spectroscopic Carbon Rod Reacting at 1200°
 Based on Density Profile and D_{eff} Data*

Radius, cm.	C_r , (g. of carbon in CO ₂)/cc. × 10 ⁴			C_r as % of C_R		
	Case 1	Case 2	Case 3	Case 1	Case 2	Case 3
0.35	0.05	0.09	0.05	14	13	16
0.40	0.08	0.15	0.08	23	20	26
0.45	0.12	0.22	0.13	36	32	40
0.50	0.18	0.31	0.19	57	47	55
0.55	0.24	0.41	0.26	69	66	73
0.60	0.31	0.51	0.35	89	88	91
$R = 0.6225$	0.35	0.56	0.39	100	100	100

ing the rate *vs.* concentration plot to zero rate, taking the negative intercept on the concentration ordinate as C_0 , and adding this constant concentration term to the concentrations in Table VI, thereby arriving at Fig. 19. By this method, C_0 is estimated as 0.14×10^{-4} g. of carbon per cc. at 1200°. A similar plot for the rod reacted at 1305° is given in Fig. 20. Clearly, the reaction is not first order at either temperature, nor do the data fit a Langmuir expression of the form $dn/dt = aC/(1 + bC)$. The data fit an expression of the form $1/(dn/dt) = (a/C) - (1/b)$, as seen in Fig. 21. Such an expression is consistent with the idea of carbon monoxide inhibition, as discussed below.

Figure 22 presents the change of over-all reaction rate with change in partial pressure of carbon dioxide in the main gas stream. Nitrogen was used as the diluent, and the total flow rate was maintained constant. The over-all order of reaction is found to be *ca.* 0.5 from 950 to 1200°. An over-all order of reaction of *ca.* 0.5 close to the start of Zone II has been interpreted to mean a true reaction order of zero (70, 79). In this case, however, as has been shown in Fig. 19, the true order is not zero at 1200°. Therefore, the above reasoning is not valid. An over-all order of 0.5 would be expected (for reaction in Zone II) if the mechanism of the reaction is represented by

$$\frac{dn}{dt} = \frac{a}{1 + \left(\frac{C_{CO}}{C_{CO_2}}\right)b} = F \left(\frac{C_{CO}}{C_{CO_2}}\right) \quad (59)$$

as suggested by Ergun (45). Both a and b vary exponentially with temperature, a increasing and b decreasing with increase in temperature. By similar reasoning to that used to derive Equation (A18), it can be shown that for

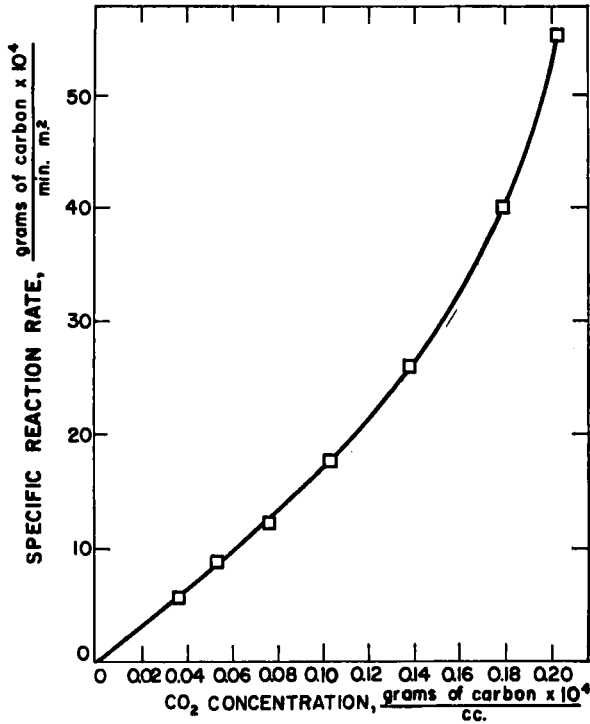


FIG. 20. Relation between specific reaction rate and carbon dioxide concentration in rod undergoing reaction at 1305°.

reaction through a specimen,

$$C_{CO} = \Gamma(\rho - C_{CO_2}) \quad (60)$$

with Γ varying between 1 and 2 depending upon the pressure buildup which occurs in the material. Assuming $\Gamma = 1$, for simplicity,

$$\frac{C_{CO}}{C_{CO_2}} = \frac{\rho}{C_{CO_2}} - 1 \quad (61)$$

The carbon dioxide concentration can be expressed as a fraction of the exterior gas concentration; that is, $C_{CO_2}/\rho = f$, with f varying from 1 to 0 from the exterior to the interior of the carbon. For any given value of f , C_{CO}/C_{CO_2} is fixed, and therefore, dn/dt is a function of f and not of C_{CO_2} alone, or

$$\frac{dn}{dt} = F(C_{CO_2}/\rho) \quad (62)$$

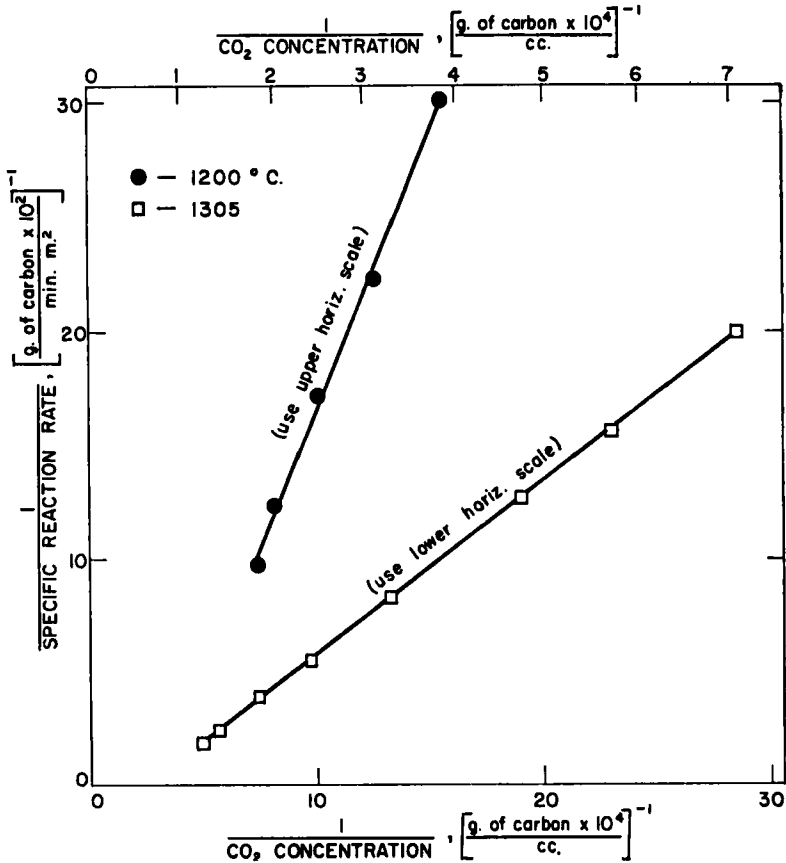


FIG. 21. Relation between reciprocal of specific reaction rate and reciprocal of carbon dioxide concentration in rods undergoing reaction at 1200 and 1305°.

Consider now a plane specimen of carbon (of uniform specific internal surface area and uniform D_{eff}) reacted in Zone II at two exterior carbon dioxide concentrations ρ_1 and ρ_2 . For a given temperature, Equation (62) shows that the specific reaction rate at a given value of C_{CO_2}/ρ is fixed. Therefore, in the two cases, since C_{CO_2}/ρ covers the same range of values, the specific reaction rates will cover the same range of values. However, in going from one fixed value of C_{CO_2}/ρ to another fixed value, the change in concentration and, therefore, the diffusional mass transport, will not be the same in both cases even though the specific reaction rate covers the same range of values. Clearly, for the higher concentration case, penetration will occur deeper into the specimen and the given specific reaction rate range will apply over a larger section of carbon. The fall in C_{CO_2}/ρ through

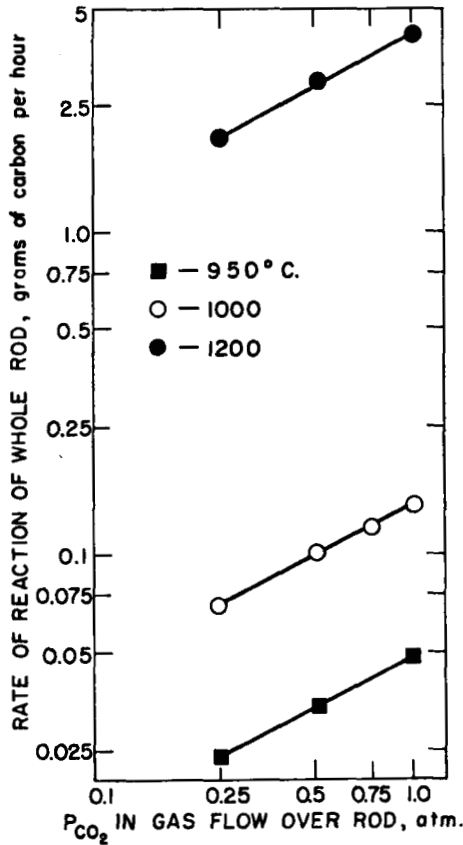


FIG. 22. Apparent order of reaction for whole rod at reaction temperatures between 950 and 1200°.

the material is as illustrated in Fig. 23, where the curves are of the same shape, but the penetration scale at the higher external concentration is expanded uniformly. Consider the two infinitesimal sections ΔL and δL at the same C_{CO_2}/ρ value. Let $\delta L = \lambda \Delta L$, then from Equation (62):

$$\text{Reaction in volume element } \delta L = S_v (dn/dt) \delta L \quad (63)$$

where S_v is the internal surface area per unit volume and the specimen is considered to be of unit cross sectional area. Also

$$\text{Reaction in volume element } \Delta L = S_v (dn/dt) \Delta L = 1/\lambda (\text{reaction in } \delta L) \quad (64)$$

Therefore,

$$\int_{C_{CO_2}/\rho=1}^{C_{CO_2}/\rho=0} \frac{dn}{dt} \delta L = \lambda \int_{C_{CO_2}/\rho=1}^{C_{CO_2}/\rho=0} \frac{dn}{dt} \Delta L \quad (65)$$

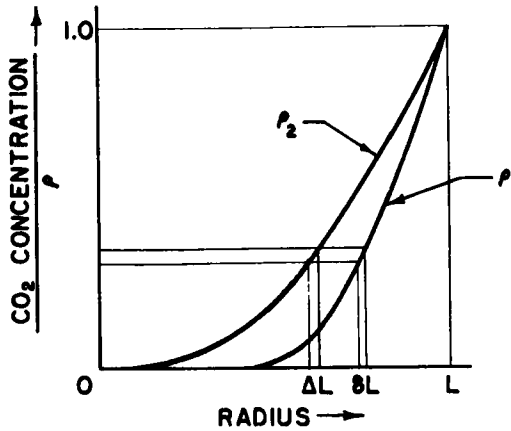


FIG. 23. Illustrations of fractional carbon dioxide concentrations through reacting specimen, when exterior face is exposed to reacting gas of concentration ρ_1 or ρ_2 , $\rho_2 > \rho_1$.

That is,

$$\left(\frac{dw}{dt}\right)_1 = \lambda \left(\frac{dw}{dt}\right)_2 \tag{66}$$

Considering the gradient of C_{CO_2}/ρ at the external reacting face

$$\left[\frac{d(C_{CO_2}/\rho_1)}{dx}\right]_1 = \frac{1}{\lambda} \left[\frac{d(C_{CO_2}/\rho_2)}{dx}\right]_2 \tag{67}$$

That is,

$$\left[\frac{d(C_{CO_2})}{dx}\right]_1 = \frac{\rho_1}{\rho_2 \lambda} \left[\frac{d(C_{CO_2})}{dx}\right]_2 \tag{68}$$

Now the overall rate of reaction is equal to $D_{eff} \left(\frac{dC}{dx}\right)_{\text{surface}}$, therefore

$$\left(\frac{dw}{dt}\right)_1 = \frac{\rho_1}{\rho_2 \lambda} \left(\frac{dw}{dt}\right)_2 \tag{69}$$

Eliminating λ from Equations (69) and (66) and rearranging

$$\frac{\left(\frac{dw}{dt}\right)_2}{\left(\frac{dw}{dt}\right)_1} = \sqrt{\frac{\rho_2}{\rho_1}} \tag{70}$$

Thus, the over-all rate should be proportional to the gas concentration in the main gas stream to the half power.

The above derivation applies to reaction completely in Zone II. From Equation (59) it is seen that in Zone I, where C_{CO} is small, the reaction should be zero order. Hence, over the transition region the apparent order of the over-all reaction should range from 0 to 0.5. This is not the case in the present work, as shown in Fig. 21, where the order is approximately 0.5 from 950 to 1200°. The discrepancy may be due to Equation (59) not being the correct equation for small values of carbon monoxide concentration.

As was discussed in Sec. III, the rate of the carbon-carbon dioxide reaction can be expressed as

$$\frac{dn}{dt} = \frac{i_1 C_{CO_2}}{1 + \frac{j_1}{j_3} C_{CO} + \frac{i_1}{j_3} C_{CO_2}} \quad (71)$$

which can be written in the form

$$\frac{1}{\frac{dn}{dt}} = \left(\frac{1 + \frac{j_1}{j_3} \rho}{i_1} \right) \frac{1}{C_{CO_2}} + \left(\frac{i_1 - j_1}{i_1 j_3} \right) \quad (72)$$

by substituting for the C_{CO_2} Equation (60) with $\Gamma = 1$. Equation (72) is of the form found to correlate the reaction rate *vs.* concentration data presented in Fig. 21. When the pressure of carbon monoxide becomes appreciable, Equation (71) can take the form

$$\frac{dn}{dt} = \frac{i_1 C_{CO_2}}{\frac{j_1}{j_3} C_{CO} + \frac{i_1}{j_3} C_{CO_2}} = \frac{j_3}{1 + \left(\frac{j_1}{i_1} \right) \left(\frac{C_{CO}}{C_{CO_2}} \right)} \quad (73)$$

which is of the form of Equation (59). Substituting for C_{CO} Equation (60) with $\Gamma = 1$,

$$\frac{dn}{dt} = \frac{i_1 C_{CO_2}}{\frac{j_1}{j_3} \rho + C_{CO_2} \left[\left(\frac{i_1}{j_3} \right) - \left(\frac{j_1}{j_3} \right) \right]} \quad (74)$$

which again can be arranged in a form to satisfy the reaction rate versus concentration correlation presented in Fig. 21. Substituting $K = i_1/j_1$ and simplifying

$$\frac{dn}{dt} = \frac{i_1 j_3 C_{CO_2}}{j_1 \rho \left[1 + \frac{C_{CO_2}}{\rho} (K - 1) \right]} \quad (75)$$

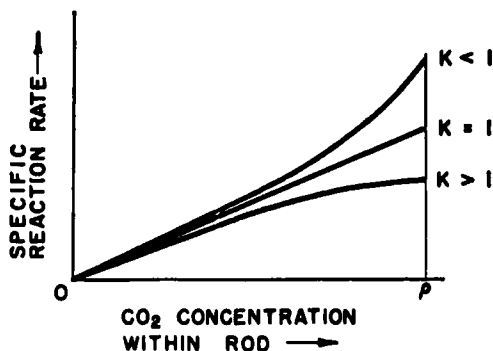


FIG. 24. Effect of K [Eq. (75)] on the relation between the specific reaction rate and carbon dioxide concentration in a rod. $K < 1$ (order $>$ first); $K = 1$ (order = first); $K > 1$ (order $<$ first).

The order of the reaction through the rod will depend on the value of K with respect to 1, the various cases being illustrated in Fig. 24. In all cases the order is approximately first when the carbon dioxide concentration is small. It should be kept in mind that all cases are derived from Equation (73), where the over-all order of reaction in the rod has been shown to be 0.5 when reaction is proceeding in Zone II.

At 1200 and 1305°, K is found to be less than 1, whereas Ergun (45) quotes values of 1.8 and 2.4 (see Fig. 4) for reaction at 1200 and 1300°, respectively.

E. SUMMARY

The primary purpose of this section has been to show the possibilities for using density and area profile data to aid in the better understanding of gas-carbon reactions. In order to determine specific reaction rates and carbon dioxide concentrations at given penetrations, it has been necessary to make assumptions which can only be approximations to the truth. Several major anomalies in the results have been found, however. The calculated concentrations of carbon dioxide at the external surface of rods reacted at 1200 (Table VI) and 1305° are not in agreement with the known carbon dioxide concentrations. Clearly, more information is required on the variation of D_{eff} with temperature and its variation with porosity produced at different reaction temperatures. It is feasible that at high temperatures, considerable porosity may be produced without increasing D_{eff} to such a marked extent as found at 900°. Another anomaly is the non-uniformity of reaction found at 925°, when it would be expected that the reaction should be in Zone I. The preliminary assumption of a completely interconnecting pore system may not be valid. It should also be noted that neither the value of K in Equation (75) nor the low-temperature activa-

tion energy of 93 kcal./mole agree with the values found by Ergun (45). The activation energy value agrees much better with that suggested by Rossberg (32) and those found by Armington (62).

VII. Some Factors, Other than Mass Transport, Which Affect the Rate of Gas-Carbon Reactions

The hope of attaining a quantitative understanding of the factors affecting the reactivity of carbons to gases has been the stimulus behind much work on gas-carbon reactions. At present, however, there is no clear understanding of why a given carbon reacts at a particular rate with a given gas under a fixed set of operating conditions. In this section, the possible effects on carbon reactivity of crystallite orientation, crystallite size, surface area, impurities in the carbon, heat treatment of the carbon, addition of halogens to the reacting gas, and irradiation are discussed briefly.

A. CRYSTALLITE ORIENTATION

In catalysis, one does not expect the activity of a catalyst to be proportional to its surface area, since there is good evidence that in many instances catalytic action is limited to certain active regions which may constitute only a small fraction of the total surface area (129). As would be expected, the same reasoning holds true for gas-carbon reactions. Carbon is a multicrystalline material, which can present varying degrees of surface heterogeneity depending upon the size and orientation of the crystallites. In the broadest sense, two main orientations of crystallites in the carbon surface need be considered—(1) crystallites with their basal planes parallel to the surface and (2) crystallites with their basal planes perpendicular to the surface.

According to Grisdale (130), the rate of oxidation of carbon crystallites is *ca.* 17 times faster in the direction parallel to the basal planes (along their edges) than perpendicular to them. Therefore, it would be expected that the specific reactivity of a carbon would be at a minimum when its surface contains a maximum of crystallites with their basal planes parallel to the surface. Smith and Polley (131) showed this to be the case. They compared the oxidation rates of original and graphitized* (2700°) samples of Sterling FT carbon black, which have very close to the same surface areas (15.4 and 16.6 m.²/g.) and particle sizes (2,094 and 1,940 Å. from electron micrographs). Figure 25 shows what they envision the orientation of the crys-

* It is to be emphasized that "graphitized" is used in this section to mean "heated to an elevated temperature above *ca.* 2200°." This is in line with the popular usage of the word, and should not be interpreted to mean that after graphitization the carbon has a 100% graphitic structure. As discussed by Walker and Imperial (132), artificial "graphite" approaches closely but does not have a 100% graphitic structure even after heat treatment to 3600°.

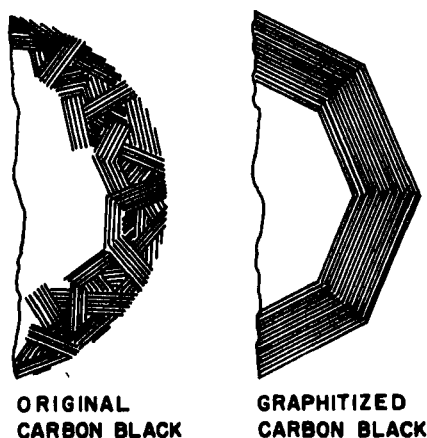


FIG. 25. Arrangement of crystallites in an original and graphitized (2700°) particle of Sterling FT carbon black. [After W. R. Smith, and M. H. Polley, *J. Phys. Chem.* **60**, 689 (1956).]

tallites in the two samples to be. In the original carbon black, there are a number of exposed edges in the surface for reaction to occur at a relatively high rate. On the other hand, they picture the graphitized carbon black as being in the shape of a polyhedron with its entire surface composed of crystallites with their basal planes parallel to the surface.* Smith and Polley find comparable rates of oxidation for the original and graphitized carbon blacks at temperatures of *ca.* 600 and 800° , respectively. If an activation energy of 50 kcal./mole (92) is assumed for the oxidation of both carbons, the ratio of reaction rates at the same temperature is *ca.* 200.

Walker and co-workers (134) investigated the reactivity of a series of graphitized carbon plates to carbon dioxide in the apparatus previously described (85). The majority of the plates were fabricated from mixtures of 65% petroleum coke (produced by delayed coking) and 35% coal tar pitch, using standard techniques (135). Using X-ray diffraction, they determined the relative tendency of the different petroleum cokes to orient with their basal planes parallel to the surface of the carbon plates. A qualitative correlation is found showing that the reactivity of the plates decreases as the percentage of basal plane structure in the surface increases. Plates produced from a fluid coke (136, 137) are found to have a gas reactivity lower than all plates produced from the delayed cokes, which is attributed to the fluid coke particles graphitizing in a manner similar to the Sterling FT carbon black, as previously discussed.

* The authors (131) and Kmetko (133) have confirmed definitely, from electron micrographs, that graphitization of carbon blacks of low surface area produces polyhedral particles.

B. IMPURITIES IN THE CARBON

Much work has been done on the effect of the addition of impurities (salts and metals, chiefly) on the reactivity of carbon. Quantitatively, the effects are difficult to understand, since they are functions of the location of the impurity in the carbon matrix and the extent of interaction of the impurity with the matrix. Long and Sykes (94) suggest that impurities affect carbon reactivity by interaction with the π -electrons of the carbon basal plane. This interaction is thought to change the bond order of surface carbon atoms, which affects the ease with which they can leave the surface with a chemisorbed species. Since the π -electrons in carbon are known to have high mobility in the basal plane, it is not necessary that the impurity be adjacent to the reacting carbon atom. Indeed, it is thought that the presence of the impurity at any location on the basal plane is sufficient for it to affect the reaction.

Impurities can either accelerate or retard carbon reactivity. Day (138) studied the effect of impurities on the oxidation of acetylene black by mixing equal weights of black and metallic oxides. He finds that a number of the impurities, including boron, titanium, and tungsten, inhibit oxidation, whereas iron, cobalt, nickel, copper, and manganese, among other metals, accelerate oxidation. Perhaps of greater significance is the finding that different methods of adding the impurity can affect markedly the degree of oxidation acceleration or retardation. For example, the addition of nickel originally as the nitrate is more effective than the addition of nickel originally as the hydroxide.

Earp and Hill (99) find that the addition of salts to graphite usually accelerates oxidation markedly; the notable exceptions being most of the borates and phosphates.

Sato and Akamatu (139) report that alkali metals enhance the chemisorption of oxygen on carbon and weaken the carbon-carbon bonds at the surface so as to accelerate combustion. On the other hand, they report that phosphorus, while catalyzing the adsorption of oxygen on carbon, has a retarding effect on the release of the surface oxide.

Nebel and Cramer (140) show that the addition of a series of lead compounds to carbon at a concentration of *ca.* 5 wt. % lowers the ignition temperature (raises the combustion rate) of the carbon. Of importance is the finding that the extent of the catalytic effect depends on the particular salt. Lead acetate is the most effective, lowering the ignition temperature 293°; lead sulfate is the least effective, lowering the ignition temperature only 39°. Lead pyrophosphate and lead orthophosphate are found not to lower the ignition temperature.

Tuddenham and Hill (72) investigated the effect of addition of cobalt, iron, nickel, and vanadium to spectroscopic graphite on its gasification with

steam at 1100°. They added the impurities as the nitrate. They report that relative gasification rates increase from 19-fold for nickel to 32-fold for iron.

Gulbransen and Andrew (141) investigated the effect of iron on the reactivity of spectroscopic graphite to carbon dioxide. The porous graphite was impregnated with an iron nitrate solution and then heated to a relatively low temperature to convert the iron nitrate to iron oxide. In one run, they then pretreated the sample by holding it at 850° for 1 hr. at 10^{-6} mm. Hg, prior to reacting the sample at 700° in 76 mm. Hg carbon dioxide pressure. Over the 10 min. of reaction time, the impregnated sample (containing 0.078% iron) is reported to have a reaction rate 530 times that of the original graphite. In another run, they pretreated under similar vacuum conditions but at a temperature of 700° for 16 hrs. They find negligible change in gasification rate following this pretreatment. Gulbransen and Andrew conclude that the iron impurity must be present as either the re-

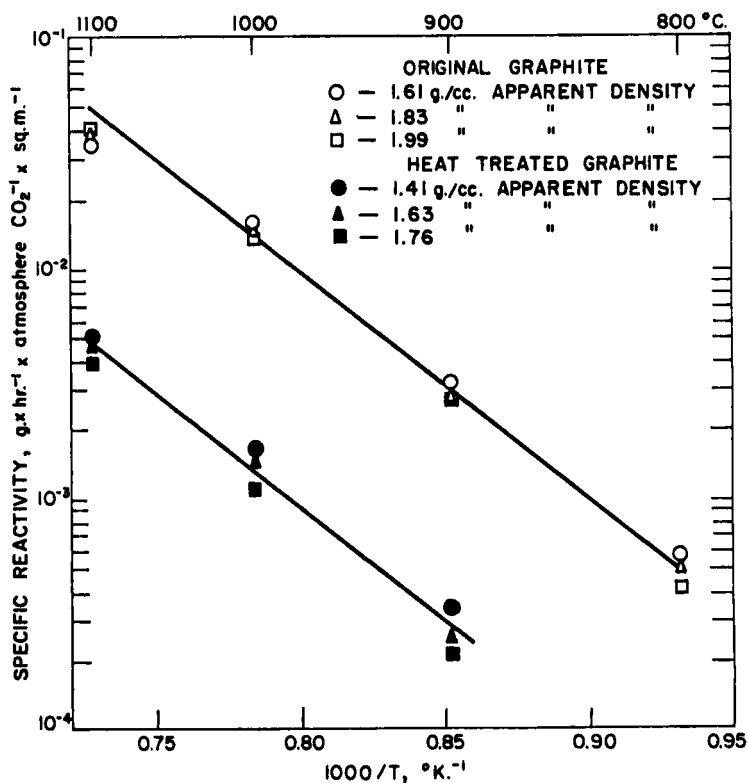


FIG. 26. Arrhenius plots for reaction of raw and heat-treated rods of Ceylon graphite with carbon dioxide at 1 atm. pressure. [After F. Rusinko, Jr., Ph.D. Thesis, The Pennsylvania State University, 1958.]

duced metal or as the carbide to catalyze the carbon dioxide reaction. They suggest that their vacuum pretreatment at 700° did not effectively reduce the iron oxides.

Rusinko (89) investigated the reactivity of pelletized natural graphite rods, before and after heat treatment at 2600°, with carbon dioxide at a series of temperatures from 800 to 1100°. On heat treatment, the ash content is found to decrease from *ca.* 2% to less than 0.1%. The crystallite size and specific surface area are found to undergo negligible change. Figure 26 correlates reactivity data on rods of various densities with temperature using an Arrhenius plot. Heat treatment is seen to reduce the specific reactivity of the rods by a factor of *ca.* 10 but not to change the activation energy (42 kcal./mole). The implication in this case is that the removal of impurities decreases the number of carbon sites able to participate in the reaction, but the removal does not change the mechanism by which the active sites react. It is known that the activation energy obtained is less than E_t , since the specific reactivity of the rods increases as the diameter of the rods reacted is decreased. It appears that reaction is proceeding in the transition region between Zone I and Zone II.

C. CRYSTALLITE SIZE

Usually it is difficult to separate the effect of crystallite size on carbon reactivity from the effects of crystallite orientation and impurity content. However, Armington (62) attempted to do so by reacting a series of graphitized carbon blacks with oxygen and carbon dioxide, as discussed earlier in this article. Assuming that upon graphitization all the carbon blacks are converted to polyhedral particles with the surface composed almost completely of basal plane structure, it is possible to eliminate crystallite orientation as a variable. Spectroscopically, the total impurity content of all the graphitized carbon blacks is quite low; and to a first approximation, the analyses of the individual constituents are similar.

By selecting carbon blacks of a wide range of particle size, Armington was able to control the extent of crystallite growth upon graphitization, since crystallites only grow to a fraction (usually from $\frac{1}{5}$ to $\frac{1}{10}$) of the carbon particle size. The graphitized carbon blacks range in crystallite size from *ca.* 20 to 130 Å. and in particle size from *ca.* 130 to 2000 Å. Particle sizes calculated from B.E.T. surface areas (assuming no internal porosity) agree well with particle sizes approximated from electron micrographs.

Figure 27 presents data on the specific reactivity of the series of carbon blacks in 0.1 atm. of oxygen at 600° *vs.* the specific surface area of the blacks. Since the crystallite size is an inverse function of surface area, the conclusion to be drawn from Fig. 27 is that the specific reactivity of carbons increases with increase in crystallite size. Armington reports similar results for the

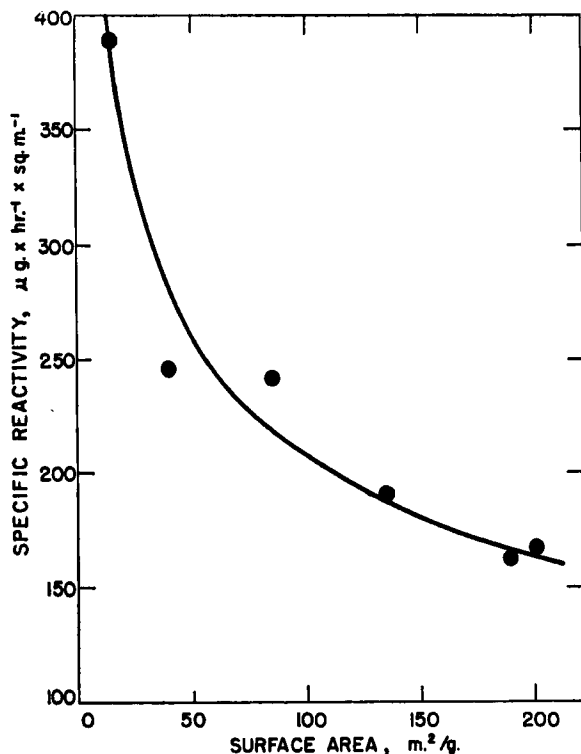


FIG. 27. Relation between specific reactivity to oxygen and specific surface area of a series of graphitized carbon blacks. [After A. F. Armington, Ph.D. Thesis, The Pennsylvania State University, 1960.]

reaction of the same graphitized carbon blacks with carbon dioxide. He suggests that catalysis of the reaction by the impurities still present in the blacks is responsible for this effect of crystallite size on reactivity. That is, assuming the same quantitative and qualitative impurity content in all blacks, the larger the crystallite size the greater the number of edge carbon atoms which can be affected by a given impurity atom by π -electron transfer through the basal plane. Edges of crystallites will serve as zones of high resistance to electron flow. Consequently, an impurity atom associated with one crystallite will have little effect on the reaction rate of edge carbon atoms on other crystallites in the matrix.

D. EFFECT OF HEAT TREATMENT OF CARBONS ON THEIR SUBSEQUENT REACTIVITY TO GASES

Several cases of the effect of heat treatment on the subsequent reactivity of carbon have already been discussed. In both the work of Rusinko (89)

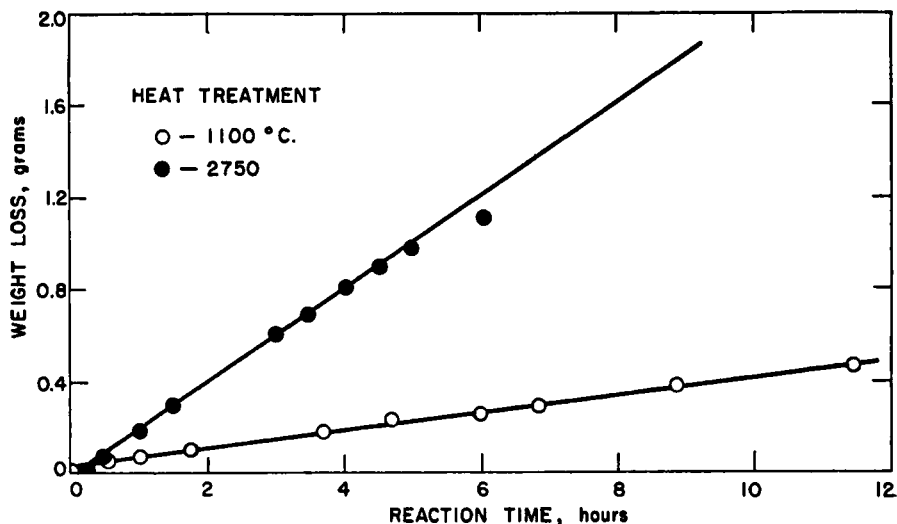


FIG. 28. Effect of heat treatment on the reactivity of carbon derived from petroleum pitch. Reaction of 2 g. of 6×8 -mesh carbon with carbon dioxide at 1100° . [After P. L. Walker, Jr., and J. R. Nichols, "Industrial Carbon and Graphite," Society of Chemical Industry, p. 334. London, 1957.]

and Smith and Polley (131), heat treatment at elevated temperatures produces a marked decrease in reactivity of the carbon. It is to be emphasized, however, that heat treatment to elevated temperatures also can increase the subsequent reactivity of carbon. Walker and Nichols (142) investigated the reactivity of cokes produced from coal tar pitch and petroleum pitch. Particle samples (2 g. of 6×8 -mesh material) having seen maximum temperatures of either 1100 or *ca.* 2750° were reacted with carbon dioxide at 1100° in the apparatus previously described (85). Figure 28 presents the reaction rate curves for the samples derived from the petroleum pitch. The graphitized sample has a reaction rate some fivefold higher than the sample which has not seen a temperature above 1100° . Similar results are found for the samples produced from the coal tar pitch with the graphitized sample having a reactivity over threefold higher than the ungraphitized sample. For both materials, graphitization produced a marked increase in crystallite size, a marked decrease in impurity content, and only a minor change in surface area.

As a follow-up to this work, Walker and Baumbach (143) investigated the effect of heat treatment on the reactivities of carbons produced from 20 different coal tar pitches and one delayed petroleum coke. Heat treatment again produced a marked increase in crystallite size, a marked decrease in impurity content, and only a minor change in surface area. They use the

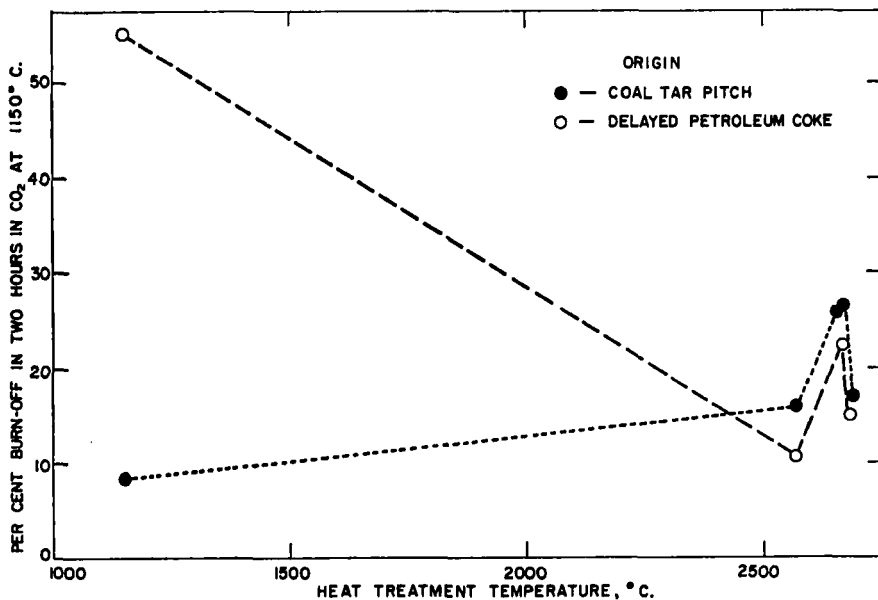


FIG. 29. Effect of heat treatment on the reactivity of carbons derived from coal tar pitch and delayed petroleum coke. Reaction with carbon dioxide at 1150°. [After P. L. Walker, Jr., and D. O. Baumbach, unpublished results 1959.]

same apparatus and procedure as that used by Walker and Nichols (142), while studying reactivities in carbon dioxide at 1150°. Of the 20 samples derived from coal tar pitch, in 19 cases the graphitized sample (2660°) has a considerably higher reactivity than the samples which have seen a maximum temperature of only 1150°. On the other hand, the reactivity of the graphitized petroleum coke is about one-half that of the coke having seen a maximum temperature of 1150°. Of even more interest is the effect of heat treatment to different elevated maximum temperatures on subsequent reactivity to carbon dioxide. In Fig. 29, results on a typical sample produced from coal tar pitch and a sample produced from delayed petroleum coke are given. Pronounced effects of graphitization temperatures in the range 2570 to 2680° are found. As noted, two separate heat treatment runs at temperatures of *ca.* 2655° were made on the sample from coal tar pitch to confirm the maximum in the reactivity. There is no doubt that the maximum exists. The relative values of temperatures reported agree well with the temperatures estimated from electrical resistivity data on the heat-treated samples. That is, room temperature electrical resistivities of carbons heated in this temperature range are known to increase with increasing heat treatment temperature.

The authors feel that these preliminary results of Walker and Baumbach on the effect of heat treatment of carbon on subsequent gas reactivity serve to indicate the complexity of the problem. At the same time, the results indicate the necessity of much additional work in this area if an understanding of the factors affecting the rate of gas-carbon reactions are to be understood. These results emphasize that total impurity content in carbons is not the decisive factor determining gas reactivities. Of more importance is the location of the impurity in the carbon matrix and its particular chemical form. It is suggested that heat treatment can bring the impurity into more intimate contact with the carbon matrix through high-temperature reactions so that a small amount of impurity can serve as a more efficient catalyst. Also to be kept in mind is the fact that the crystallite size of the carbon can increase with increasing temperature—at least up to a point. As discussed previously, the size of the crystallite determines, in part, how effectively the catalytic impurities are used.

It is suggested that a detailed examination of the effect of heat-treatment temperature on the gas reactivity of the carbons studied by Walker and Baumbach (143) might show a series of reactivity maxima which correspond to temperatures at which different catalytic impurities first begin to show significant solid state diffusion and reaction with the carbon matrix followed at higher temperatures by their complete volatilization from the sample. The advent of significant diffusion and reaction of the impurity with the carbon could result in a subsequent increase in gas reactivity. Complete volatilization of the impurity from the sample could result in a subsequent decrease in gas reactivity.

E. ADDITION OF HALOGENS TO THE REACTING GAS

The role which halogens play in raising the CO-CO₂ ratio of the product gas in the carbon-oxygen reaction has been discussed in Sec. III. Halogens can also affect markedly the rate of carbon burnoff. Day (24), for example, investigated the effect of chlorine on the carbon-oxygen reaction under high velocity conditions. The carbon was heated solely by the energy supplied by the reaction, and at 20,000 ft./min. in pure oxygen, a surface temperature of 1660° was maintained. The introduction of 0.15% chlorine to the oxygen stream lowers the surface temperature by 280°; 0.25% chlorine immediately extinguishes the reaction. The chlorine is thought to be dissociating and chemisorbing on the carbon sites preventing the formation of a carbon-oxygen complex. If the chlorine has not extinguished the reaction, subsequent removal of the chlorine from the oxygen stream results in the surface returning to its original temperature. However, the return to normal does not occur as rapidly as the poisoning, which is almost instantaneous.

Wicke (31) investigated the effect of POCl₃ on the carbon-oxygen reac-

tion. He finds a normal ignition temperature of 650° in dry air. With 1% by volume of POCl_3 added to the air, there is no reaction at 650°; and it proves impossible to remove the inhibiting material from the carbon by subsequently passing in pure air. Even at 900°, the removal is found to take several minutes. The ignition temperature of the carbon is raised 200°.

Hedden (144) investigated the effect of the addition of POCl_3 and chlorine on the rate of the carbon-carbon dioxide reaction at a temperature of 1100°. After achieving a constant rate for the reaction in the absence of halogen-containing gas, he finds upon addition of impurity gas that there is an initial sharp increase in reaction rate. This is followed by a decrease in reaction rate. For POCl_3 , the rate falls below the normal rate; for chlorine it remains above this rate. When the halogen-containing gas is stopped, the reaction rate in both cases increases sharply above the normal rate, followed by a continuing decrease back to the same value as that when no halogen-containing gas is added. The initial increase in reaction rate following halogen treatment to a value greater than the normal value is ascribed to excessive surface roughening while the halogen is present in the reacting gas. The degree of surface roughening gradually decreases after the halogen gas flow is stopped until reaching the normal value.

It can be concluded that the halogen-containing gases offer unusual possibilities for affecting the rate of attack of carbon surfaces by oxygen-containing gases.

F. IRRADIATION

With the use of graphite as a moderator in nuclear reactors becoming of increasing importance, there is concern about the effects of irradiation on the rate of reaction of the graphite with gases. Aside from the practical importance of irradiation effects, high-energy irradiation of carbons provides a powerful tool for studying the relation between imperfections in the carbon lattice and rates of gas-carbon reactions. Relatively large and controlled concentrations of imperfections can be introduced into graphite by high energy particle bombardment.

Kosiba and Dienes (145) investigated the effects of neutron irradiation on the rate of reaction of spectroscopic graphite rods with air. Figure 30 shows the effects of exposure of the graphite to *ca.* 4×10^{20} neutrons/cm.² at temperatures under 50° on its subsequent reaction rate over the temperature range 250 to 450°. Prior irradiation increases the oxidation rate by a factor of *ca.* 5 to 6 at reaction temperatures of 300 to 350°. The effect of irradiation decreases with further increase in reaction temperature, as evidenced by a larger activation energy of oxidation for the unirradiated graphite. Kosiba and Dienes estimate that at the reaction temperatures studied there is at most about 1% displaced carbon atoms remaining from the

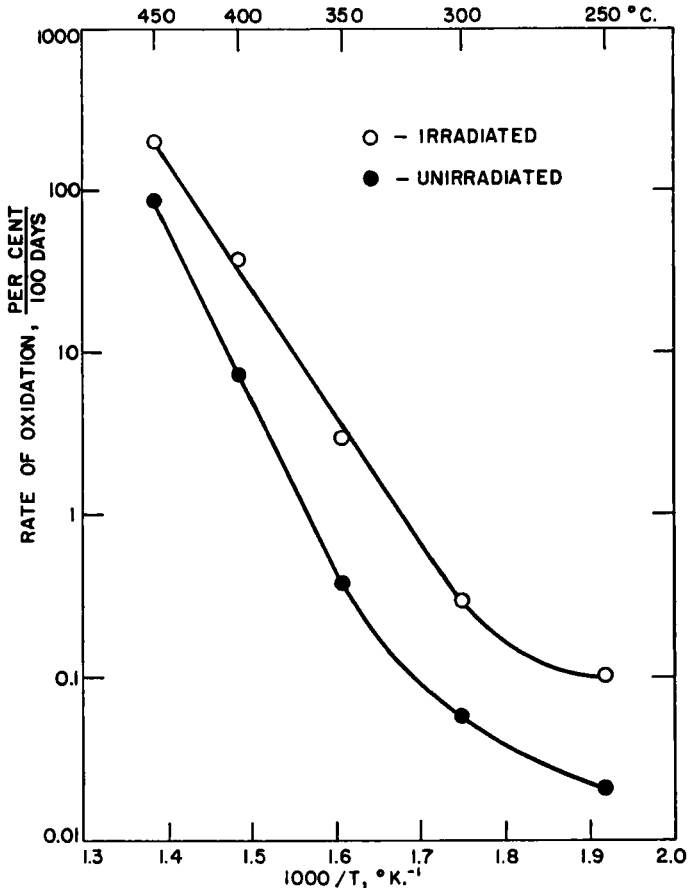


FIG. 30. Arrhenius plots for the rate of oxidation in air of both unirradiated and previously irradiated spectroscopic graphite. [After W. L. Kosiba, and G. J. Dienes, *Advances in Catalysis* 9, 398 (1957).]

previous irradiation with neutrons. On the other hand, they observe that at 400°, for example, the higher oxidation rate of the irradiated sample persists even when 20 to 25% of the sample has been oxidized. They conclude, therefore, that the displaced carbon atoms are not themselves being oxidized preferentially but facilitate in some way the over-all oxidation. They further observe that this increase in reaction rate on irradiation is not brought about by an increase in surface area, since it is known from the recent work of Spalaris (122) that the surface area decreases significantly upon irradiation at room temperature.

Kosiba and Dienes (145) also investigated the effect of exposure of the graphite to gamma-irradiation during reaction on oxidation rates. On the

unirradiated graphite, they find that the reactivity at 300° is hardly altered at a gamma-flux of 2×10^5 r./hr., whereas a significant increase in reactivity is observed at a flux of 6×10^5 r./hr. On an irradiated graphite, a flux of 2×10^5 r./hr. increases the reactivity at 300° by a factor of three over the irradiated graphite not reacted in a gamma-field. This means that the irradiated graphite subsequently reacted in a gamma-flux of 2×10^5 r./hr. at 300° had an over-all oxidation rate some 18-fold higher than the unirradiated graphite whether or not the unirradiated graphite was exposed to the above gamma-flux during reaction. Kosiba and Dienes conclude that the gamma-ray effect is probably due to the ionization of oxygen molecules, since gamma-rays have not been observed to have any effect on the properties of graphite at the exposures used.

ACKNOWLEDGMENT

We wish to express our appreciation to the following groups for support of our studies on gas-carbon reactions either through direct financial assistance or through the supplying and processing of carbon materials: U.S. Atomic Energy Commission through Contract No. AT(30-1)-1710; The Commonwealth of Pennsylvania through its continuing support of coal research; Consolidation Coal Co.; Godfrey L. Cabot, Inc.; National Carbon Co.; Plastics and Coal Chemicals Division of the Allied Chemical Corp.; Socony Mobil Oil Co.; Speer Carbon Co.; and Stackpole Carbon Co. Their support has made the writing of this article possible.

Appendix

A. SOLUTION OF DIFFERENTIAL EQUATION (21)

Equation (21) is a Bessel equation of the general solution

$$C = AJ_0(r\sqrt{-k_v/D_{\text{eff}}}) + BY_0(r\sqrt{-k_v/D_{\text{eff}}}) \quad (\text{A1})$$

However, the function Y_0 tends to infinity as r tends to zero, while the function J_0 remains finite; and as C must be finite at $r = 0$, B must be zero. Thus

$$C = A \sum_{n=0}^{\infty} \frac{(-1)^n [(r/2)\sqrt{-k_v/D_{\text{eff}}}]^{2n}}{(n!)^2} \quad (\text{A2})$$

or

$$\frac{C}{A} = \sum_{n=0}^{\infty} \frac{[(r/2)\sqrt{k_v/D_{\text{eff}}}]^{2n}}{(n!)^2} \quad (\text{A3})$$

By computation or by using tables of Bessel functions, values of C/A can be found for a range of $(r/2)\sqrt{k_v/D_{\text{eff}}}$ values. Let

$$\phi = r\sqrt{k_v/D_{\text{eff}}} \quad (\text{A4})$$

Then, by plotting $\log_{10}(C/A)$ vs. $\phi/2$, it was found that for values of $\phi > 4$

$$\log_{10}(C/A) = 0.84(\phi/2) - 0.75 \quad (\text{A5})$$

Hence,

$$\log_{10} [5.62(C/A)] \simeq 2(\phi/2) \log_{10} e \quad (\text{A6})$$

or

$$5.62(C/A) = e^\phi \quad (\text{A7})$$

When $C = C_R$, $\phi = R\sqrt{k_v/D_{\text{eff}}}$ and, therefore,

$$A = 5.62C_R \exp -R\sqrt{k_v/D_{\text{eff}}} \quad (\text{A8})$$

or

$$C_r = C_R \exp r\sqrt{k_v/D_{\text{eff}}} \exp -R\sqrt{k_v/D_{\text{eff}}} \quad (\text{A9})$$

From the plot of $\log(C/A)$ against $\phi/2$, it is found that C_r is approximately constant throughout the rod for $\phi < 0.2$. (At $\phi = 0.2$, the concentration at the center of the rod is *ca.* 20% less than C_R .)

B. DERIVATION OF EQUATIONS FOR REACTANT CONCENTRATION PROFILE THROUGH CARBON RODS DEPENDING UPON TYPE OF MASS TRANSPORT

1. *Knudsen Diffusion Only Is Occurring.* For a very fine pore material in which the effective pore diameter is less than the mean free path of the molecules, bulk diffusion and Poiseuille flow do not occur. For this case, the change in volume given when $C + \text{CO}_2 \rightarrow 2\text{CO}$ has no influence on the rate of diffusion of carbon dioxide into the rod, and D_{eff} is not dependent on the total pressure in the pores. Considering a wedge of carbon (Fig. A1),

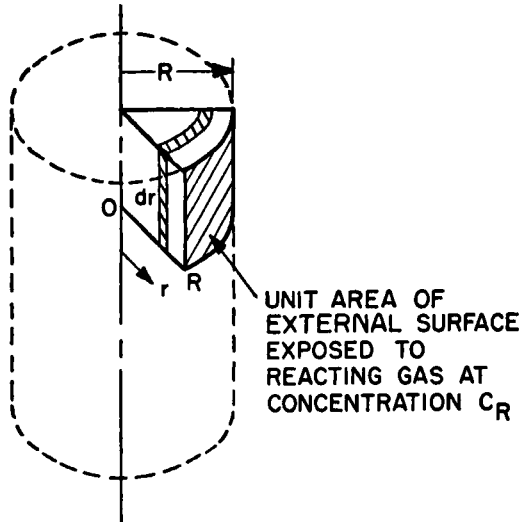


FIG. A1. Section of rod of radius R undergoing reaction.

the amount of CO_2 which diffuses through a plane at r must equal the CO_2 reacted from 0 to r . That is,

$$\int_0^r \left(\frac{dn}{dt} \right)_r dr = (D_{\text{eff}})_r \frac{r}{R} \left(\frac{dC}{dr} \right)_r \quad (\text{A10})$$

From the values of $(dn/dt)_r$ obtained experimentally,

$$\int_0^r \left(\frac{dn}{dt} \right)_r dr = f(r)$$

can be obtained by graphical integration. Then

$$dC = \frac{f(r)}{(D_{\text{eff}})_r} \frac{R}{r} dr \quad (\text{A11})$$

and integrating,

$$C_r - C_0 = \int_0^r \frac{f(r)}{(D_{\text{eff}})_r} \frac{R}{r} dr = F(r) \quad (\text{A12})$$

where C_r is the concentration of CO_2 at r in g. of carbon per cc. and C_0 is the concentration of CO_2 in the center of the rod. At high reaction rates, $C_0 \simeq 0$. $F(r)$ can be determined by graphical integration.

2. *Bulk Diffusion Occurring But Pores Too Fine to Allow Poiseuille Flow.* For bulk diffusion, $D_{\text{eff}} \propto (1/P)$, where P is the total pressure. If Poiseuille flow is negligible, then the concentration profiles of CO_2 and CO through the rod can be shown as in Fig. A2. For the reaction $\text{C} + \text{CO}_2 \rightarrow 2\text{CO}$, the increase in volume of CO over CO_2 is two; and at any point, the diffusion gradient for CO must be double that for CO_2 . If C' is the concentration of CO at a point where the concentration of CO_2 is C ,

$$\frac{dC'}{dr} = -2 \frac{dC}{dr} \quad (\text{A13})$$

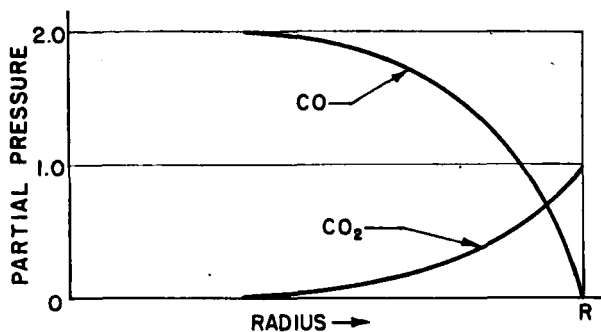


FIG. A2. Illustration of the pressure profiles through a rod when substantial bulk diffusion and negligible Poiseuille flow are occurring.

or

$$C' = -2C + A \quad (\text{A14})$$

At the external surface, let the total pressure P_R be made up of q inerts, C_R carbon dioxide and C'_R carbon monoxide. Then

$$P_R = C_R + C'_R + q \quad (\text{A15})$$

Therefore,

$$C_R + C'_R = \rho = P_R - q \quad (\text{A16})$$

where ρ is in g. of carbon per cc. When $C = C_R$, $C' = C'_R = \rho - C_R$ and

$$\rho - C_R = -2C_R + A \quad (\text{A17})$$

or

$$C' = \rho + C_R - 2C \quad (\text{A18})$$

At any point in the carbon, the total pressure P_r is given by

$$P_r = q + C + C' = q + \rho + C_R - C \quad (\text{A19})$$

Now the diffusion coefficient D_{eff} at this point under a pressure of P_r is obtained from the diffusion coefficient D'_{eff} at the same point but measured at P_R by the relation

$$(D_{\text{eff}})_r = (D'_{\text{eff}})_r \frac{P_R}{P_r} = (D'_{\text{eff}})_r \left(\frac{q + \rho}{q + \rho + C_R - C} \right) \quad (\text{A20})$$

If $q = 0$,

$$\int_0^r \left(\frac{dn}{dt} \right)_r dr = (D'_{\text{eff}})_r \frac{\rho}{\rho + C_R - C} \frac{r}{R} \left(\frac{dC}{dr} \right)_r \quad (\text{A21})$$

or

$$\int_0^r \frac{f(r)}{(D'_{\text{eff}})_r} \frac{R}{r} dr = \int_0^r \frac{\rho}{\rho + C_R - C} dC \quad (\text{A22})$$

or

$$F(r) = 2.3\rho \log \left(\frac{\rho + C_R - C_0}{\rho + C_R - C_r} \right) \quad (\text{A23})$$

If $C_0/C_R = L$, where L is clearly < 1 ,

$$C_r = (\rho + C_R) - \frac{(\rho + C_R - LC_R)}{\text{antilog} \left[\frac{F(r)}{2.3\rho} \right]} \quad (\text{A24})$$

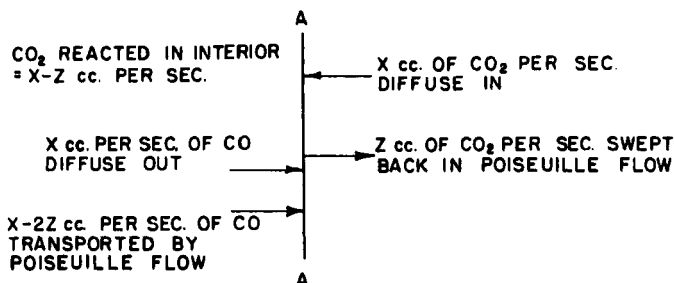


FIG. A3. Representation of flow conditions at a plane in a rod when bulk diffusion and a maximum of Poiseuille flow are occurring.

When the reaction is not in the stagnant film-controlled zone, $C_R = \rho$ and at high rates of reaction, $L \approx 0$. Therefore,

$$C_r = 2C_R(1 - e^{-r(r)/C_R}) \quad (\text{A25})$$

3. *Bulk Diffusion Occurring with a Maximum of Poiseuille Flow.* The third limiting case is where the pores are so large that negligible absolute pressure differential builds up within the pores and Poiseuille flow carries the extra volume of CO to the exterior. Under these conditions, CO will diffuse out at the same rate as CO₂ diffuses in (that is, $dC/dr = -dC'/dr$), while CO is carried out by forced flow. It is clear, however, that the forced flow will also carry out some of the CO₂ which diffuses in. This situation is represented by Fig. A3, where AA is a plane in the solid (after Thiele (100)). The total mass flow outwards in cc./sec. is given as

$$Q = X - 2Z + Z = X - Z \quad (\text{A26})$$

But $Z = Q \times C''$ where C'' equals the concentration of CO₂ in gas in cc. per cc. Therefore,

$$Z = (X - Z)C'' = \frac{C''X}{1 + C''} \quad (\text{A27})$$

If 1 cc. of CO₂ weighs ρ g. of carbon at the temperature and pressure applying, then considering 1 cm.² of external surface of rod, the rate of reaction in g. of carbon per sec. is given by

$$\int_0^r \frac{dn}{dt} dr = (X - Z)\rho \quad (\text{A28})$$

$$= \left(X - \frac{C''X}{1 + C''} \right) \rho \quad (\text{A29})$$

$$= \left(\frac{1}{1 + C''} \right) X\rho \quad (\text{A30})$$

Now

$$X\rho = (D_{\text{eff}})_r \frac{dC}{dr} \frac{r}{R}$$

Therefore,

$$\int_0^r \left(\frac{dn}{dt} \right)_r dr = \frac{1}{1 + C''} (D_{\text{eff}})_r \frac{r}{R} \frac{dC}{dr} \quad (\text{A31})$$

As C is in g. of carbon per cc., $C'' = C/\rho$. Substituting from this and

$$f(r) = \int_0^r (dn/dt)_r dr,$$

$$f(r) = \frac{1}{1 + (C/\rho)} (D_{\text{eff}})_r \frac{r}{R} \frac{dC}{dr} \quad (\text{A32})$$

That is,

$$\int_0^r \frac{f(r)}{(D_{\text{eff}})_r} \frac{R}{r} dr = \int_0^r \frac{\rho}{\rho + C} dC \quad (\text{A33})$$

or

$$F(r) = 2.3\rho \log \left(\frac{\rho + C_r}{\rho + C_0} \right) \quad (\text{A34})$$

For high rates of reaction, $C_0 \simeq 0$. If there is 100% CO_2 in the reacting gas stream

$$C_r = C_R (e^{F(r)/C_R} - 1) \quad (\text{A35})$$

REFERENCES

1. Hougen, O. A., and Watson, K. M., "Chemical Process Principles," Part I, p. 254. Wiley, New York, 1950.
2. Based on data from: "Tables of Selected Values of Chemical Thermodynamic Properties." National Bureau of Standards, Washington, D. C., 1949.
3. Trapnell, B. M. W. "Chemisorption." Academic Press, New York, 1955.
4. Loebenstein, W. V., and Deitz, V. R., *J. Phys. Chem.* **59**, 481 (1955).
5. Savage, R. H., *Ann. N. Y. Acad. Sci.* **53**, 862 (1951).
6. Gadsby, J., Long, F. J., Sleightholm, P., and Sykes, K. W., *Proc. Roy. Soc.* **A193**, 357 (1948).
7. Kefer, N. P., and Man'ko, N. M., *Doklady Akad. Nauk S.S.S.R.* **83**, 713 (1952).
8. Zelinski, J. J., Ph. D. thesis, The Pennsylvania State University, 1950.
9. Studebaker, M. L., Huffman, E. W. D., Wolfe, A. C., and Nabors, L. G., *Ind. Eng. Chem.* **48**, 162 (1956).
10. Garten, V. A., and Weiss, D. E., *Australian J. Chem.* **8**, 68 (1955).
11. Graham, D., *J. Phys. Chem.* **59**, 896 (1955).
12. Anderson, R. B., and Emmett, P. H., *J. Phys. Chem.* **56**, 753 (1952).
13. Carter, R. L., and Greening, W. J., Preprint 319, American Nuclear Society, Nuclear Eng. and Sci. Congress, Dec. 1955.

14. Norton, J. F., and Marshall, A. L., *Trans. Am. Inst. Mining Met. Engrs.* **156**, 351 (1944).
15. Ingram, D. J. E., and Austen, D. E. G., in "Industrial Carbon and Graphite," p. 19. Society of Chemical Industry, London, 1957.
16. Winslow, F. H., Baker, W. O., and Yager, W. A., *Proc. 1st and 2nd Conf. on Carbon, Univ. of Buffalo*, p. 93 (1956).
17. Hennig, G. R., and Smaller, B., *Proc. 1st and 2nd Conf. on Carbon, Univ. of Buffalo*, p. 113 (1956).
18. Ingram, D. J. E., and Bennett, J. E., *Philos. Mag.* **45**, 545 (1954).
19. Langmuir, I., *J. Am. Chem. Soc.* **37**, 1139 (1915).
20. Sihvonen, V., *Trans. Faraday Soc.* **34**, 1062 (1938).
21. Meyer, L., *Trans. Faraday Soc.* **34**, 1056 (1938).
22. Strickland-Constable, R. F., *Trans. Faraday Soc.* **40**, 333 (1944).
23. Duval, X., *J. chim. phys.* **47**, 339 (1950).
24. Day, R. J., Ph.D. thesis, The Pennsylvania State University, 1949.
25. Chukhanov, Z. F., *Fuel* **19**, 17, 49, 64 (1940).
26. Grodozovskii, M. K., and Chukhanov, Z. F., *Fuel* **15**, 321 (1936).
27. Rhead, T. F. E., and Wheeler, R. V., *J. Chem. Soc.* **103**, 461 (1913).
28. Arthur, J. R., *Nature* **157**, 732 (1946).
29. Bridger, G. W., *Nature* **157**, 236 (1946).
30. Arthur, J. R., *Trans. Faraday Soc.* **47**, 164 (1951).
31. Wicke, E., "Fifth Symposium on Combustion," p. 245. Reinhold, New York, 1955.
32. Rossberg, M., *Z. Elektrochem.* **60**, 952 (1956).
33. Lewis, W. K., Gilliland, E. R., and Paxton, R. R., *Ind. Eng. Chem.* **46**, 1327 (1954).
34. Arthur, J. R., Bangham, D. H., and Bowering, J. R., "Third Symposium on Flame, Combustion, and Explosion Phenomena," p. 466. Williams and Wilkins, Baltimore, 1949.
35. Walker, P. L., Jr., and Wright, C. C., *Fuel* **31**, 45 (1952).
36. Arthur, J. R., and Bowering, J. R., *Ind. Eng. Chem.* **43**, 528 (1951).
37. Reif, A. E., *J. Phys. Chem.* **56**, 785 (1952).
38. Marsh, J. D. F., Publication No. 393, The Institution of Gas Engineers, London, 1951.
39. Lewis, W. K., Gilliland, E. R., and McBride, G. T., Jr., *Ind. Eng. Chem.* **41**, 1213 (1949).
40. Wu, P. C., D.Sc. thesis, Mass. Inst. Technol., Cambridge, Mass., 1949.
41. Graham, H. S., D.Sc. thesis, Mass. Inst. Technol., Cambridge, Mass., 1947.
42. Semechkova, A. F., and Frank-Kamenetskii, D. A., *Acta Physicochim. U.R.S.S.* **12**, 879 (1940).
43. Long, F. J., and Sykes, K. W., *Proc. Roy. Soc.* **A193**, 377 (1948).
44. Reif, A. E., *J. Phys. Chem.* **56**, 778 (1952).
45. Ergun, S., *J. Phys. Chem.* **60**, 480 (1956).
46. Key, A., *Gas Research Board Commun. (London)* No. G.R.B. 40 (1948).
47. Strickland-Constable, R. F., *J. chim. phys.* **47**, 356 (1950).
48. Strickland-Constable, R. F., *Proc. Roy. Soc.* **A189**, 1 (1947).
49. Paxton, R. R., Sc.D. thesis, Mass. Inst. Technol., Cambridge, Mass., 1949.
50. Bonner, F., and Turkevich, J., *J. Am. Chem. Soc.* **73**, 561 (1951).
51. Brown, F., *Trans. Faraday Soc.* **48**, 1005 (1952).
52. Orning, A. A., and Sterling, E., *J. Phys. Chem.* **58**, 1044 (1954).

53. Gadsby, J., Hinshelwood, C. N., and Sykes, K. W., *Proc. Roy. Soc.* **A187**, 129 (1946).
54. Johnstone, H. F., Chen, C. Y., and Scott, D. S., *Ind. Eng. Chem.* **44**, 1564 (1952).
55. Jolley, L. J., and Poll, A., *J. Inst. Fuel* **28**, 33 (1953).
56. Dolch, P., *Brennstoff-Chem.* **14**, 261 (1933).
57. Neumann, B., Kroger, C., and Fingas, E., *Gas- u. Wasserfach* **74**, 565 (1931).
58. Ingles, O. G., *Trans. Faraday Soc.* **48**, 706 (1952).
59. Zielke, C. W., and Gorin, E., *Ind. Eng. Chem.* **47**, 820 (1955).
60. Vulis, L. A., and Vitman, L. A., *J. Tech. Phys. (U.S.S.R.)* **11**, 509 (1941).
61. Thring, M. W., and Price, P. H., *Iron and Coal Trades Rev.* **169**, 347 (1954).
62. Armington, A. F., Ph.D. thesis, The Pennsylvania State University, 1960.
63. Vastola, F. J., Ph.D. thesis, The Pennsylvania State University, 1959.
64. Duval, X., *J. chim. phys.* **44**, 296 (1947).
65. Karzhavina, N. A., *Doklady Akad. Nauk S.S.S.R.* **73**, 971 (1950).
66. Batchelder, H. R., Busche, R. M., and Armstrong, W. P., *Ind. Eng. Chem.* **45**, 1856 (1953).
67. Mayers, M. A., *J. Am. Chem. Soc.* **56**, 70 (1934).
68. Pilcher, J. M., Walker, P. L., Jr., and Wright, C. C., *Ind. Eng. Chem.* **47**, 1742 (1955).
69. Key, A., and Cobb, J. W., *J. Soc. Chem. Ind.* **49**, 440T (1930).
70. James, V. E., Ph.D. thesis, West Virginia University, 1957.
71. Goring, G. E., Curran, G. P., Tarbox, R. P., and Gorin, E., *Ind. Eng. Chem.* **44**, 1057 (1952).
72. Tuddenham, W. M., and Hill, G. R., *Ind. Eng. Chem.* **47**, 2129 (1955).
73. Binford, J. S., Jr., and Eyring, H., *J. Phys. Chem.* **60**, 486 (1956).
74. Mayers, M. A., *Trans. Am. Inst. Mining Met. Engrs.* **119**, 304 (1936).
75. Scott, G. S., and Jones, G. W., *U. S. Bur. Mines, Rept. Invest.* 3405 (1938).
76. Sihvonen, V., *Z. Electrochem.* **36**, 806 (1930).
77. Chen, M. C., Christensen, C. J., and Eyring, H., *J. Phys. Chem.* **59**, 1146 (1955).
78. Gulbransen, E. A., and Andrew, K. F., *Ind. Eng. Chem.* **44**, 1034 (1952).
79. Blyholder, G., and Eyring, H., *J. Phys. Chem.* **61**, 682 (1957).
80. Gilliland, E. R., and Harriott, P., *Ind. Eng. Chem.* **46**, 2195 (1954).
81. Wicke, E., and Hedden, K., *Z. Elektrochem.* **57**, 636 (1953).
82. Rossberg, M., and Wicke, E., *Chem.-Ingr.-Tech.* **28**, 181 (1956).
83. Arthur, J. R., Newitt, E. J., and Raftery, M. M., *Nature* **178**, 157 (1956).
84. Lambert, J. D., *Trans. Faraday Soc.* **34**, 1080 (1938).
85. Walker, P. L., Jr., Foresti, R. J., Jr., and Wright, C. C., *Ind. Eng. Chem.* **45**, 1703 (1953).
86. Walker, P. L., Jr., and Rusinko, F., Jr., *J. Phys. Chem.* **59**, 241 (1955).
87. Petersen, E. E., and Wright, C. C., *Ind. Eng. Chem.* **47**, 1624 (1955).
88. Walker, P. L., Jr., and Raats, E., *J. Phys. Chem.* **60**, 370 (1956).
89. Rusinko, F., Jr., Ph. D. thesis, The Pennsylvania State University, 1958.
90. Hedden K., private communication, 1957.
91. Mayers, M. A., *J. Am. Chem. Soc.* **61**, 2053 (1939).
92. Hunt, B. E., Mori, S., Katz, S., and Peck, R. E., *Ind. Eng. Chem.* **45**, 677 (1953).
93. Dotson, J. A., Holden, J. H., and Koehler, W. A., *Ind. Eng. Chem.* **49**, 148 (1957).
94. Long, F. J., and Sykes, K. W., *J. chim. phys.* **47**, 361 (1950).
95. Lambert, J. D., *Trans. Faraday Soc.* **32**, 452 (1936).
96. Letort, M., and Magrone, R., *J. chim. phys.* **47**, 576 (1950).
97. Golovina, E. S., *Izvest. Akad. Nauk S.S.S.R., Otdel, Tekh. Nauk* p. 1343 (1949).

98. Klibanova, T. M., and Frank-Kamenetskii, D. A., *Acta Physicochim. U.R.S.S.* **18**, 387 (1943).
99. Earp, F. K., and Hill, M. W., in "Industrial Carbon and Graphite," p. 326. Society of Chemical Industry, London, 1957.
100. Thiele, E. W., *Ind. Eng. Chem.* **31**, 916 (1939).
101. Wheeler, A., *Advances in Catalysis* **3**, 249-327 (1951).
102. Wheeler, A., in "Catalysis" (P. H. Emmett, ed.), Vol. 2, pp. 105-165. Reinhold, New York, 1955.
103. Weisz, P. B., and Prater, C. D., *Advances in Catalysis* **6**, 143-196 (1954).
104. Frank-Kamenetskii, D. A., "Diffusion and Heat Exchange in Chemical Kinetics." Princeton University Press, Princeton, N. J., 1955.
105. Petersen, E. E., *Am. Inst. Chem. Eng. J.* **3**, 443 (1957).
106. Walker, P. L., Jr., and Raats, E., *J. Phys. Chem.* **60**, 364 (1956).
107. Aris, R., *Chem. Eng. Sci.* **6**, 262 (1957).
108. Weisz, P. B., *Z. physik. Chem. (Frankfurt)* **11**, 1 (1957).
109. Walker, P. L., Jr., Rusinko, F., Jr., and Raats, E., *J. Phys. Chem.* **59**, 245 (1955).
110. Rice, C. W., *Ind. Eng. Chem.* **16**, 460 (1924).
111. Parker, A. S., and Hottel, H. C., *Ind. Eng. Chem.* **28**, 1334 (1936).
112. Mayers, M. A., *Trans. Am. Inst. Mining Met. Engrs.* **130**, 408 (1938).
113. Chukhanov, Z. F., and Karzhavina, N. A., *Fuel* **20**, 73 (1941).
114. Kuchta, J. M., Kant, A., and Damon, G. H., *Ind. Eng. Chem.* **44**, 1559 (1952).
115. Tu, C. M., Davis, H., and Hottel, H. C., *Ind. Eng. Chem.* **26**, 749 (1934).
116. Graham, J. A., Brown, A. R. G., Hall, A. R., and Watt, W., in "Industrial Carbon and Graphite," p. 309. Society of Chemical Industry, London, 1957.
117. "Handbook of Chemistry and Physics," 33rd ed., p. 1837. Chemical Rubber Publishing Co., Cleveland, 1951.
118. Wilke, C. R., *Chem. Eng. Progr.* **46**, 95 (1950).
119. Bromley, L. A., and Wilke, C. R., *Ind. Eng. Chem.* **43**, 1641 (1951).
120. Petersen, E. E., Ph.D. thesis, The Pennsylvania State University, 1953.
121. Emmett, P. H., *Am. Soc. Testing Materials Tech. Publ.* **51**, 95 (1941).
122. Spalaris, C. N., *J. Phys. Chem.* **60**, 1480 (1956).
123. Dresel, E. M., and Roberts, L. E. J., *Nature* **171**, 170 (1953).
124. Petersen, E. E., Wright, C. C., and Walker, P. L., Jr., *Ind. Eng. Chem.* **47**, 1629 (1955).
125. Carman, P. C., "Flow of Gases Through Porous Media." Academic Press, New York, 1956.
126. Kaye, G. W. C., and Laby, T. H., "Physical and Chemical Constants," p. 37. Longmans, Green, London, 1936.
127. O'hern, H. A., Jr., and Martin, J., Jr., *Ind. Eng. Chem.* **47**, 2081 (1955).
128. Golovina, E. S., *Doklady Akad. Nauk S.S.S.R.* **85**, 141 (1952).
129. Emmett, P. H., ed., "Catalysis," Vol. I, p. 53. Reinhold, New York, 1954.
130. Grisdale, R. O., *J. Appl. Phys.* **24**, 1288 (1953).
131. Smith, W. R., and Polley, M. H., *J. Phys. Chem.* **60**, 689 (1956).
132. Walker, P. L., Jr., and Imperial, G., *Nature* **180**, 1184 (1957).
133. Kmetko, E. A., *Proc. 1st and 2nd Conf. on Carbon, Univ. of Buffalo*, p. 21 (1956).
134. Walker, P. L., Jr., Rusinko, F., Jr., Rakszawski, J. F., and Liggett, L. M., *Proc. 3rd Conf. on Carbon, Univ. of Buffalo*, p. 643 (1958).
135. Abbott, H. W., "Encyclopedia of Chemical Technology," Vol. 3, pp. 1-23. Interscience Encyclopedia, Inc., New York, 1949.
136. Johnson, F. B., and Wood, R. E., *Petrol. Refiner* **33**, 157 (1954).
137. Molstedt, B. V., and Moser, J. F., Jr., *Ind. Eng. Chem.* **50**, 21 (1958).

138. Day, J. E., *Ind. Eng. Chem.* **28**, 234 (1936).
139. Sato, H., and Akamatu, H., *Fuel* **33**, 195 (1954).
140. Nebel, G. J., and Cramer, P. L., *Ind. Eng. Chem.* **47**, 2393 (1955).
141. Gulbransen, E. A., and Andrew, K. F., *Ind. Eng. Chem.* **44**, 1048 (1952).
142. Walker, P. L. Jr., and Nichols, J. R., in "Industrial Carbon and Graphite," p. 334. Society of Chemical Industry, London, 1957.
143. Walker, P. L., Jr., and Baumbach, D. O., unpublished results (1959).
144. Hedden, K., *27th Intern. Congr. Ind. Chem.* **2**, 68 (1954).
145. Kosiba, W. L., and Dienes, G. J., *Advances in Catalysis* **9**, 398 (1957).